

THE USE OF THERMOGRAVIMETRIC ANALYSIS TO FOLLOW CHANGES DURING SHORT-CONTACT-TIME COAL LIQUEFACTION

He Huang, Keyu Wang, William H. Calkins* and Michael T. Klein
Dept of Chemical Engineering, University of Delaware, Newark, DE 19716

Key words: thermogravimetric analysis, coal liquefaction, short-contact-time

INTRODUCTION

The study of the chemical reactions involved in coal liquefaction is aided by elucidation of the processes occurring in the very early stages (low conversions), before secondary reactions of the products become significant. To this end, as reported in previous papers^{1,2}, we have developed a reactor system capable of carrying out liquefaction reactions at accurately known reaction times from as short as a few seconds (low conversions) to as long as 60 min or more. The analytical methods to monitor these reactions must provide sensitive measures of the coal conversion and product yield information. We have found thermogravimetric analysis (TGA) useful since it provides sensitive, rapid and reproducible results concerning the various weight loss changes that can be connected to the physical and chemical changes occurring during coal liquefaction.

Thermogravimetric analysis has other desirable features as well. First, only very small samples (about 30 mg) are required for each TG run. Second, by suitable adjustments in the work-up procedures and the TG running parameters, such as heating rate and atmosphere, thermogravimetric analyses yield important information concerning the reaction pathways.

It is to illustrate the usefulness of thermogravimetric analysis of coal liquefaction products that this paper is presented.

EXPERIMENTAL

Apparatus. The design and operation of the SCTBR reactor system have been described in detail previously¹. In brief, both the empty preheater and reactor are immersed in a Techne IFB-52 fluidized sand bath. They are brought up to the predetermined reaction temperature prior to the start of the reaction. High pressure nitrogen gas provides the driving force to deliver the reaction mixture of a coal-tetralin slurry from a small blow case into the empty reactor through the preheater tubing. Nitrogen gas is then bubbled through the reactor from the bottom to provide the agitation needed in the heterogeneous reaction system. The degree of agitation is controlled by the exit gas flow rate from the top of the reactor. The temperature of the reactant mixture (ca. 30 g) approaches the desired reaction temperature to within 5-8 °C of preset temperature during the transport process (approximately 0.3 seconds). This temperature is maintained within ± 2 °C during the experiment. At a preselected reaction time, high pressure nitrogen gas is again used to drive the reactor contents from the reactor into a cold receiver through the precooler. Both receiver and precooler are immersed in a water bath. Cooling of the product mixture to about 25 °C is achieved within 0.3 seconds.

Coal Liquefaction Runs. All reactions were run as mixtures of tetralin (T, the H-donor solvent) and coal (C) at ratio of T/C = 8. About 4 grams of coal were used for each reactor run together with added tetralin to make up the reactant slurry. The reactor runs are summarized in Table I. Hold up of material on the surfaces of the reactor, preheater, and precooler prevented complete recovery of the reaction products. However, the recoveries were high, and varied from about 80-90 wt%. The measure of conversion and subsequent analytical results were therefore based on representative aliquots.

Thermogravimetric Analysis. The thermogravimetric analyzer (TGA) was a Model 51 TGA (TA Instruments, New Castle, Delaware). A representative TG scan on the Illinois #6 coal from the Argonne Premium Coal Sample program is shown in Figure 1. The weight loss resulting from heating in nitrogen at 100 cm³(STP)/min with a heating rate of 10°C/min to 950°C and hold for 7 min at 950 °C defines the amount of volatile matter (VM). For this illustrative sample VM was 36.64 wt%. Further weight loss occurred at 950°C after the introduction of oxygen. This was due to the oxidation of the remaining combustible material, the so called "fixed carbon (FC)", in the char, which amounted to 48.42 wt% for the illustrative sample of Figure 1. The residue represents the ash content (14.94 wt%). Thus the two phases, i.e., 1) the heating rate to 950°C in nitrogen and hold for 7 min; and 2) the oxidation at 950°C, provided measures of VM, FC, and Ash, respectively. The experimental error for determination of these TGA characteristic variables (VM, FC, and Ash) is less than $\pm 2\%$ of the measured values.

Thermogravimetric analysis can also be run in a hydrogen atmosphere. This provides additional information regarding the structure of coal and liquefaction residue. However, it is required that nitrogen be introduced to replace hydrogen in the TGA system for about 10 min before the introduction of oxygen.

RESULTS AND DISCUSSION

Effect of Heating Rate and Atmosphere in TG Runs. The effect of heating rate on the DTG analysis of the Illinois #6 coal is illustrated in Figure 2. The two small peaks in the VM portion of the DTG curves gradually disappear as heating rate increases. This is due to the lower resolution of DTG profile at the higher heating rate. The DTG curves of the Illinois #6 coal in nitrogen and in hydrogen demonstrated in Figure 3 show the similar pyrolysis rate patterns. However, all three peak temperatures in the VM portion of TG pyrolysis in hydrogen are shifted to lower temperatures than those of TG pyrolysis in nitrogen.

Figures 4(a), 4(b) and 4(c) show plots of VM for Illinois #6, Utah Blind Canyon bituminous coals and Wyodak Black Thunder subbituminous coal, respectively. They were determined by TG pyrolysis in nitrogen and in hydrogen at heating rates varying from 10°C/min to 200°C/min. The heating rate had a strong effect on the volatile matter in nitrogen and in hydrogen. The VM yields in nitrogen (VM_{N_2}) increased with increasing heating rate until it leveled off at about 50 °C/min. This can be tentatively attributed to an unstable component in the coal when the volatile product is only slowly removed from the coal in nitrogen which results in free radical retrograde reactions and low volatile yields. The VM yields in hydrogen (VM_{H_2}) are always higher than those in nitrogen. This is because the presence of hydrogen in the TG pyrolysis apparently stabilizes or quenches these radicals to give the higher VM yields. VM_{H_2} decreased with increasing heating rate. This may be due to the longer pyrolysis times at the low heating rates. The different behavior in VM determined by TGA shown by the various coals in nitrogen and in hydrogen (see Figure 4) may represent an indication of the potential relative instabilities of the various coals. While the Illinois and Utah bituminous coals showed similar behavior with heating rate in hydrogen or nitrogen atmosphere, the Wyodak subbituminous coal showed only a small effect of heating rate on VM in the presence of nitrogen and quite a strong and reverse effect in the presence of hydrogen. Further research is being directed toward a better understanding of these phenomena.

Conversion Determination and Work-up Procedures for Coal Liquefaction Runs.

During coal liquefaction, the mineral matter of the coal primarily remains with the unconverted coal, and is essentially insoluble in the tetralin. The coal liquids, however, are largely extracted into the tetralin solvent, although some remain with the coal residue. This provides a means of measuring the conversion of the coal by determining the ash content of the residue when it has been washed free of the coal liquids. All the tetralin and tetralin-derived products must also be removed or an error in the conversion calculation will result. The conversion can be calculated using Eq. 1:

$$\text{Conversion} = \left(1 - \frac{X_0}{X}\right) \times 100 \text{ (wt\%)} \quad (1)$$

where X_0 and X are the ash contents of the control sample and the coal liquefaction residue, respectively. The control sample is the original coal which is processed exactly as a liquefaction residue except running at room temperature.

After a liquefaction run, the product mixture is filtered and the residue washed with tetralin thoroughly and dried in a vacuum oven at about 105°C for 48 hours. A DTG curve for one of these samples is shown in Figure 5. Comparison of this curve with that of unreacted coal shows that there is an incomplete peak on the low temperature side of the principal VM peak in the coal residue. That this is due to the presence of residual tetralin is shown by a control sample treated by processing a tetralin-coal slurry through the reactor at room temperature. To measure the coal conversion accurately, the tetralin and the tetralin-derived materials as well as the coal liquefaction liquid products must be removed from the residue. The most satisfactory solvent we have found for this purpose is methylene chloride (see Figure 5). The tetralin peak disappears after methylene chloride washing. For this reason, we have adopted the work-up procedure including the methylene chloride treatment.

The conversion of Illinois #6 in tetralin vs. time at 390°C under 1000 psig nitrogen gas determined by Eq. 1 is illustrated in Figure 6. Within 30-60 seconds, the coal conversion has reached about 18 wt%. This rapid liquefaction may be resulted from the extraction of a soluble portion of coal into the tetralin. From the contact time of 1 min to 30 min, the coal conversion only increase about 19 wt% (reaching 37 wt%), probably due to the coal matrix itself being attacked. Finally, the coal conversion reached 47 wt% at 60 min.

Change of DTG Profiles with Conversion during Coal Liquefaction in Tetralin.

Figure 7 shows DTG vs temperature curves for the residues of the Illinois #6 coal after liquefaction in tetralin at 390 °C under 1000 psig nitrogen at selected times. The two small peaks in the VM portion gradually disappear. Such chemical changes have been supported by previously observed changes in the total oxygen content and hydroxyl content^{3,5} of the

coal during the early stages in coal liquefaction.

Change of Volatile Matter in N_2 and in H_2 with Conversion during Coal Liquefaction in Tetralin. Interesting insights into the coal structure and the coal liquefaction process can be obtained by running thermogravimetric analyses in nitrogen and in hydrogen at various heating rates on the samples taken at various reaction times. The coal liquefaction process, even at low conversion, greatly changes the TG behavior of the partially reacted coal residue. Figure 8 shows an example of the VM determined by TG pyrolysis in nitrogen and in hydrogen at various heating rates for the liquefaction residue of the Illinois #6 coal reacted in tetralin under 1000 psig nitrogen gas at 390°C for 30 seconds. The VM_{N_2} no longer shows the strong sensitivity to heating rate. Furthermore, it decreased with increasing heating rates. This suggests that the unstable component of the coal may have been stabilized in the very early stage of the liquefaction process.

SUMMARY AND CONCLUSIONS

Thermogravimetric analysis provides various weight changes in coal residua arising from coal liquefaction and these reveal significant information concerning the underlying chemical and physical processes.

A workup protocol including the methylene chloride washing to eliminate the error due to the presence of tetralin and/or coal liquids has been devised which is being used along with TGA to determine liquefaction conversion.

Interesting differences have been observed in the three Argonne Premium Coal Samples (Illinois #6 bituminous coal, Utah Blind Canyon bituminous coal, and Wyodak Black Thunder subbituminous coal) studied by running TGA at different heating rates and in nitrogen or hydrogen atmosphere. These experiments suggest the presence of an unstable component in the coal or coal-derived liquid which is rapidly removed or stabilized by very short contact time under liquefaction conditions.

Acknowledgements. The support of this work by the Department of Energy under DE-FG22-93PC93205 is gratefully acknowledged. The use of the Argonne Premium Coal Samples provided by Dr. Karl Vorres is also gratefully acknowledged. Additional funds for purchase of thermal analysis equipment was provided by the University of Delaware.

References

1. Huang, H.; Calkins, W.H.; Klein, M.T. A Novel Short Time Reactor System for Studying the Initial Stages of High Temperature and High Pressure Reactions. *ACS Fuel Chem Div. Preprints* **1993**, *38* (3), 1080.
2. Huang, H.; Calkins, W.H.; Klein, M.T.; A Novel Laboratory Scale Short Contact Time Batch Reactor System for Studying Fuel Processes. 1. Apparatus and Preliminary Experiments, submitted in *Energy & Fuels*.
3. Huang, H.; Provine, W.D.; Jung, B.; Jacintha, M.A.; Rethwisch, D.G.; Calkins, W.H.; Klein, M.T.; Dybowski, C.R.; Scouten, C.G. Short Time Reactor System for Studying the Initial Stages of Coal Liquefaction. *Proceedings of the International Conference on Coal Science*, **1993**, Ed. K.H. Michaelian, Vol. I, 266.
4. Jung, B.; Provine, W.D.; Calkins, W.H.; Klein, M.T.; Scouten, C.G. Changes in Organic Oxygen Contents of Illinois #6 Coal during Coal Liquefaction. *ACS Fuel Chem Div. Preprints* **1992**, *37* (2), 670.
5. Provine, W.D.; Jung, B.; Jacintha, M.A.; Rethwisch, D.G.; Huang, H.; Calkins, W.H.; Klein, M.T.; Scouten, C.G.; Dybowski, C.R. A Kinetic Investigation of Coal Liquefaction at Short Reaction Times. *Catalysis Today*, **1994**, Ed. D.B. Dadyburjor and J.W. Zondlo, Vol. *19*, No. *3*, 409.

Table I Illinois #6 Coal Liquefaction Runs

Sample	Contact time min	T/C (wt)	Temperature °C	Recovery wt%
DOE001	15.00	8	15	78%
DOE012	0.17	8	390	86%
DOE015	0.50	8	384	92%
DOE016	0.75	8	385	89%
DOE017	1.00	8	386	88%
DOE021	5.00	8	387	87%
DOE013	10.00	8	390	82%
DOE009	30.00	8	390	85%
DOE010	60.00	8	390	81%

Sample: Illinois #6
 Size: 44.7080 mg
 Method: DDE Coal Liquefaction
 Comment: 10 °C/min to 950 °C, N₂, 100 ml/min (after drying)

TGA

File: C: ILL6N2.016
 Operator: Keyu Wang
 Run Date: 19-May-94 16: 59

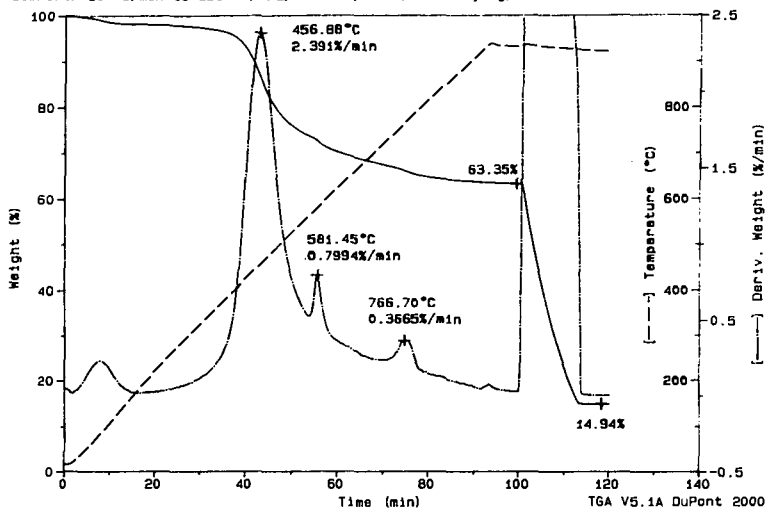


Figure 1. A TG scan on the Illinois #6 coal

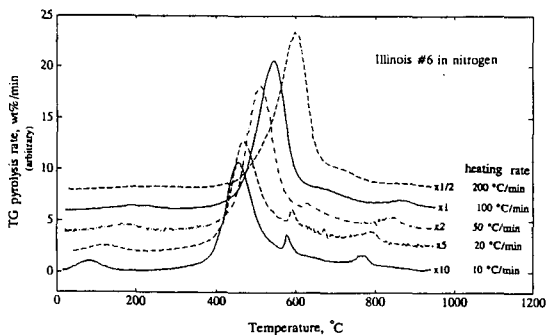


Figure 2. Effect of heating rate on DTG of the Illinois #6 coal pyrolysis in N₂

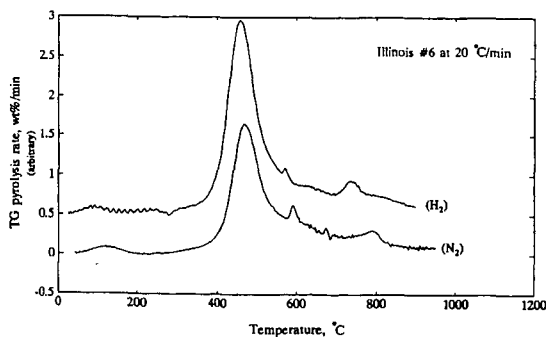


Figure 3. Effect of gas atmosphere on DTG of the Illinois #6 coal pyrolysis at heating rate of 20 °C/min

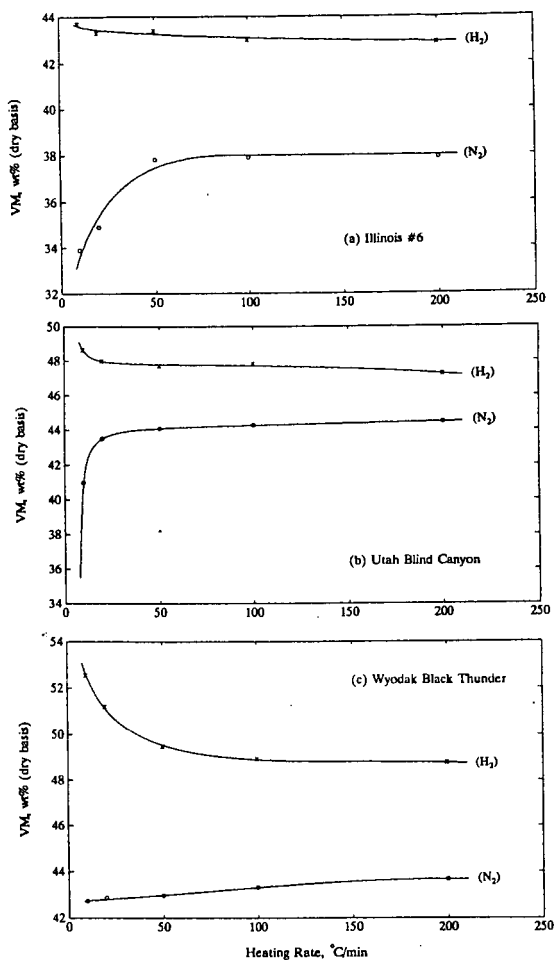


Figure 4. Effect of heating rate on the VM yields determined by TG pyrolysis in N_2 and in H_2

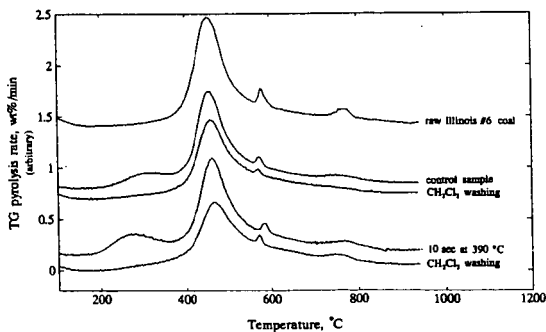


Figure 5. Disappearance of the incomplete peak on the low temperature side of the principal VM peak due to the presence of residual tertalin in the control sample and the reacted solid residue by methylene chloride washing

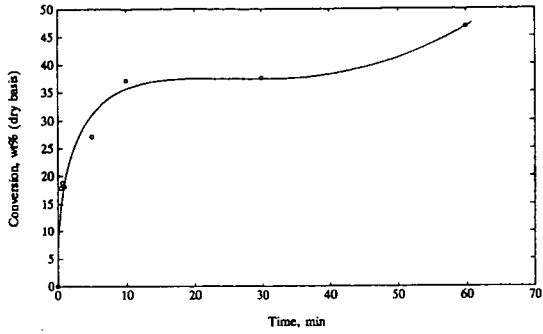


Figure 6. Kinetics of the Illinois #6 coal liquefaction in tetralin (1000 psig N_2 gas; 390 °C; T:C = 8:1)

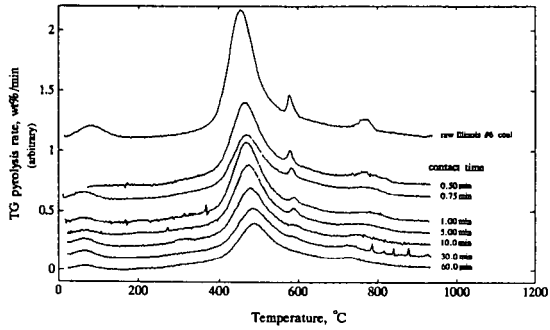


Figure 7. DTG profiles for residues of the Illinois #6 coal after liquefaction in tetralin at the selected contact times (TG scan at 10 °C/min in N_2 ; liquefaction run at 390 °C under 1000 psig N_2 with T:C = 8:1)

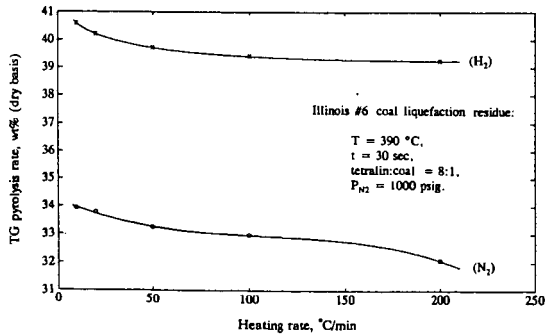


Figure 8. Effect of heating rate on VM yields of Illinois #6 coal liquefaction residue determined by TG pyrolysis in N_2 and in H_2

THE RELEASE OF NITROGEN IN THE COMBUSTION AND PYROLYSIS OF COALS AND MACERALS

C.J. Hindmarsh, J.E. Varey and K.M. Thomas
Northern Carbon Research Laboratories, Dept. of Chemistry,
Bedson Building, University of Newcastle, Newcastle upon Tyne,
NE1 7RU, U.K.

Keywords: Coal, char, combustion, pyrolysis, macerals, NO_x

Introduction

The release of nitrogen and sulphur oxides during coal combustion is a major environmental problem. NO_x and SO_x are contributors to acid rain whereas N₂O is a 'greenhouse' gas. In coal combustion the following stages occur: 1) rapid devolatilization followed by 2) ignition of volatiles and 3) the slower char gasification [1]. The nitrogen and sulphur species are partitioned into the volatiles and the char. The minimization of the environmental impact of coal combustion by improved burner technology and flue gas desulphurization is currently underway. In the case of NO_x emissions, the retrofitting of 'low NO_x' burners in power stations has been undertaken. In these combustion systems, the char nitrogen is the major contributor to NO_x emissions [2]. The volatiles are released in a zone where the oxygen concentration is low and the formation of molecular nitrogen is favoured. Therefore the release of nitrogen and sulphur oxides during coal combustion has major implications for the environment.

The release of nitrogen oxides is controlled to an extent by the combustion conditions but there are also variations due to coal properties [3-5]. In low NO_x burners and fluidized bed combustion, fuel nitrogen is the major contributor to NO_x formation. Therefore an understanding of the nitrogen in coal and its release during combustion is an important consideration. Coals are a complex heterogeneous material with a cross-linked macromolecular structure. This gives rise to problems when characterising the coal for combustion purposes. This structural heterogeneity can be described at a variety of levels. At the macroscopic level coals may have a banded structure. At the microscopic level the structure may be described as microscopic components, macerals or associations of macerals which are termed microlithotypes. Macerals can be separated and have distinct physical and chemical properties, for example, volatile matter, nitrogen content, reactivity etc. When considering coal the heterogeneity must be considered since the small particles used in pulverised fuel (pf) combustion, depending on the coal, may be regarded as pure macerals or associations of macerals [6-9]. When considering the nitrogen in coal at the molecular level the nitrogen functionality must be considered. The nitrogen may be described as pyrrolic, pyridinic or quaternary nitrogen.

The objective of this paper was to study the release of coal nitrogen as NO_x during temperature programmed combustion of coals and macerals, with the emphasis being on the identification of reactive intermediate species and a comparison of the differences between macerals.

Experimental

Materials used

The characterisation data for the coals and maceral concentrates used in this study are given in Table 1. Maceral concentrates were obtained by the density gradient centrifugation (DGC) technique [10-12].

Temperature Programmed Combustion

The temperature programmed combustion studies were carried out using a Thermal Sciences thermogravimetric analysis - mass spectrometer system (TG-MS). This system consisted of a thermogravimetric analysis (TGA) instrument coupled with a VG Quadrupoles 300 amu mass spectrometer. Gas sampling was carried out at two positions: 1) approximately 1 cm directly above the sample and 2) at the exit of the thermogravimetric analyser. The former sampling point allows reactive intermediate species to be detected while the latter essentially samples the gases at equilibrium. The evolved gas profiles were measured at both sampling positions. Approximately 5 mg of the coal was used in each run. The sample was heated at 15 K min⁻¹ in 20% oxygen/helium and the evolved gas profiles recorded. The following mass/charge (m/z) ratios were monitored throughout the course of the reaction: 2, 14-65.

Temperature Programmed Pyrolysis

The temperature programmed pyrolysis was carried out in argon at a flow rate of 50 cc min⁻¹ at a heating rate of 15 K min⁻¹ in a similar manner to the combustion experiments. In this case gas sampling was carried out at the exit of the thermogravimetric analyser.

Results

A comparison of the temperature programmed combustion required evolved gas profiles for Illinois No. 6, in 20% oxygen/helium with sampling directly above the sample and at the exit of the thermogravimetric analyser. These are shown in Figures 1(a) and 1(b) respectively. It is apparent that whilst there are similarities between the two sets of evolved gas profiles there are also marked differences. The profiles have a complex series of emissions. The integrated gas concentration ratios for some of the species evolved during the temperature programmed combustion of the Illinois No. 6 coal are given in Table 2. The CO and CO₂ profiles show a shoulder on the low temperature side. This corresponds to the evolution of small hydrocarbons and tars. In addition, the CO/CO₂ ratios for gas sampling directly above the sample and at the exit of the thermogravimetric analyser were 0.535 and 0.096 respectively. This clearly indicates that CO is being formed and released into the gas phase where it is converted to CO₂ by homogeneous gas phase reactions. Another noticeable difference in intensities is the increase in m/z 30 concentration and decrease in m/z 27 concentration when comparing sampling directly above the sample and at the exit of the TGA. This can be explained by the conversion of HCN released in the gas combustion process and converted to NO by gas phase oxidation reactions. The fraction of coal nitrogen converted to NO is 0.362 when measured by sampling directly above the sample and this increases to 0.961 when the gas sampling is carried out at the exit of the TGA. Not all of the m/z 27 and m/z 30 are HCN and NO respectively. Undoubtedly there are small contributions from hydrocarbons, and/or fragmentation in the mass spectrometer which make a contribution for some m/z ratios. When gas sampling is carried out directly above the sample, a high CO concentration is observed. Since NO is in relatively low concentration, there may be a significant contribution to the NO peak from ¹²C¹⁸O. This

contribution can be corrected for by subtracting $0.002 \cdot \text{CO}$ peak. The peak which occurs at the lowest temperature $\sim 300^\circ\text{C}$ is consistent with the release of hydrocarbons. This precedes the release of tars when the coal starts to pyrolyse. Figure 1(a) shows that intermediate species such as COS and HCN are released during the temperature programmed combustion. Evolved gas profiles have been monitored for all m/z values in the range 14-65. It is apparent that when gas sampling is carried out directly above the sample many of the masses have weak profiles. It is difficult to assign the peaks unequivocally to various species due to the complex nature of the mixture of gases evolved and fragmentation effects in the mass spectrometer. However, it is apparent that in some coals, a peak was observed for m/z 52 at the beginning of the char gasification region whereas no corresponding peaks were observed at m/z 51 and 53. This peak was observed at the same temperatures as peaks at m/z 26 and 27 corresponding to HCN and its fragments. Therefore it is reasonable to assign the peak at m/z 52 to $(\text{CN})_2$. The evolved gas profiles for m/z 41, 42 and 43 were all bimodal. The lowest temperature peak for m/z 43 occurs at a position coincident with m/z values which can be assigned to the evolution of small hydrocarbon species. The higher temperature peak for m/z 43 which occurs at a similar temperature to m/z 52 and 27 is possibly due, in part, to HOCN. The evolved gas profiles at 41, 42, 43, 52, 60 etc are either not observed or are very weak when gas sampling is carried out at the exit of thermogravimetric analyser thereby confirming that reactive intermediate species can be detected by gas sampling close to the sample during temperature programmed combustion. A suite of coals with a range of rank have been studied in detail, in addition, to the coal described above. These include Blind Canyon and Pocohontas from the Argonne Premium Coal Sample Bank and Illinois No. 6 from SBN. These reveal significant differences in the release of species such as COS, $(\text{CN})_2$ etc. during temperature programmed combustion.

The corresponding temperature programmed pyrolysis profiles are shown in Figure 1(c). In this case the gas sampling was carried out at the exit of the TGA. The results show that a range of small gaseous molecules CO_2 , CO, NO, N_2 , HCN, SO_2 and CH_4 are evolved over a range of temperatures. At the lowest temperatures low molar mass hydrocarbons were detected. Tars were condensed out and not detected. It is apparent that the temperature programmed pyrolysis technique is capable of distinguishing the release of gaseous species. Some of the peaks, for example, m/z 27 (HCN) occurs at the same temperature for both the pyrolysis and combustion.

The temperature programmed combustion evolved gas profiles for the entrained flow reactor chars prepared from Illinois No. 6 are shown in Figure 2. The results show similarities to the temperature programmed combustion of the raw coal. The CO concentration measured by sampling directly above the sample is high but this is reduced when evolved gas sampling is carried out at the exit. The CO/ CO_2 ratio decreases from 0.355 measured directly above the sample to 0.076 measured at the exit of the TGA. It is apparent that the primary product CO is again converted to CO_2 by gas phase homogeneous reactions as in the coal studies. In addition the m/z 27 peak (mainly HCN) virtually disappears and the m/z 30 (NO) increases slightly when gas sampling is carried out at the exit. The fraction of char nitrogen converted to NO measured directly above the sample was 0.225 and this increased to 0.399 when measured at the exit of the TGA. This is similar to the results for the corresponding coals but the effect is much smaller. This is consistent with the HCN released being converted to NO in the gas phase. Reactive species released during temperature programmed coal combustion, for example, COS, are not observed when gas sampling is carried out at the exit of the TGA.

The temperature programmed combustion evolved gas profiles for vitrinite (density 1.2 - 1.27 g cm⁻³) and fusinite (density 1.5 - 1.60 g cm⁻³) with gas sampling directly above the sample and at the exit of the TGA are given in Figure 3. As expected the vitrinite profiles are very similar to those obtained for raw coals with a pronounced shoulder on the low temperature side of the evolved gas profile. The corresponding CO and CO₂ profiles for the fusinite are more complex consisting of several peaks and reach a maximum at a higher temperature than the vitrinite fraction as expected from the lower reactivity of the inertinite fraction. This is observed when gas sampling is carried out at both directly above the sample and at the exit of the TGA. The observation that the CO and CO₂ evolved gas profiles of the fusinite are more complex than the profiles of the vitrinite fraction may be due to a number of factors. The samples were prepared by the DGC and it may be that different types of inertinite fraction are being resolved in the temperature programmed combustion. Also, higher concentrations of mineral matter were observed in the fusinite fraction and this may give rise to catalytic gasification effects. The NO evolved gas profile for the fusinite showed a peak at ~300°C followed by profile in the char gasification region which could be resolved into three peaks with similar temperatures to the CO and CO₂ profiles. The m/z 27 (mainly HCN) evolved gas profiles for gas sampling directly above the sample for the vitrinite and fusinite are both bimodal but these peaks virtually disappear when sampling is carried out at the exit of the TGA. It is surprising that the m/z 27 peaks occur at a higher temperature in the vitrinite concentrate than the fusinite. This may indicate structural differences. The m/z 14 peak is also bimodal when gas sampling is carried out directly above the sample. The high temperature peak in the profile is also observed when gas sampling is carried out at the exit of the TGA. This suggests that this peak is due to nitrogen.

The integrated gas concentration ratios for some of the species evolved in the temperature programmed combustion of the macerals are given in Table 2. A comparison of gas concentration ratios obtained when sampling directly above the sample and at the exit of the TGA shows similar trends to those observed for the raw coals. It is evident from the CO/CO₂ ratio that substantial amounts of CO formed in the combustion are converted in the gas phase to CO₂. Similarly a comparison of the two sampling positions indicates that the NO/N ratio is higher while the (m/z 27)/N *i.e.* mainly HCN/N, was virtually absent when gas sampling is carried out at the exit of the TGA. This is most probably due to the conversion of HCN and other nitrogen containing species to NO in the gas phase and is similar to the results obtained for the coals.

Discussion

Temperature programmed combustion is a useful technique for studying the release of nitrogen and sulphur species during the combustion of coals and chars. The evolved gas profiles have the following general characteristics [7, 8, 13-16].

1. For coals, there is a shoulder on the low temperature side of the CO and CO₂ evolved gas profiles for the coals. This shoulder corresponds to the release of low molecular mass species and tars and it is absent in the corresponding evolved gas profiles of the chars.
2. The release of NO and HCN during temperature programmed combustion is complex with several peaks. For low rank coals the NO peak is observed for the release of volatiles and the gasification of the char. The latter is sometimes asymmetric consisting of a number of peaks.

3. The NO profiles for the chars are delayed relative to the CO and CO₂ profile. The NO profiles always reach a maximum at a higher temperature than the corresponding CO₂ profiles. As a result the NO/CO₂ and NO/CO profiles usually increase with increasing burn-off. The NO/CO and NO/CO₂ ratios tend to decrease in the region where volatiles are released from the coals.

In this study, two gas sampling positions have been used: 1) ~1 cm above the sample and 2) at the exit of the thermogravimetric analyser. The results of this study show that reactive intermediate species can be detected by sampling close to the sample undergoing combustion. Some of the reactive species which have been identified are COS, (CN)₂, HCN and CO as well as hydrocarbon species. These species are either not detected or are observed in very much lower concentrations for sampling at the exit of the TGA. These studies have shown that under temperature programmed conditions there are a number of well defined stages which can be assigned to the release of low molecular mass gases, tars and combustion products and char gasification. Therefore the thermogravimetric analyser - mass spectrometer allows the extent of gas phase reactions to be assessed. In comparison, pyrolysis studies can also be carried out under temperature programmed conditions.

Previous temperature programmed combustion studies [6-9, 13-16] of a suite of coals and chars covering a wide range of rank have shown that the fraction of coal/char nitrogen converted to NO decreases with increasing reactivity. These studies were carried out with the gas sampling directly above the sample. In the case of the coals, substantial amounts of HCN were detected and if this were assumed to be converted to NO this would modify the trend for conversion of the coal nitrogen to NO for gas sampling at that position. In these studies the suite of coals studied covered a range of reactivities. Therefore the nitrogen species are released over the different temperature ranges. The release of the NO may vary with temperature and this may be a factor which influences the observed trend. Isothermal reactivity studies have also shown that a similar correlation exists [16] between char reactivity and the fraction of char nitrogen converted to NO. Hence it is apparent from the trends that gas sampling of the temperature programmed combustion of the coals allows reactive nitrogen species to be detected and that the NO release is similar to that for the char. The results of a more detailed investigation show that a range of reactive species can be detected.

Conclusions

The use of temperature programmed combustion for studying the release of reactive intermediate species from coal has been investigated. It is apparent that a comparison of gas sampling carried out directly above the sample and at the exit of the TGA shows that reactive species can be detected. Species detected include CO, COS, HCN, (CN)₂. The conversion of the nitrogen intermediate species to NO has been followed by the technique. It is apparent that temperature programmed combustion is a useful technique for following the release of nitrogen and sulphur during coal and char combustion.

Acknowledgements

The authors would like to thank SERC for support under Grant No.GR/J 12161

References

1. Laurendeau N.M.,
Prog. in Energy and Combustion Science, 4, 221-270, 1978.
2. Phong-Anant D., Wibberley L.J. and Wail T.F.,
Combustion and Flame, 62, 21, 1985.
3. Shimizu T., Sazawa Y., Adschin T. and Furusawa T.,
Fuel 71, 361, 1992.
4. Pels J.R., Wojtowicz M.A. and Moulijn J.A.,
Fuel 72, 373, 1993.
5. Gavin D.G. and Dorrington M.D.,
Fuel 72, 381, 1993.
6. Crelling J.C., Thomas K.M. and Marsh H.,
Fuel 72, 359, 1993.
7. Crelling J.C., Thomas K.M. and Marsh H.,
Ironmaking Proceedings-Iron and Steel Society of AIME, 51, 407-413, 1992.
8. Hindmarsh C.J., Wang W.X., Thomas K.M. and Crelling J.C.,
Fuel (in press).
9. Crelling J.C. and Thomas K.M.,
Abstracts of Papers of the American Chemical Society, 207, p. 3, 1994.
10. Dyrkacz G., Blomquist C. and Ruscic L.,
Fuel 63, 1367, 1984.
11. Dyrkacz G., Blomquist C. and Horwitz P.,
Sep. Sci. Technol. 16, 1571, 1981.
12. Dyrkacz G. and Horwitz P.,
Fuel 61, 3, 1982.
13. Brown S.D. and Thomas K.M.,
Fuel 72, 359, 1993.
14. Wang W.X., Brown S.D., Thomas K.M. and Crelling J.C.,
Fuel 73, 341, 1994.
15. Wang W.X., Brown S.D., C.J. Hindmarsh, A.I. Gonzalez de Andres
and Thomas K.M.,
Proc Int. Conf. Coal Sci., Banff, Canada 2, 144, 1993.
16. Gonzalez de Andres A.I. and Thomas K.M.,
Fuel 73, 635, 1994.
17. Brown S.D., Wang W.X. and Thomas K.M.,
(Unpublished results).

Table 1 Characterisation data for the coal, char, and maceral concentrates.

Coal/ Maceral	Illinois No6 (APCS) Coal	Illinois No6 (APCS) Char	Coal A Vitrinite	Coal A Fusinite
Proximate Analysis				
Volatile Matter (daf)/ %	47.39	4.43	41.97	35.76
Ash (dry)/ %	15.48	29.84	1.21	31.26
Elemental Analysis				
C (daf)/ %	77.67	99.63	82.57	79.01
H (daf)/ %	5.00	0.67	5.28	4.25
N (daf)/ %	1.37	1.82	1.72	0.83
O (daf)/ %	13.51		12.16	15.68
Random Relectance/ %	0.43	0.43	0.65	0.65
Maceral Analysis				
Vitrinite/ %	85.00			
Liptinite/ %	5.00			
Inertinite/ %	10.00			
Minerals/ %	18.10			

Table 2 Temperature programmed combustion evolved gas concentration ratios

Sample	CO/ CO ₂	NO/ N	HCN/ N
Illinois No6 (APCS) Coal			
-Above the Sample	0.535	0.362	0.209
-At the Exit	0.096	0.961	0.036
Illinois No6 (APCS) Char			
-Above the Sample	0.355	0.225	0.096
-At the Exit	0.076	0.399	0.016
Coal A Vitrinite Concentrate			
-Above the Sample	0.606	0.356	0.167
-At the Exit	0.067	0.546	0.025
Coal A Fusinite Concentrate			
-Above the Sample	0.314	0.797	0.325
-At the Exit	0.082	0.893	0.053

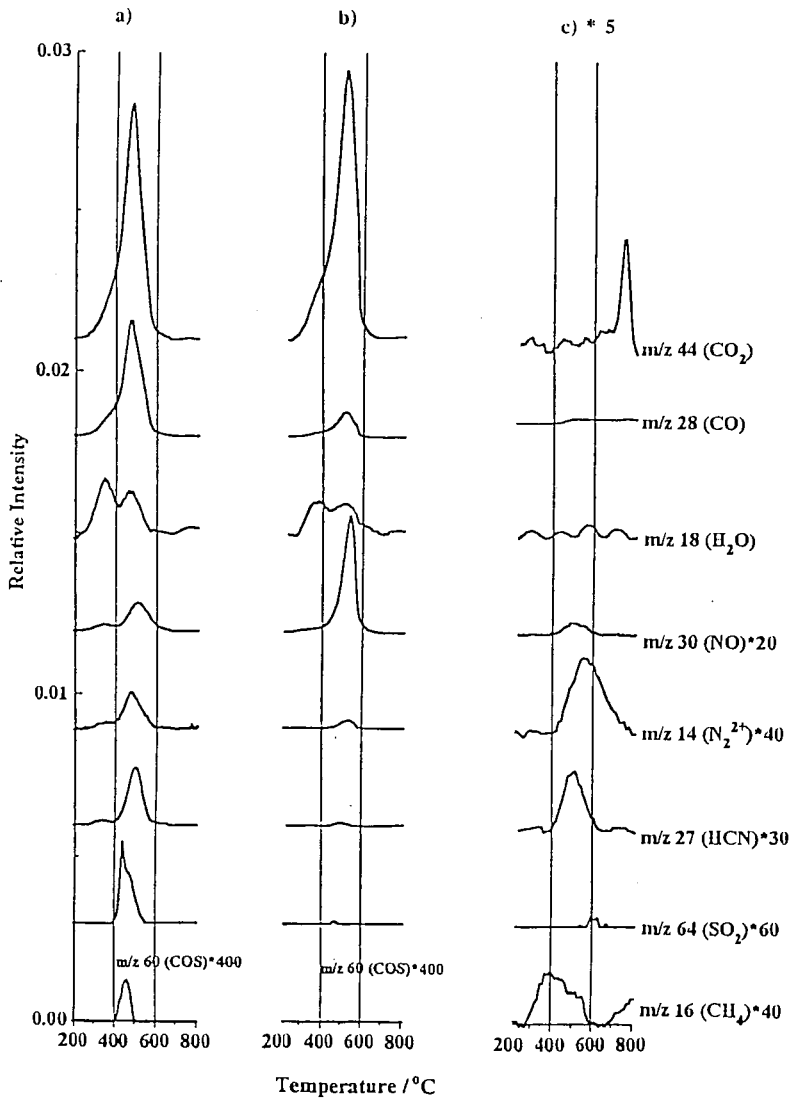


Figure 1 Temperature programmed evolved gas profiles for Illinois No6 (Argonne) coal in a) 20% oxygen/ helium with gas sampling directly above the sample, b) in 20% oxygen/ helium with gas sampling at the exit of the thermogravimetric analyser and c) in argon with gas sampling at the exit of the thermogravimetric analyser.

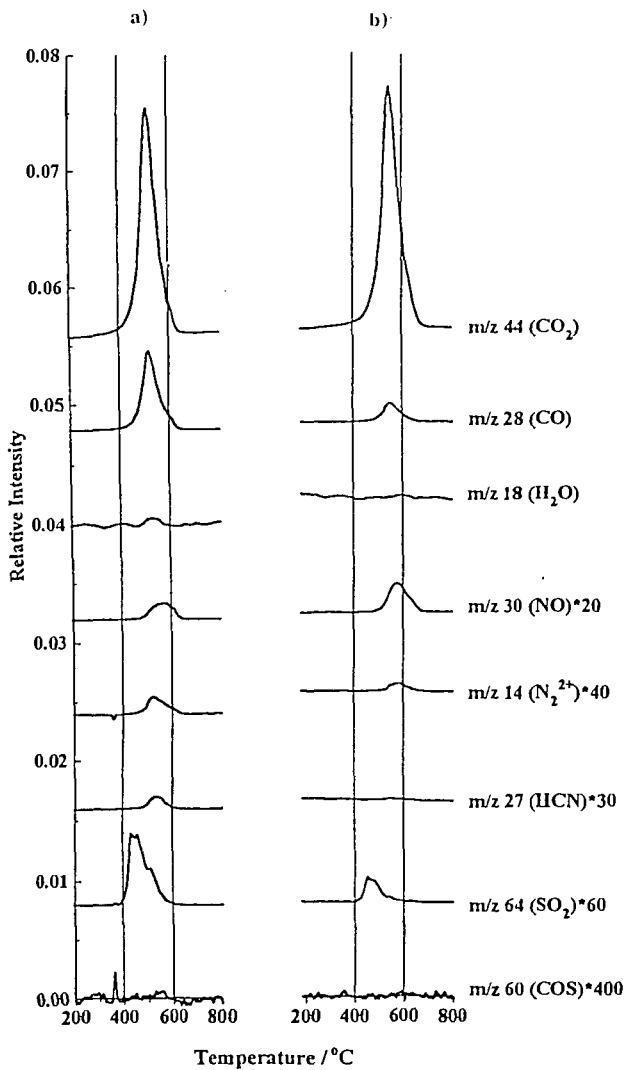


Figure 2 Temperature programmed combustion evolved gas profiles for Illinois No6 (Argonne) EFR char (HTT 1273 K) in 20 % oxygen/helium with gas sampling a) directly above the sample and b) at the exit of the thermogravimetric analyser.

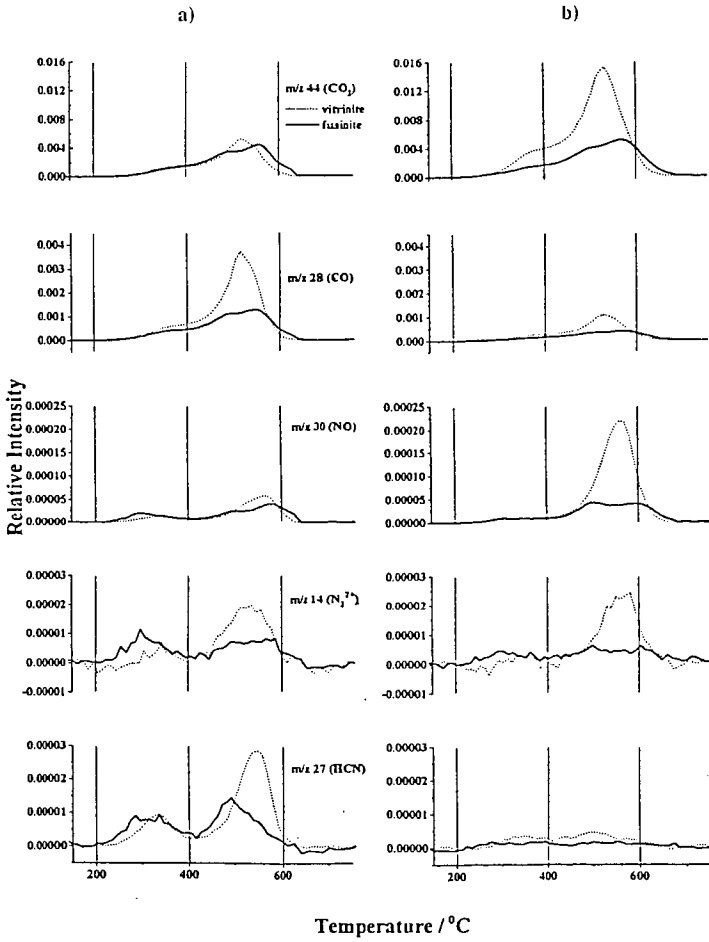


Figure 3 Temperature programmed combustion evolved gas profiles for maceral concentrates derived from coal A in 20 % oxygen/ helium with gas sampling a) directly above the sample and b) at the exit of the thermogravimetric analyser.

THE CHEMISTRY OF SULFUR DURING HYDROPYROLYSIS OF COALS

M. L. Gorbaty, S. R. Kelemen, S. N. Vaughn, M. Sansone, P. J. Kwiatek

Exxon Research and Engineering Company
Annandale, NJ 08801

G. N. George

Stanford Synchrotron Radiation Laboratory
Stanford, CA 94309

Keywords: Sulfur, XANES, XPS, Hydropyrolysis

Sulfur K-edge X-Ray Absorption Near Edge Structure Spectroscopy (XANES) and sulfur 2p X-Ray Photoelectron Spectroscopy have been used to identify organically bound sulfur forms in coals (1-3), and to follow the chemistry of organic sulfur during various treatments including mild oxidation (4), pyrolysis (5-7) and chemical reductions (8). This paper focuses on the changes which take place with organically bound sulfur functionalities in coals of various ranks when they are subjected to hydropyrolysis conditions. Data from both X-Ray techniques and temperature programmed decomposition-mass spectrometry were used in tandem.

Experimental Section

Most coal samples used in this study were obtained from the Argonne Premium Coal Program (9). The sample of Rasa coal was obtained from Dr. C. M. White of PETC. The procedures for obtaining and interpreting XPS and XANES spectra of coals have been reported and discussed previously (1, 2). XPS spectra were obtained on a Vacuum Generators (VG) ESCA lab system using Mg K_{α} non-monochromatic radiation using a five channel detection system. XANES spectra were recorded at the National Synchrotron Light Source at Brookhaven National Laboratory on beam line X-10C. Fluorescence spectra were recorded using a Stern-Heald-Lytle detector. Hydropyrolysis char thermal reactivity data were obtained using a temperature programmed decomposition (TPD) apparatus, the design and use of which are described elsewhere (5, 6). Samples were heated under ultrahigh vacuum from room temperature to 750 °C at a rate of 0.5 °C/s, while the off gases were monitored by a mass spectrometer. Hydropyrolysis experiments were carried out in a closed reactor pressurized at room temperature to 70 atm with a 95% hydrogen - 5% helium gas mixture. Pyrolysis was done in helium, at 1 atm in a quartz lined reactor (5). For pyrolysis experiments, the samples were heated at a linear heating rate of 0.5 °C/s to 400 °C followed by holding at that temperature for 5 minutes. The reactor temperature program for hydropyrolysis was similar except that the maximum temperature was 427 °C and the samples were held for 30 minutes under isothermal conditions. Samples were analyzed after the linear heatup and isothermal stages. These kinetic conditions favored the retention of coal liquid products in the pyrolysis and hydropyrolysis residues.

Results and Discussion

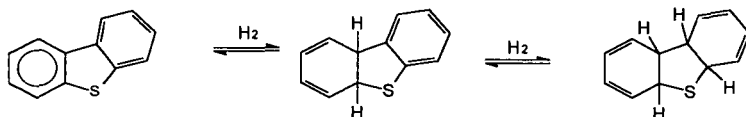
The coals were subjected to hydropyrolysis conditions and the hydropyrolysis residues were collected and examined by elemental analysis to determine sulfur loss, by XPS and XANES to determine the forms of bound sulfur remaining, and by TPD to determine the thermal reactivity of the residues. Table 1 shows the sulfur to carbon atomic ratios for samples of starting Rasa and Illinois No. 6 coals, as well as those for the residues from heating to 400 °C under helium pyrolysis and hydropyrolysis after heating to 427 °C as determined from bulk elemental analysis and from XPS by integration of the areas for sulfur and carbon (1). The bulk and XPS elemental analyses are in good agreement for Rasa coal, which contains virtually no pyrite, and are not in agreement for Illinois No. 6. The discrepancy between the bulk elemental and XPS data for Illinois No. 6 coal is due to the fact that the surface concentration of pyrite and its oxidation products are different on this coal's surface relative to that in the bulk(10). However, both analyses indicate that more sulfur was lost during hydropyrolysis than pyrolysis under nitrogen. The bulk elemental analyses indicate that about 22% of the sulfur was lost from Rasa and 32% from Illinois No. 6 under these hydropyrolysis conditions. XPS sulfur 2p spectra of the 427 °C hydropyrolysis residues from Rasa and Illinois No. 6 coal are shown in Figure 1. Included in the figure are the actual spectra and the curve resolved aromatic and aliphatic sulfur components. The results of the curve resolution analysis (1, 2) of these

spectra are shown in Table 2. The table shows the XPS results for aliphatic sulfur for the initial coals, hydroxyprolysis residues obtained at 200, 350 and 427 °C, and previously obtained data (5) on helium pyrolysis chars. The results indicate that the hydroxyprolysis chars contain the same ratio of aliphatic to aromatic sulfur as the starting coals, and considerably more than that contained in the pyrolysis residues. XANES data on the same samples confirm these findings. In addition, the feature attributed to pyrite in the fresh Illinois No. 6 coal and its 200 °C hydroxyprolysis residue largely disappears in the 350 °C residues and is replaced by a feature attributed to pyrrhotite.

The effect of temperature on the reactivity of bound sulfur on the hydroxyprolysis residues was examined by TPD. Traces of the relative intensities of the $m/e = 34$ mass spectra of the initial Rasa and Illinois No. 6 coals and their hydroxyprolysis residues prepared at 200, 350 and 427 °C are plotted as a function of temperature in Figure 2. These were normalized so that the data for a given coal appear on the same relative intensity scale. Up to 350 °C, Rasa coal continues to evolve H_2S , but at 427 °C the amount released is considerably diminished. The TPD traces for fresh Illinois No. 6 coal and its 200 °C hydroxyprolysis residue show evolution of H_2S from both aliphatic sulfur and pyrite, but the total amount of H_2S released from the 350 °C residue is diminished, and that from pyrite is virtually gone. There is even less H_2S evolution from the 427 °C hydroxyprolysis residue.

Taken together the data present an apparent discrepancy. It is known that on pyrolysis in an inert environment at 400 °C, aliphatic sulfur is lost from the coal as H_2S (5, 6). Aromatic sulfur does not evolve at these temperatures (11). Somewhat more sulfur is lost during hydroxyprolysis than pyrolysis, but the differences are not great. TPD data indicate that most of the reactive sulfur in the hydroxyprolysis residues had evolved at 427 °C. Nevertheless, XPS and XANES analyses indicate that the hydroxyprolysis residues contain about as much aliphatic sulfur as the starting coals; the ratio of aliphatic to aromatic sulfur is about the same, even though significant amounts of H_2S evolved during the hydroxyprolysis.

To account for these observations, we postulate that molecules containing aromatic sulfur forms are partially hydrogenated under hydroxyprolysis conditions as follows:



To the XPS and XANES probes, the sulfur in the hydrogenated molecules appear as aliphatic sulfurs. However, during heating, carbon sulfur bonds are not cleaved; rather the molecules lose hydrogen to regain their aromaticity.

Conclusions

Unlike pyrolysis under inert gas, pyrite in coals is converted to pyrrhotite during hydroxyprolysis, and significant quantities of aliphatic sulfur are detected in the residues. It is believed that these aliphatic sulfur forms result from partial hydrogenation of aromatic sulfur species. While these sulfur species appear to be aliphatic to the X-ray probes, they are not, and do not behave thermally as aliphatic species.

References

- Kelemen, S. R.; Gorbaty, M. L.; George, G. N. *Fuel*, **1990**, *69*, 939, 945.
- George, G. N.; Gorbaty, M. L.; Kelemen, S. R.; Sansone, M. *Energy Fuels*, **1991**, *5*, 93.
- Huffman, G. P.; Mitra, S.; Huggins, F. E.; Shah, N.; Vaidya, S.; Lu, F. *Energy Fuels*, **1991**, *5*, 574.
- Gorbaty, M. L.; Kelemen, S. R.; George, G. N.; Kwiatek, P. J. *Fuel*, **1992**, *71*, 1255.
- Kelemen, S. R.; Gorbaty, M. L.; George, G. N.; Kwiatek P. J.; Sansone, M. *Fuel*, **1991**, *70*, 396.

6. Kelemen, S. R.; Vaughn, S. N.; Gorbaty, M. L.; Kwiatek, P. J. *Fuel*, **1993**, 72, 645.
7. Taghiei, M. M.; Huggins, F. E.; Shah, N.; Huffman, G. P. *Energy Fuels*, **1992**, 6, 293.
8. Chatterjee, K.; Stock, L. M.; Gorbaty, M. L.; George, G. N.; Kelemen, S. R. *Energy Fuels*, **1991**, 5, 773.
9. Vorres, K. *Energy Fuels*, **1990**, 4, 420.
10. Kelemen, S. R.; Gorbaty, M. L.; George, G. N.; Kwiatek, P. J. *Energy Fuels*, **1991**, 5, 720.
11. Calkins, W.H.; Torres-Ordonez, R. J.; Jung, B.; Gorbaty, M. L.; George, G. N.; Kelemen, S. R. *Energy Fuels*, **1992**, 6, 411.

TABLE 1

<u>RASA</u>	SULFUR/CARBON ATOM RATIO (x100)	
	<u>XPS</u>	<u>BULK</u>
INITIAL	6.20	6.10
PYROLYSIS	4.70	5.30
HYDROLYSIS	4.51	4.82
<u>ILLINOIS #6</u>		
INITIAL	1.25	2.32
PYROLYSIS	0.98	2.25
HYDROLYSIS	0.96	1.58

TABLE 2

	XPS MOLE PERCENT SULFIDIC SULFUR	
	<u>RASA</u>	<u>ILLINOIS #6</u>
INITIAL	26	29
HYDROLYSIS (200 °C)	25	30
HYDROLYSIS (350 °C)	26	--
HYDROLYSIS (427 °C)	25	26
PYROLYSIS (400 °C)	8	13

FIGURE 1

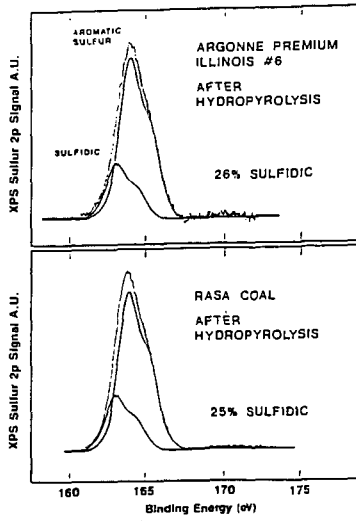
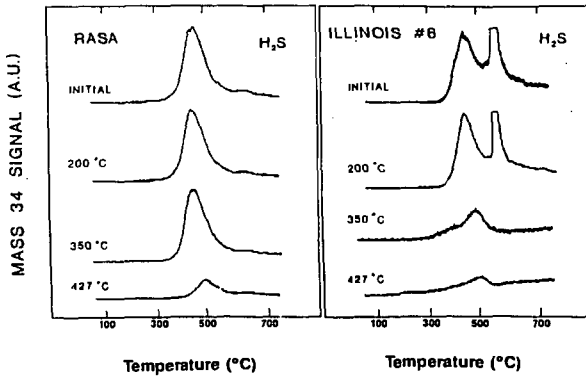


FIGURE 2



REMOVAL AND RECOVERY OF NITROGEN AND SULFUR COMPOUNDS
FROM COAL TAR FRACTIONS USING SUPPORTED ALUMINIUM
SULFATE UNDER SUPERCRITICAL CO₂ CONDITIONS

Kinya Sakanishi, Hiroaki Obata, Isao Mochida*, and Tsuyoshi Sakaki¹⁾

Institute of Advanced Material Study, Kyushu University,

Kasuga, Fukuoka 816, Japan

²⁾ Kyushu National Industrial Research Institute,

Tosu, Saga 841, Japan

Keywords: Recovery of nitrogen compounds, Supported aluminium sulfate, Supercritical CO₂

ABSTRACT

Removal and recovery of nitrogen and sulfur compounds from coal tar fractions such as crude naphthalene and methylnaphthalene oils are examined using 10 wt% Al₂(SO₄)₃/SiO₂ as a solid acid under atmospheric or supercritical CO₂ (50°C, 80 atm) conditions. Repeated use of the solid acid is achieved by purging adsorbed nitrogen compounds with higher pressure (150 atm) CO₂ and methanol as an entrainer solvent, recovering effectively quinoline bases as well as purifying methylnaphthalenes.

Benzo[thiophene] (BT) is dimerized over Al₂(SO₄)₃/SiO₂ catalyst under supercritical CO₂ conditions in order to separate BT from crude naphthalene as well as to purify naphthalene. BT was more selectively dimerized under supercritical CO₂ conditions (100°C, 100 atm) than in atmospheric n-octane solution at 100°C, allowing its selective dimerization and adsorption on the solid acid with selective extraction of naphthalene.

Effects of supercritical CO₂ conditions on the above adsorptions and reactions are discussed based on the analysis of recovered fractions and products.

INTRODUCTION

Crude methylnaphthalene oil (CMNO) is prepared as a residue of naphthalene oil (b. p. 210~260°C) of coal tar after the recovery of crude naphthalene.¹⁾ CMNO is further extracted with sulfuric acid and then neutralized with alkali to recover basic quinoline oil.^{2,3)} However, because of the consumption of both acid and base as well as sludge formation, such a purification procedure appears no more feasible in the modern industry.⁴⁾

The present authors have reported that a consecutive solvent extraction with first methanol and then hexane concentrates the pyrroles and phenols in the hexane insoluble-methanol soluble fraction (HI-MS).⁵⁾ Major basic nitrogen species staying in the methanol insoluble fraction (MI) are captured and recovered by adsorption and desorption, using nickel sulfate.⁶⁻⁸⁾ The sulfate is known acidic and neutral, respectively, when it is dehydrated or rehydrated.⁹⁾ High dispersion and proper heat-treatment of the sulfate increase the number and strength of acidic sites by supporting on silica gel for larger capacity against the adsorption of basic nitrogen compounds.^{7,8)}

The present authors succeeded in removing nitrogen compounds from CMNO and recovering them in concentrated form using aluminium sulfate on silica gel as the adsorbent.¹⁰⁾ The supporting on silica gel disperses the sulfate on the surface, increasing the acidic strength and number of acidic sites. Hence, the surface which can get access to quinoline bases is essential as the support, larger pores being preferable. It was also reported that non-polar and poor solvents such as hexane and pentane appear to behave as an anti-solvent to expel the polar as well as basic compounds in methylnaphthalenes onto the adsorbent. Poorer solvents such as supercritical propane and carbon dioxide appear attractive.

In the present study, the removal and recovery of nitrogen compounds in crude methylnaphthalene oil (CMNO) obtained from coal tar were investigated using Al₂(SO₄)₃, more acidic than NiSO₄, supported on silica gel to obtain highly denitrogenated CMNO as well as to recover

basic quinoline bases under atmospheric or supercritical CO₂ conditions.

Crude naphthalene is commercially purified by hydrotreatments to remove nitrogen and sulfur compounds, however these heterocyclic compounds such as indole and benzothiophene could be used as valuable chemicals and medicines if they could be recovered. In the present study, recovery of benzothiophene(BT) was also examined using the Al₂(SO₄)₃ catalyst by designing the selective dimerization of BT with extraction of purified naphthalene followed by BT de-dimerization under the supercritical CO₂ conditions.

EXPERIMENTAL

Aluminium sulfate(10 wt%) was supported by impregnation from aqueous solution on silica gel of MB-4B provided by Fuji-Davison Chemical Ltd. The surface area and mean pore diameter of the silica gel were 500 m²/g and 64 Å, respectively. The adsorbent was calcined at 350°C for 4 h in air.

Model methylnaphthalene oil (quinoline:Q 8wt%, isoquinoline:IQ 8wt%, 1- and 2-methylnaphthalenes: 1- and 2-MN 42wt% each) was prepared for the supercritical extraction experiments. Figure 1 shows the supercritical CO₂ extraction apparatus used in the present study. The model feed was charged to extraction vessel, and supercritical CO₂ (50°C, 80 atm) was flowed at 6 l/min to carry the feed to the fixed bed column filled with the Al₂(SO₄)₃ adsorbent. After the adsorbent was saturated with nitrogen compounds, higher pressure CO₂ and then methanol was flowed to recover the adsorbed species and to regenerate the adsorbent for its repeated use. The eluted and recovered fractions were analyzed and quantified by GC-FID (50 m capillary OV-101 column, 110°C).

Benzothiophene(BT) in crude naphthalene was extracted and dimerized using several catalysts in atmospheric hexane and octane, respectively or supercritical CO₂ solvent at 100°C for 3 h in order to separate BT from naphthalene. The fractionated and reaction products were analyzed by the elemental analysis, LC and FD-MS.

RESULTS AND DISCUSSIONS

Removal and Recovery of Quinolines from Model Methylnaphthalene Oil

Figure 2 shows the elution profile of the model methylnaphthalene oil using 10 wt% Al₂(SO₄)₃/SiO₂ as an adsorbent in the fixed bed apparatus under supercritical CO₂ conditions. No nitrogen compounds were eluted until the extraction time of 120min, only denitrogenated methylnaphthalenes being recovered at the separation vessel. At the extraction time of 220 min when the adsorbed compounds were hardly extracted, CO₂ was pressurized upto 150 atm which was kept for 60 min to recover the adsorbates, and then methanol was added to CO₂ flow as an entrainer, almost all the adsorbed nitrogen compounds being desorbed and recovered from the adsorbent.

Figure 3 illustrates the elution curve of each compound in the model methylnaphthalene feed, where the elution conditions are same as Figure 2. 62% of methylnaphthalenes in the feed was recovered without nitrogen compounds, in other words, quinoline and isoquinoline were not eluted until about 60% of the feed was eluted. The activity of the adsorbent in the repeated adsorption/desorption cycle is shown in Figure 4. The adsorption capacity of 10wt% Al₂(SO₄)₃/SiO₂ was restored to almost the same level of the first run in the second run by purging almost completely the remaining adsorbates which consist mainly of nitrogen compounds. The adsorption activity of the adsorbent was gradually decreased with the repetition number of the adsorption/desorption cycle, indicating that some deactivation of the adsorbent should take place during the adsorption/desorption repetition. More polar and/or dried entrainers may be very effective in achieving the complete recovery of nitrogen compounds without the deterioration of the adsorbent. Adsorbents should be designed in combination with eluting solvents for the completely reversible adsorption/desorption performances.

Removal of Benzothiophene from Crude Naphthalene

Table 1 summarizes the adsorption treatment of crude naphthalene with various adsorbents in

atmospheric n-hexane solution followed by filtration to recover hexane-eluted fraction and washing of the adsorbent with benzene to recover adsorbed compounds. Sulfur as well as nitrogen compounds were removed from crude naphthalene, purified naphthalene and hetero-atom compounds being concentrated in hexane and benzene eluates, respectively, although the sulfur removal was not so effective as the nitrogen removal, because the basicity of sulfur compounds is not so strong as nitrogen compounds.

Recovery scheme of purified naphthalene(Np) and benzothiophene(BT) under supercritical CO₂ conditions is illustrated in Figure 5. BT is selectively dimerized and adsorbed on solid acid catalyst, naphthalene being purified and recovered by extraction with supercritical CO₂. BT dimer may be converted to BT monomer at a higher temperature, BT being recovered by supercritical CO₂ extraction. Figures 6 and 7 show the FD-MS spectra of the oligomerization products from the reaction of BT with 10wt% Al₂(SO₄)₃/SiO₂ catalyst at 100°C for 3 h in atmospheric octane and supercritical CO₂ solvent, respectively. It is noted that BT is more selectively converted to its dimer in supercritical CO₂ solvent than in atmospheric octane solution, suggesting a remarkable solvent effect on the reactivity of BT and the selectivity to its dimer. Such a highly selective dimerization in supercritical CO₂ solvent was also observed in the oligomerization reaction of the mixture of BT and naphthalene under the same reaction conditions. More cross-oligomerization products between BT and naphthalene were produced in atmospheric octane solution at 100°C, suggesting that the supercritical CO₂ solvent may enhance the more preferable interaction of BT with the catalyst to that of naphthalene.

Reaction conditions including temperatures and pressures of dimerization and extraction, and catalyst should be further optimized to achieve more selective conversion to BT dimer and recovery of BT monomer after selective extraction of purified naphthalene.

REFERENCES

- 1 "Handbook of Aromatics and Tar Industry", Nihon Houkoushoku Kougyoukai, 1965, p.81 .
- 2 Japanese Patent 61-50942(1986).
- 3 Horita, Y., Togari, O., Komoto, T., Nakamura, M., Tanji, H., J. Petrol. Inst. Jpn., 1987, 30, 94.
- 4 Horita, Y., Komoto, T., Arioka, H., Nakamura, M., Tanji, H., J. Petrol. Inst. Jpn., 1987, 30, 149.
- 5 Fei, Y. Q., Sakanishi, K., Sun, Y. N., Yamashita, R., Mochida, I., Fuel, 1990, 69, 261.
- 6 Mochida, I., Fei, Y. Q., Sakanishi, K., Usuba, H. and Miura, K., Chem. Lett., 1990, 515.
- 7 Mochida, I., Sakanishi, K., Usuba, H. and Miura, K., Fuel, 1991, 70, 761.
- 8 Mochida, I., Fei, Y. Q., Sakanishi, K., Korai, Y., Usuba, H., Miura, K., Carbon, 1992, 30, 241.
- 9 Tanabe, K., Takeshita, T., "Acid-Base Catalysis", Sangyo Tosho Pub. Co., Ltd. (Tokyo), 1966.
- 10 Sakanishi, K., Sun, Y. N., Mochida, I., Usuba, H., Fuel Process. Technol., 1992, 32, 143.

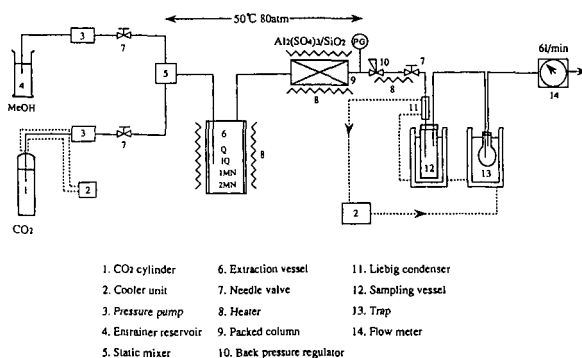


Fig 1 Supercritical CO₂ extraction apparatus

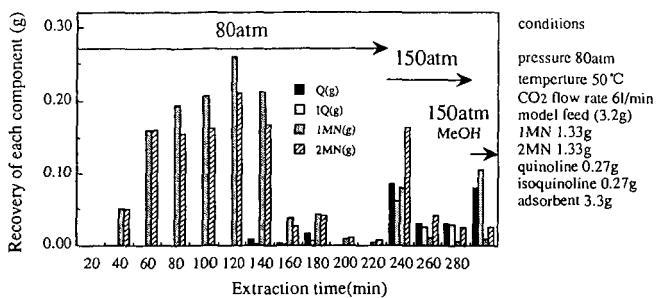


Fig2 Elution profile of model methylnaphthalene oil under supercritical CO₂ conditions

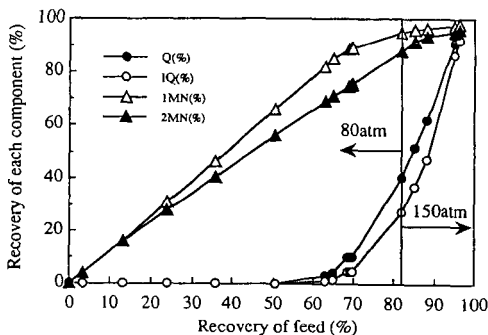


Fig3 Elution curve of each compound in the model methylnaphthalene oil under supercritical CO₂ extraction conditions (conditions; see Fig2)

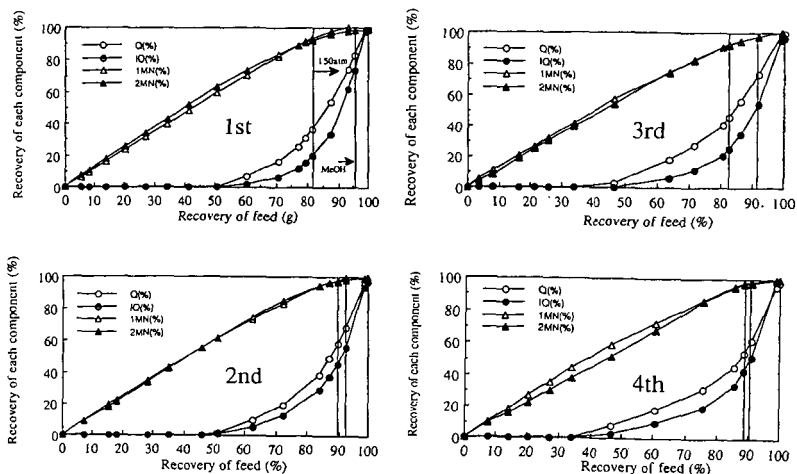


Fig 4 Repeated activity of the adsorbent for adsorption / desorption treatment of model methylnaphthalene oil under supercritical CO₂ conditions (conditions; 50 °C-80atm catalyst 2.3g)

Table 1 Adsorption treatment of crude naphthalene with various adsorbents in atmospheric hexane solution

Adsorbent	Eluting solvent	Recovery (wt%)	Elemental analysis	
			S(%)	N(ppm)
Original crude naphthalene		—	1.6	500
10%Al ₂ (SO ₄) ₃ /SiO ₂	hexane	91.0	1.0	50
	benzene	6.1	3.1	1700
reduced CoMo/Al ₂ O ₃	¹⁾ hexane	93.3	1.2	31
	benzene	4.3	5.6	—
reduced NiMo/Al ₂ O ₃	¹⁾ hexane	92.1	1.3	25
	benzene	6.4	4.2	—

1) Catalyst reduction pretreatment ; H₂ flow , 360°C·3h

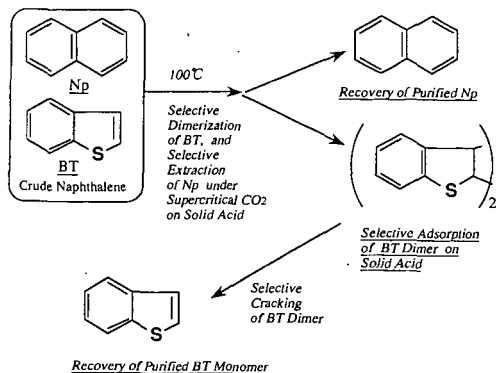


Fig 5 Recovery Scheme of Purified Np and BT through Selective Dimerization of BT and Extraction of Np under Supercritical CO₂ Conditions on Solid Acid Catalyst

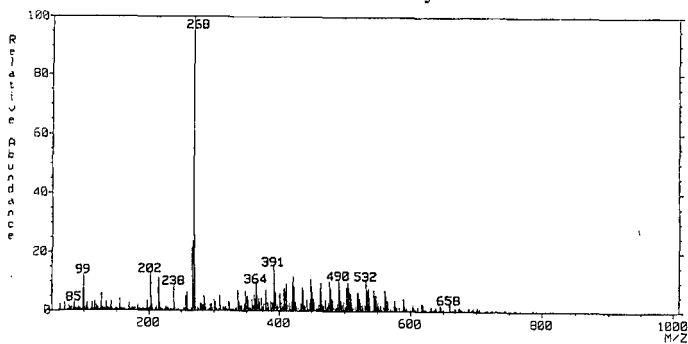


Fig6 FD-MS spectra of B.T oligomerization products conditions in atmospheric octane solution

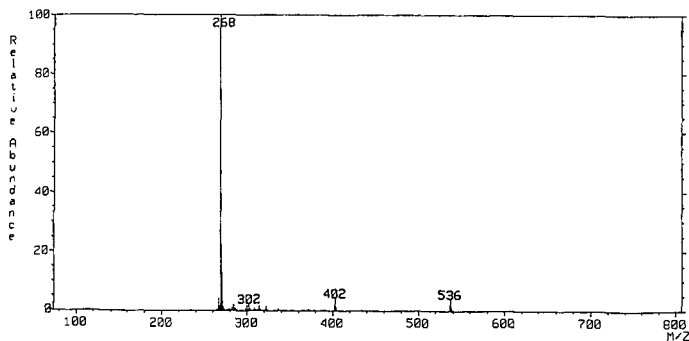


Fig 7 FD-MS spectrum of B.T oligomerization products under supercritical CO₂ conditions

CHARACTERIZATION OF NITROGENOUS COMPOUNDS IN DISTILLATES
DERIVED FROM TWO-STAGE COAL LIQUEFACTION

C. Bradley, R.E. Pauls, D.C. Cronauer and M.E. Bambacht
Amoco Research Center
P.O.Box 3011
Naperville, IL 60566-7011

Keywords: nitrogen compounds, coal liquids, GC/MS

INTRODUCTION

The nitrogen compounds in coal distillates have not been characterized as fully as the predominant hydrocarbon components, but are of considerable importance due to their adverse effect on fuel stability (1-3) and catalyst lifetime (4) and the potentially adverse health and environmental impact (5-7). A number of different classes of nitrogen compounds are commonly found in coal liquids (e.g. quinolines, indoles, carbazoles (7-10)). These each will affect catalyst deactivation and product stability to different extents.

This report specifically addresses the nature of nitrogen compounds found in Wilsonville streams. In the current study, gas chromatography with a nitrogen-selective detector (GC/N) and gas chromatography/mass spectrometric (GC/MS) techniques were employed to identify and quantitate the major nitrogen-containing components found in concentrates prepared from coal-derived distillates from two series of Wilsonville pilot plant runs. These runs were made with Illinois No. 6 and Wyodak Coals.

While direct GC/N analysis can be done on the whole, untreated distillate, the nitrogen detector is a poor identification tool. Therefore, GC/MS was necessary for compound identification. Consequently, pretreatment of the distillates to obtain N-rich fractions was a necessary step to minimize hydrocarbon interference in GC/MS analyses and allow more detailed examination of the nitrogen components in coal distillates. However, once a typical nitrogen profile has been characterized, GC/N should allow rapid quantitation of the nitrogen compounds in an untreated distillate.

EXPERIMENTAL

Samples

The coal-derived liquids were obtained from the Advanced Coal Liquefaction R & D Facility at Wilsonville, AL. The products from five runs were characterized, three from the liquefaction of Illinois No. 6 bituminous coal (runs 250D, 250H, and 251E) and two from Wyodak subbituminous coal (runs 251-IIB and 251-IIIB). Details of these coals and their processing are given in reference 11.

Samples from the Wilsonville product streams were obtained soon after the runs and stored in a cold room to avoid degradation. Product liquid blends were prepared just before experimentation and their elemental analyses are given in Table I.

Preparation of Nitrogen Concentrates

Nitrogen-containing concentrates were prepared in the following manner. Approximately 80g of coal liquid oil was added to twice that weight of 10% NaOH aqueous solution. The resulting oil and aqueous phases were separated; phenolics were extracted into the aqueous layer. Toluene was added to the oil layer which was added to Amberlyst-15 cation ion exchange resin in a ratio of 4:2:1 of toluene:raffinate:resin, respectively. After three days of gentle mixing, the "OH, N-free" oil was recovered by filtration.

The resin was flushed with pentane and dried in a stream of N₂ at ambient temperature. It was then contacted with methanol saturated with NH₃ to recover the concentrates. About 70% of the methanol was gently stripped from these concentrates by rotary evaporation.

To confirm that essentially no organic nitrogen compounds remained on the resins after NH₃ treatment, resins from the 250D, 250H, and 251E treatments were treated with H₂SO₄. The recovered liquids were neutralized and extracted with CH₂Cl₂. These extracts contained no organic N-containing compounds. The samples of regenerated resin were checked for nitrogen content. The recovered

resins and a sample of fresh resin subjected to NH₃ and H₂SO₄ regeneration all contained nitrogen levels of 4.1 +/- 0.1%.

Chromatographic Separations and Component Identification

Detailed analytical experimental conditions for component separations and identification are given in Table II. Dichloromethane was used as the solvent for GC/MS. Methyl t-butyl ether was the solvent used in GC/N work because of severe peak tailing and detector response problems when dichloromethane was used.

Nitrogen Compound Quantification

The thermionic nitrogen detector (TID) for GC/N quantification work was calibrated using blends of pyridines, anilines, quinolines, indoles, carbazoles, and indoline. Each of these seven types of nitrogen compounds gives a different TID response. Therefore, seven different linear calibration equations were generated. Figure 1 shows a typical GC/N calibration plot and calibration equation of an aniline.

Based on the nitrogen components identified by GC/MS, the nitrogen components in a sample were grouped by types and quantitated using the calibration equations corresponding to the nitrogen types detected. Responses relative to 4-methylpyridine were determined for available model compounds as listed in Table III. As shown, the response factors for a given nitrogen compound type are similar but vary for different types of nitrogen compounds. For the majority of alkylated nitrogen components identified by GC/MS in the samples, we have no standards. Therefore, for a given nitrogen compound class, e.g. C₉-C₁₀ indoles, a single calibration equation based on the parent compound, e.g. indole, was used. There were several nitrogen components boiling above carbazole for which we had no standard whatsoever. In such cases, the peak area of these components were summed and the carbazole calibration equation used to quantitate them.

RESULTS AND DISCUSSION

Ion-Exchange

The A-15 resin adsorbed between 90 and 95% of the nitrogen compounds from the OH-free raffinate generated from the phenolics stripping step. Essentially no organic nitrogen compounds were retained in the A-15 resin after stripping with the ammonia/methanol solution.

Analytical Results

GC/MS was used to identify the nitrogen components in the nitrogen concentrates of the blends and to determine relative amounts of the various nitrogen components. Seven major types of nitrogen-containing compounds were detected in the bituminous coal liquid distillates--pyridines, anilines, quinolines, hydro-quinolines, indoles, indolines, and carbazoles. Four of these types (pyridines, anilines, hydroquinolines, and indoles) were the nitrogen classes in the subbituminous coal liquid distillates. Side-chains on the ring compounds ranged from C₁ through C₁₀ chains. The parent types of nitrogen compounds detected are shown in Figure 2.

The nitrogen compounds identified by GC/MS and quantitated by GC/N are grouped by classes in Table IV. This Table also shows boiling point data for representative nitrogen-containing compounds. Boiling points range from 300°F (C₂ pyridines) up to 700°F (carbazoles). The majority of the nitrogen compounds detected boiled in the 350-700°F range. In addition, the majority of the nitrogen compounds were alkyl substituted (designated herein by the total alkyl carbon number, e.g., C₂ pyridines).

Anilines (C₆-C₈) were the major nitrogen components in all blends, with the catalytic/catalytic run (251E) bituminous product having relatively more anilines and the subbituminous products having relatively fewer anilines than that of the other runs. Run 251E product also had fewer pyridines compared with that of the other runs. The levels of anilines found in the bituminous products are consistent with the fact that the first stage catalyst would increase the extent of hydrogenation and cracking of quinolines and multiple ring species to anilines. However, it was not anticipated that the level of anilines would be so high.

In addition to nitrogen species, GC/MS detected a number of aromatic hydrocarbons, primarily biphenyls, naphthalenes, anthracenes, phenanthrenes, and pyrenes in the nitrogen concentrates of all runs. These occurred because of non-specific adsorption onto the resin. The hydrocarbons accounted for about 30% of the total peak area of the GC/MS data. There was 1-2% phenolic material in the nitrogen concentrates of 250D and 250H (none detected in the 251E nitrogen concentrate).

Table V shows comparative quantitative GC/N and GC/MS data for the bituminous 251E coal liquid distillate. The data compare very well in spite of the semi-quantitative nature of GC/MS.

CONCLUSIONS

For the characterization of coal-derived distillates for nitrogen compound distribution, it is highly beneficial to concentrate a nitrogen-component rich fraction prior to analysis. Extraction of phenolics followed by ion-exchange to concentrate nitrogen compounds appears to work well for pyridines through carbazoles boiling up to about 700°F. Analysis by GC/MS and GC/N selective detection are the preferred techniques to obtain a distribution of the nitrogen components.

Data indicate that the nitrogen concentrates derived from IL No. 6 coal contain seven types of nitrogen ring structures: pyridines, anilines, quinolines, hydroquinolines, indoles, indolines, and carbazoles. Nitrogen concentrates from Wyodak sub-bituminous coal contain mostly pyridines, anilines, hydroquinolines, and indoles. Essentially all of the nitrogen compounds in both types of coal liquids are alkyl substituted. Sidechains on the aromatic rings are C₁ to C₁₀. It was not possible to determine if there was single attachment of longer alkyl chains or multiple attachment of short chains.

High levels of anilines are present, namely about 44% of the total nitrogen components detected in the bituminous coal liquids and 29% in the subbituminous coal liquids. Other investigators have reported anilines in coal-derived liquids (9,10,12). These anilines are presumably the result of the hydrogenation and opening of aromatic nitrogen-containing rings. Anilines should donate hydrogen during coal liquefaction; however, there is a high likelihood that the resulting product forms adducts quickly, thereby resulting in measurable retrogressive reactions. Most retrogressive products have high nitrogen content.

ACKNOWLEDGEMENTS

We are grateful to P. L. Baldwin for her extraction work, D. Parisi and E. G. Lesko who analyzed the samples, and W. H. Weber, J. M. Lee, and others at the Wilsonville facility who helped obtain the samples and operating data. We also acknowledge the funding of the Wilsonville facility by the DOE, The Electrical Research Institute, and Amoco Oil Company.

REFERENCES

1. Brown, F. R. and Karn, F. W., Fuel, 59, 431 (1980).
2. Ford, C. D., Holmes, S. A., Thompson, L. F. and Latham, D. R., Anal. Chem., 53, 831 (1981).
3. Drushel, H. V. and Sommers, A. L., Anal. Chem., 38, 19 (1966).
4. Hartung, G. K., and Jewell, D. M., Anal. Chem. Acta, 26, 514 (1962).
5. Guerin, M. R., Ho, C. H., Rao, T. K., Clark, B. R. and Epler, J. L., Environ. Res., 23, 42 (1980).
6. Lee, M. L., Novotny, M. V. and Bartle, K. D., Analytical Chemistry of Polycyclic Aromatic Compounds, Academic Press, N. Y. and London, 1981, Chp.3.
7. Schiller, J. E., Anal. Chem., 49, 2292 (1977).
8. Schweighardt, F. K., White, C. M., Friedman, S. and Schultz, J. L., Organic Chemistry of Coal, (Gould, F. R., ed.), ACS, Sec. No.71, ACS, Washington DC, 1978, Chp. 18.
9. Paudler, W. W. and Cheplen, M., Fuel, 58, 775 (1979).
10. Felice, L. J., Anal. Chem., 54, 869 (1982).
11. Puls, R. E., Bambacht, M. E., Bradley, C., Scheppelle, S. E. and Cronauer, D. C., Energy and Fuels, 4, 236 (1990).
12. Novotny, M., Komp, R., Merli, F., Todd, L. J., Anal. Chem., 52, 401 (1980).

TABLE I

Elemental Analyses of the Product Blends

Run No.	Carbon	Hydrogen	Nitrogen	Oxygen	Sulfur
250D	86.9	11.4	0.19	1.4	0.09
250H	87.2	11.6	0.13	1.4	0.17
251E	87.5	11.6	0.14	0.8	0.03
251-IIIB	85.7	11.3	0.31	2.60	0.06
251-IIIB	86.3	12.7	0.15	0.84	0.06

TABLE II

Analytical Operating Conditions

	GC/MS		GC/MS
GC Unit:	Varian 3700 with a Thermionic # detector (TID); 6.70 base current; 17 psig H ₂ ; 4.0V bias; 1.0E ⁻¹⁰ ation	GC Unit:	Varian 3500
Column:	60 m fused silica capillary, 0.25 mm i.d.	Column:	60 m fused silica capillary, 0.25 mm i.d.
Coating:	DB-1, 0.25 µm film	Coating:	DB-1, 0.25 µm film
Temperature:	50 to 300°C at 6°/min with a 20 min hold Injector: 300°C; Detector: 350°C	Temperature:	50 to 300°C at 6°/min with a 20 min hold (oven) Injector: 310°C
Carrier:	Helium (37 psig)	Carrier:	Helium (20 psig and 5 ml/min split)
Inlet Split Ratio:	60/1	Sample:	10 µg diluted with 250 µl of CH ₂ Cl ₂
Sampler:	0.2µl of the sample diluted 1:2 with N ₂ S	MS Unit:	PCLAB-2P
		Data System:	Data General Nova 3 with Kratos software
		Mass Resolution:	3000
		Source Temperature:	230°C
		Operational Mode:	Electron Impact
		Sample Rate:	0.5 sec/mass decade

TABLE III

Nitrogen Detector Response Factors

Component	TID Response relative to 4-methyl pyridine = 1.00
pyridine	1.01
2,4,6-trimethylpyridine	1.00
aniline	0.856
2,5-dimethylaniline	0.860
p-methylaniline	0.860
quinoline	0.962
2,4-dimethylquinoline	0.956
tetrahydroquinoline	0.974
indole	1.07
carbazole	0.849
indoline	1.03

TABLE IV
Nitrogen Compounds in Coal Liquids

Component	Boiling Range, °F ^a	WEX Component				
		Bituminous ^b			Subbituminous ^c	
		Run 230D	Run 230E	Run 231E	Run 251-11E	Run 251-11EB
Pyridine	239	0.0	0.0	0.0	0.0	0.0
C ₁ PF	230-300	0.4	1.0	0.0	1.8	1.1
C ₂ PF	303-340	1.4	2.1	0.4	4.2	1.6
C ₃ PF	342-373	1.7	2.0	1.0	3.7	1.6
C ₄ PF	370-393	1.3	1.0	0.4	1.9	4.9
C ₅ PF	400-420	0.0	0.0	0.0	0.6	1.6
Total Pyridines		4.8	6.1	1.8	13.2	10.8
Aniline	363	2.3	3.1	2.9	1.0	1.3
C ₁ An	376-390	7.4	11.0	8.0	2.5	2.7
C ₂ An	400-423	6.8	6.3	11.6	2.3	4.0
C ₃ An	435-470	4.9	4.0	7.4	3.7	4.3
C ₄ An	500-525	5.0	3.9	5.1	1.9	3.6
C ₅ An	529-530	2.0	0.6	0.6	0.6	0.8
C ₆ An	573-590	0.0	0.0	0.0	0.2	0.3
Total Anilines		28.6	29.1	33.6	12.4	17.2
Quinoline	462	0.0	0.0	0.0	0.0	0.0
C ₁ Q	478-498	1.3	1.4	0.1	0.0	0.0
C ₂ Q	513-560	0.3	0.2	0.4	0.0	0.0
C ₃ Q	576-597	0.7	0.7	0.7	0.0	0.0
C ₄ Q	572-593	0.4	0.8	0.1	0.0	0.0
C ₅ Q	607-635	0.0	0.0	0.0	0.0	0.0
C ₆ Q	640-671	0.0	0.0	0.0	0.0	0.0
C ₇ Q	673-690	1.2	0.1	0.1	0.0	0.0
C ₈ Q	685-700	1.2	0.0	0.0	0.0	0.0
Total Quinolines		5.3	3.2	1.4	0.0	0.0
Tetrahydroquinoline (THQ)	480	0.0	1.5	0.0	0.0	0.0
C ₁ THQ	483-489	3.4	3.3	1.9	0.7	1.1
C ₂ THQ	540-580	3.4	1.8	4.7	4.6	4.8
C ₃ THQ	546-585	1.3	0.3	1.6	3.3	4.8
C ₄ THQ	585-600	1.8	0.2	2.7	0.7	1.3
C ₅ THQ	590-613	0.0	0.0	0.0	0.1	0.3
Total THQs		9.9	7.3	10.9	10.4	12.2
Indole	489	0.0	0.0	0.0	0.0	0.0
C ₁ Indole	530-530	0.3	0.0	0.7	0.3	1.1
C ₂ Indole	563-570	0.5	0.6	1.1	1.4	2.1
C ₃ Indole	563-583	0.0	0.0	0.0	1.3	1.6
C ₄ Indole	570-590	0.0	0.0	0.0	0.3	0.3
C ₅ Indole	573-613	2.9	1.7	4.6	2.1	1.3
C ₆ Indole	617-636	6.4	3.9	4.9	2.1	0.8
C ₇ Indole	640-660	3.0	0.7	1.7	1.2	0.3
C ₈ Indole	670-680	0.7	0.0	0.3	0.1	0.0
C ₉ Indole	673-689	0.0	0.0	0.0	0.7	0.0
C ₁₀ Indole	680-693	0.0	0.0	0.0	0.3	0.0
Total Indoles		14.0	8.9	13.3	10.9	7.4
Indoline	466	0.0	0.0	0.0	0.0	0.0
C ₁ Indoline	514-540	0.0	0.3	0.0	0.0	0.0
C ₂ Indoline	540-563	0.0	0.0	0.2	0.0	0.0
C ₃ Indoline	563-580	0.0	1.3	0.0	0.0	0.0
C ₄ Indoline	570-590	0.0	0.1	0.0	0.0	0.0
Total Indoline		0.0	1.9	0.2	0.0	0.0
Carbazole	671	0.4	0.7	0.9	0.1	0.0
C ₁ C	643-670	1.3	1.3	1.0	0.9	0.0
C ₂ C	680-690	0.0	0.0	0.0	0.3	0.0
C ₃ C	673-700	0.0	0.0	0.1	0.4	0.0
Total Carbazoles		1.9	2.2	2.0	1.7	0.0
Tetrahydrocarbazoles	617-690	0.8	0.4	0.4	1.8	0.3
Phenylisoquinoline	520-535	2.0	4.0	2.9	0.0	0.0
Methylisoquinoline	480-530	0.9	0.2	0.3	0.0	0.0
C ₂ diphenylamine	630-630	1.3	0.1	0.3	0.0	0.0
C ₃ diphenylamine	630-670	0.0	0.0	0.2	0.0	0.0
Other H compounds ^d		4.0	3.2	1.6	0.0	0.0
Total Misc. H		9.0	7.9	5.7	1.8	0.3

^a estimated boiling ranges for alkylated compounds
^b CC/N quantitation
^c CC/MS quantitation
^d N.W. 193 and 209

TABLE V
Comparison of GC/N and GC/MS Quantitation

Nitrogen Component	Run 251E, % Components	
	GC/N	GC/MS
C ₁ -C ₄ pyridines	1.8	1.9
C ₀ -C ₅ anilines	35.6	36.5
C ₁ -C ₇ quinolines	1.5	1.6
C ₁ -C ₄ THQs	10.9	11.0
C ₁ -C ₈ indoles	13.3	12.9
C ₂ indolines	0.2	0.4
C ₀ -C ₃ carbazoles	2.0	2.0

Figure 1

A GC/N Calibration Plot

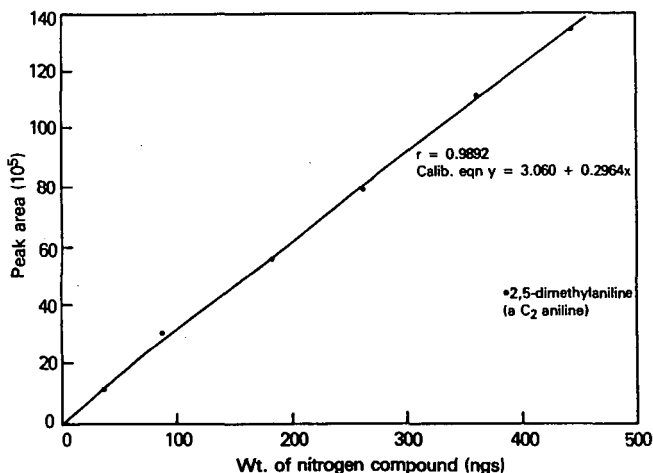
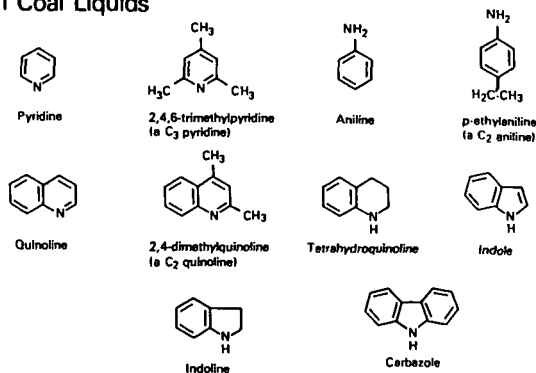


Figure 2

Types of Nitrogen Compounds Detected in Coal Liquids



PREPARATIVE SEPARATION AND CHARACTERIZATION OF COAL LIQUID AROMATICS

James N. Story
AMOCO Corporation
Naperville, IL 60566

Keywords: liquid chromatography, coal liquids

INTRODUCTION

Information concerning the degree and nature of aromaticity in a hydrocarbon feedstock is a very important characterization parameter for refining processes designed to convert high boiling feedstocks into more valuable products. This is especially true in catalytic cracking because feeds of higher aromaticity tend to be more difficult to crack and form coke more easily. Products of the liquifaction of coals are generally highly aromatic in nature and therefore a detailed knowledge of the aromatic structures present in coal liquids is very important in predicting their processing properties.

This work describes the preparative separation and characterization of the aromatics fraction of three Wilsonville coal liquids produced by different two-stage reaction processes. The coals, the liquifaction processes, and the reaction product liquids have been described by Fatemi et. al. (1). The Black Thunder sample was produced by a two stage thermal-catalytic process, while the Illinois No. 6 and Pittsburgh No. 8 liquids were produced using a more severe catalytic-catalytic process.

An additional objective of this work was to characterize the behavior of the DNAP stationary phase in aromatic ring number separations in real samples. Several workers, including this author, have verified the accuracy of the ring number separations on analytical scale DNAP columns using model compounds. However, the limited number of model compounds available, especially of alkyl and naphtheno substituted polynuclear aromatics, and the extremely complex nature of real samples of interest require that such separations be validated more completely using real samples.

EXPERIMENTAL

The samples consisted of the 650-1000 F aromatics fractions of the three Wilsonville coal liquids. One typical petroleum gas oil (650-1000 F) was included for comparison purposes. The aromatics fractions were produced by removal of polar compounds using ion exchange resins, followed by isolation of the aromatics by silica gel chromatography. One milliliter of a 20-30 mg/mL solution of sample dissolved in cyclohexane was injected manually via HPLC sampling valve. The sample was separated by gradient elution using a hexane-MTBE gradient.

The separation on this column is produced via a charge-transfer mechanism in which structures containing larger numbers of aromatic rings (more extensive pi electron systems) are retained by the electron-withdrawing dinitroaniline stationary phase. Use of this phase has been described by Grizzle et. al. (2,3). Data obtained in our laboratory using solutions of model compounds on an analytical scale column showed that the model compounds studied in all cases eluted in the same grouping with others of the same ring number and at increasing retention time with increasing ring number. There was no case in which a compound eluted in the "wrong" group. Alkyl substitution was found to generally not affect retention time enough to move the species out of its ring number group, although small shifts may occur.

The fractions produced were individually characterized by GC-MS and GC. GC-MS was used to identify individual components of the fractions and as an additional validation of the ring number boundary determinations. Single ion plots of ions representing common structures of different aromatic ring number were used to verify ring number regions. The fraction boundaries were also monitored spectroscopically using a Diode Array Spectrophotometer. The coal liquid fractions were collected in such a way as to attempt to obtain "heart-cuts" from each ring number group, and "boundary cuts" at the borders between groups. Solvents were removed from the fractions by evaporation using a Rotovap and fraction weights were obtained. Total recoveries of injected sample were 97% to 104%.

RESULTS

Cut points for the ring number fractions were initially estimated using model compounds. Model compounds known to lie on the boundaries of ring number regions were injected to define initial cut points between regions. These initial cut points were determined to be approximately 19.5 minutes for the 1-2 ring separation, 40 min for 2-3 ring, 60 min for 3-4 ring, and 80 min for 4-5+ ring. A 30 minute backflush step was included to completely elute the sample. Since total column capacity was limited to 20-25 milligrams to avoid overloading, and about twenty fractions were taken, fraction sizes were limited to a few milligrams at most in each fraction.

The samples used for this work were in the boiling range of petroleum gas oils, 650-1000 F. The molecular weight range was typically 200-600 Daltons with an average of about 350, as measured by mass spectroscopy. This means that for a molecule to contain only one aromatic ring, typically 70-80 percent of the atoms must be present in nonaromatic portions of the molecule. In general, increasing nonaromatic content results in increasing fraction complexity. Increasing aromaticity restricts the number of possible compound structures within a particular molecular weight range by constraining the hydrocarbons to a limited number of structures, since those structures must contain aromatic rings. Hence one of the effects were observe is that the ring number fractions become less complex as we go to higher ring numbers as a result of the decreasing variety of alkyl and naphthene substitution.

For comparison and validation purposes mass spectral data were collected by low resolution, high voltage MS using the so-called "Robinson" method (4). Table I shows a comparison of the normalized ring number distributions obtained by preparative HPLC, compared to those obtained from hydrocarbon type analysis by mass spectroscopy. Good agreement is obtained generally within the limits of the techniques used.

The liquid chromatographic separations showed the bulk of the mass isolated from the Illinois No. 6 and the Pittsburgh No. 8 liquid to consist of one and two ring material, which is consistent with the MS results. Chromatograms for these samples are very similar. These two samples represent the coals produced from a two stage, catalytic-catalytic process described in Reference (1). The fractions isolated from the Black Thunder (Wyodak) coal liquid, which were produced by a Thermal-Catalytic process, showed a much larger fraction of 3 and 4 ring material, compared to the Pittsburgh and Illinois coal liquids. The amount of one and two ring material is relatively small. Petroleum gas oil fractions showed a wide distribution of ring number structures with 1- and 2- ring structures predominating.

CHARACTERIZATION OF FRACTIONS

UV Spectra

All HPLC separations were monitored spectrophotometrically by continuous collection of spectra in the ultraviolet region. Aromatic compounds show characteristic spectra which differ significantly depending on ring number. This is a result of the extension of the aromatic ring system, which increases the probability of lower energy, longer wavelength transitions. Shifts to absorption at longer wavelengths will occur as the aromatic structures are extended to larger ring numbers. UV absorption spectra were used to help define the boundaries of the separation. Spectra from the separation of the Pittsburgh coal liquid are shown in Figure 1 to illustrate the distinct spectral changes which occur in the ring number separation. Figure 1a shows how the spectra change in the 1-2 ring transition region of the Pittsburgh coal liquid separation. All spectra are normalized to the absorbance maximum. It is clear that a distinct change occurs in the spectra of eluted sample components as we go from spectrum C in Figure 1a, taken at 19 minutes, to D, taken at 20 minutes. Spectrum C is much more typical of a one ring aromatic while spectrum D more closely resembles a two ring aromatic compound. These spectral changes are consistent with model compound data which shows the 1-2 ring transition to occur at about 19.5 minutes.

Figure 1b shows the sharp spectral transition occurring over just two minutes in the portion of the separation where 3 ring compounds begin to emerge. The much more extended absorption of spectrum B is indicative of the partial transition to 3 ring structures.

Figure 1c shows evidence of the emergence of 4 ring structures. Spectrum A is a typical 3 ring region spectrum, while spectrum B shows the emergence of

a series of bands in the region from 300 to 340 nm which is typically characteristic of 4 ring aromatics.

Figure 1d shows more clearly the difference between characteristic spectra taken from the middle region of each ring type.

Gas Chromatography and GC-MS

All of the fractions from the Pittsburgh No. 8 separation, and selected fractions from the other separations, were analyzed by high resolution capillary gas chromatography. Peak identification was performed by gas chromatography-mass spectroscopy and retention time matching with standard solutions of polynuclear aromatic mixtures. The variety of structures can be qualitatively compared by means of the number of distinct peaks observable in the chromatograms. All of the 1 ring fractions appeared to possess a large variety of structures and individual components are not well resolved into distinct peaks. Chromatographic resolution is also not complete enough to be able to identify individual components unambiguously by GC-MS. However, GC-MS data obtained from these fractions is consistent with the predominance of heavily alkyl substituted one ring aromatic structures. The two ring region was found to contain primarily alkyl diaromatics, including hexahydronaphthalenes, naphtho and dinaphthenonaphthalenes, as well as alkyl acenaphthenes, but there was no evidence of 3 ring aromatics. The 2-3 ring boundary fraction contained hexahydropyrene, alkyldihydroanthracenes, and alkyl phenanthrenes. The 3 ring region showed alkylated anthracenes, phenanthrenes, and naphthenophenanthrenes as well as alkyl benzofluorenes. The chromatograms from the four ring region showed exclusively alkylated tetraaromatics, including pyrenes, benzophenanthrenes, and benzanthracenes. A number of components, including pyrene and methyl pyrenes appear in several of the later fractions, providing evidence of significant bandspreading in this part of the liquid chromatographic separation. All gas chromatograms from this region show relatively few compounds and demonstrate a tremendous reduction in complexity which can be achieved by using LC and GC together to characterize complex hydrocarbon mixtures. Even the petroleum gas oil is vastly reduced in complexity. The backflush fraction of the Pittsburgh coal liquid shows the presence of 4, 5, and 6 ring aromatics. Model compound data from HPLC separations on DNAP indicate that ring number separations are increasingly poorly resolved above 5-6 rings, and this appears to be borne out by the wider variety of multi-ring structures appearing in this fraction.

GC-MS Verification of HPLC Ring Number Regions

GC-MS data obtained from the individual fractions were used in an additional way to verify ring number region assignments. Constraints imposed by structural and molecular weight requirements mean that some fragment masses will be much more likely to appear in the mass spectra of aromatics and substituted aromatics than others. The problem is greatly simplified by the absence of large amounts of nitrogen, oxygen, and sulfur containing compounds. Low sulfur content allows us to eliminate consideration of sulfur containing structures for the coal liquids, but not the petroleum gas oil, which contains 2.8 per cent sulfur. A consideration of the likely representative structural combinations and ions produced from those structures shows that by monitoring for a limited set of single ions representing likely fragments or molecular ions from those structures, we can characterize the ring number distribution for the sample by determining whether the observed masses are consistent with the expected ring number. For example, masses 270 and 280 are likely masses from 1 ring aromatics possessing typical alkyl or naphthenic substitution. The region of mass 270-280 was chosen because it is the minimum mass range of 6 ring aromatics. Since the average MW of these compounds is about 350, ions in this mass range will almost always represent the larger of any fragment ions produced. Unsubstituted, or minimally substituted 3 ring or 4 ring compounds such as pyrene and methyl pyrenes will not be observed within this mass range, but their elution positions in the HPLC separation are already well known from model compound studies. Masses 280 and 276 are likely products of 2 ring aromatics, and mass 276 of 3 ring aromatics. Likely masses for 4, 5 and 6 ring aromatics are derived from the same set, 270 and 276 for 4 rings, 280 for 5 rings, and 276 for 6 rings. Thus by monitoring for only three ions, 270, 280, and 276, and by reasoning that 4 ring aromatics will not likely fall into the same LC ring fraction as 1 or 2 ring aromatics, and 5 ring aromatics will not coelute with 2 ring, etc. we can obtain additional confirmation of the ring number content of each fraction by GC-MS. Of course this procedure may not work for some unusual structure types, some of which

we must expect, but it should hold true for most common structures such as those found in these fractions.

Figure 2 shows the GC-MS single ion chromatograms for 1 through 4 ring fractions of the Illinois coal liquid. Figure 2a shows the predominance of masses 270 and 280 in the 1-ring fraction. The absence of mass 276 suggests the absence of significant 2 or 3 ring material in this fraction. A heart cut of the 2 ring region taken from the Illinois coal liquid is shown in Figure 1b. No significant signal at mass 270 is found in this Figure indicating that no 1 ring material overlapped the fraction. Figure 2c shows exclusively 3 ring material in the 3 ring fraction as evidenced by the presence in significant quantity of only mass 276. Figure 2d shows a fraction from the 4 ring region containing exclusively ion mass 270, suggesting a relatively pure 4 ring fraction, without significant 3 or 5 ring "contamination". Similar ion chromatograms from later fractions showed significant overlap between 5 and 6 ring components.

CONCLUSIONS

The preparative DNAP column was found to effectively separate coal liquid aromatics fractions by ring number with only limited overlap. Distinct changes in UV spectra and GC-MS data were observed in the same boundary regions between ring numbers determined by use of model compounds. Boundary regions were less sharp for the petroleum gas oil as a result of the greater degree of alkyl substitution and the presence of significant sulfur containing components. Preparative HPLC is seen to be a very effective way of simplifying complex hydrocarbon mixtures for further study and characterization. The coal aromatics were found to consist mainly of polynuclear aromatics with limited alkyl substitution. This was especially true of the Black Thunder Coal liquid, which contained primarily 3, 4 and 5 ring material. The larger ring structures in the Black Thunder material were probably the result of the thermal-catalytic two-stage liquification process used in its preparation. The Pittsburgh and Illinois coals were produced using a more severe catalytic-catalytic process and, as a result, contained generally smaller aromatic ring structures. The petroleum gas oil was found to contain more heavily alkyl substituted structures than the coal liquids, based on differences in UV spectra and gas chromatogram complexity. Gravimetric quantification of coal liquid ring fractions yielded results for ring number distributions similar to those obtained by low resolution, hydrocarbon type mass spectroscopy.

REFERENCES

1. S. M. Fatemi, D. C. Cronauer, and R. T. Lagman, "Separation and Characterization of Coal Liquids from Wilsonville", 1992 ACS Meeting, Div. of Fuel. Chem., Washington, D.C.
2. P. L. Grizzle and J. S. Thomson, *Anal. Chem.*, **54**, 1071 (1982)
3. J. S. Thomson and J. W. Reynolds, *Anal. Chem.*, **56**, 2434 (1984)
4. C. J. Robinson and G. L. Cook, *Anal. Chem.*, **41**, 1548 (1969)

TABLE I

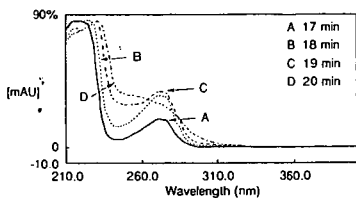
RING NUMBER DISTRIBUTION BY PREPARATIVE HPLC COMPARED TO MASS SPECTROSCOPY

	Aromatic Rings				
	1	2	3	4	5+
Illinois No. 6					
HPLC	22.7%	48.2%	20.2%	8.5%	0.4%
MS	23.3	37.3	21.7	11.4	0.4
Black Thunder					
HPLC	12.1	24.8	19.3	37.1	6.7
MS	14.4	23.0	23.9	29.5	2.1
Pittsburgh No. 8					
HPLC	30.2	36.9	18.9	11.9	1.7
MS	29.7	33.2	18.4	13.7	1.1

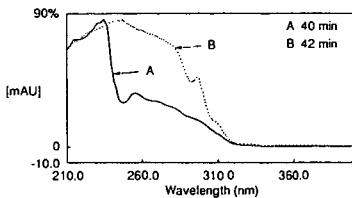
Notes:

1. All HPLC data were obtained using the same dividing points. Dividing points were identified by spectra, model compounds, and GC-MS.
2. MS data do not add up to 100% because of the presence of unidentified species in the MS results.

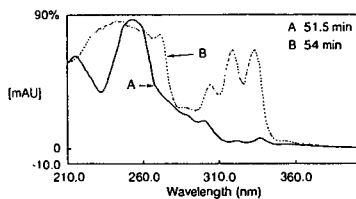
1 - 2 Ring Transition



2 - 3 Ring Transition



3 - 4 Ring Transition



Spectra by Ring Number

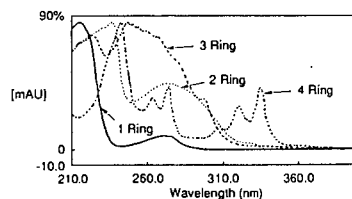


Figure 1. UV Spectra at different retention times.

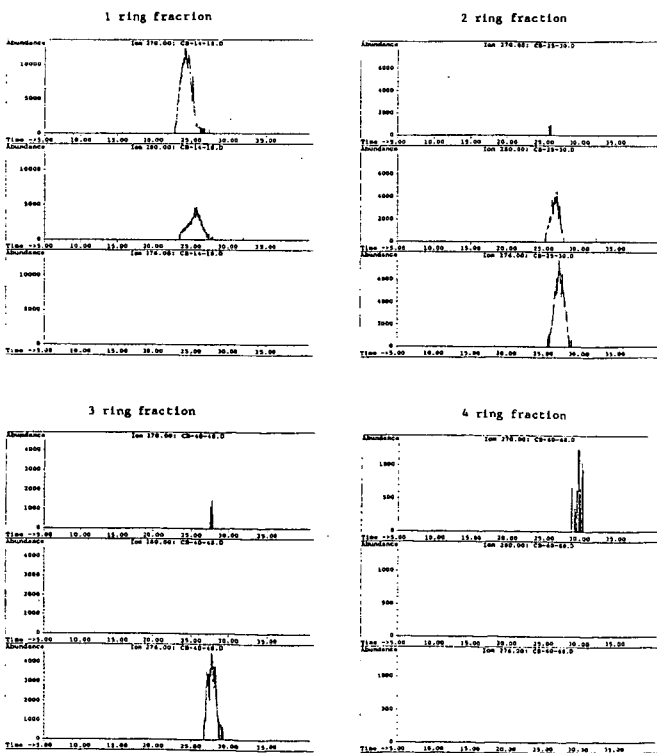


Figure 2. GC-MS ion chromatograms of ring fractions of Illinois No. 6 coal liquid.

CHARACTERISATION OF PITCH FRACTIONS BY QUANTITATIVE SOLID STATE ^{13}C NMR

J.M. Andresen ⁽¹⁾, P.R. Dennison ⁽¹⁾, M.M. Maroto-Valer ⁽¹⁾, C.E. Snape ⁽¹⁾,
R. Garcia ⁽²⁾ and S.R. Moinelo ⁽²⁾

- (1) University of Strathclyde, Dept. of Pure & Applied Chemistry,
Glasgow G1 1XL, UK
(2) Instituto Nacional del Carbon, CSIC, 33080 Oviedo, Spain

Keywords: ^{13}C NMR, single pulse excitation, quaternary aromatic carbon

INTRODUCTION

Thermal and other pretreatments of pitch fractions are being widely investigated as a means to increase the extent of mesophase formation in relation to the production of high performance carbons ⁽¹⁻³⁾. The structural changes that occur can be assessed using carbon skeletal parameters but, although solid state ^{13}C NMR has been used for this purpose ⁽⁴⁻⁷⁾, the quantitative reliability of the technique has still to be established for pitch fractions. It was demonstrated previously ⁽⁷⁾ that, as for coals ⁽⁸⁾, cross-polarisation (CP) can vastly underestimate quaternary aromatic carbon concentrations. A combination of a low magnetic field strength to avoid problems with spinning sidebands and the simple Bloch decay or single pulse excitation (SPE) technique is now generally recognised as offering the most satisfactory approach for obtaining quantitative ^{13}C NMR results for coals and related materials ⁽⁸⁻¹¹⁾. In this study, single pulse excitation (SPE) and associated relaxation measurements have been conducted at low field on coal-derived pitches and their toluene-insoluble (TI) fractions, together with a biomass-derived pitch and the results compared with those from CP.

EXPERIMENTAL

The elemental compositions of the whole coal tar pitch (CTP), the TI fraction from a CTP and the biomass pitch prepared from Eucalyptus Saligna wood are listed in Table 1.

All the ^{13}C NMR measurements were carried out at 25 MHz on a Bruker MSL100 spectrometer with MAS at 5.0 kHz as described previously ⁽⁸⁾ to give spectra in which the sideband intensities are only *ca* 7-8% of the central aromatic bands. Typically, *ca* 250 mg of sample was packed into the zirconia rotors. The ^1H decoupling and spin-lock field was *ca* 60 kHz and, for SPE, the 90° ^{13}C pulse width was 3.3 μs . ^{13}C thermal relaxation times (T_1 s) of the pitch fractions were determined using the CP pulse sequence devised by Torchia ⁽¹²⁾ with a contact time of 5 ms in most cases. Tetrakis(trimethyl)silane (TKS) was added to the samples as an intensity standard. Variable contact time CP experiments were used to estimate ^1H rotating frame relaxation times ($T_{1\rho}$ s) and the characteristic time constant for CP (T_{CH}).

Table 1 Elemental compositions of the pitch samples investigated

	Whole CTP	Toluene-insolubles	Biomass pitch
% C	94.8	92.1	72.0
H	5.7	4.8	6.6
N	1.0	1.1	0.6
S	N.D.	0.4	N.D.
O ^(a)	<1	1.6	20.8
H/C	0.57	0.62	0.91

(a) = by difference. N.D. = not determined

Depending upon the ^{13}C T_{1s} , relaxation delays between 50 and 80 s were used for all the normal and variable delay dipolar dephasing (DD) SPE measurements. At least 5 dephasing periods in the range of 50 to 500 μs were used before the first rotational modulation and this was sufficient to allow an estimate of the decay constant of the non-protonated aromatic carbon. In order to allow for variations in tuning for the variable delay DD and CP experiments, blocks of 64 scans were successively accumulated for each delay, the total number of scans being 512. No background signal was evident in the SPE spectra from the Kel-F rotor caps. All the FIDs were processed using a line broadening factor of either 20 or 50 Hz. The measurement of the small aliphatic peak areas was conducted manually as this was found to be generally more precise than using the integrals generated by the spectrometer software.

RESULTS AND DISCUSSION

Quantitative reliability Table 2 summarises the relaxation parameters determined for the whole CTP and TI fraction. The variation of the aromatic carbon peak intensity in the Torchia ^{13}C T_1 method for the CTP is presented in Figure 1. The ^{13}C T_{1s} for the quaternary aromatic carbons (longer component where two are listed, Table 1) are *ca* 10 and 15 s, respectively for the whole CTP and TI fraction meaning that recycle delays of 50 and 75 s are required in SPE to ensure virtual complete relaxation of the ^{13}C spins between successive pulses. The hydrogen T_{1s} ($T_{1\text{H}}$, Table 1) and rotating frame relaxation times ($T_{1\rho\text{H}}$) are shorter for the TI fraction, mainly due to the presumed higher concentration of free radicals. The long $T_{1\text{H}}$ for the whole CTP means that, even in CP, a recycle delay of *ca* 10-15 s is appropriate to ensure complete relaxation of the proton spins.

Table 2. Relaxation parameters for the coal tar pitch samples

Sample	$T_{1\text{H}}/\text{ms}$	$T_{\text{CH}}/\mu\text{s}$	$T_{1\rho}/\text{ms}$	$T_{1\text{C}}/\text{s}$
Whole pitch	1100 (77%)	42 (44%)	5.4	15.2 (a)
	3200 (23%)	780 (56%)		
Toluene-insolubles	0.2 (59%)	27 (68%)	1.5 (68%)	1.0 (32%)
	60 (41%)	310 (32%)	11 (32%)	10.0 (68%)

(a) = for quaternary aromatic carbon only.

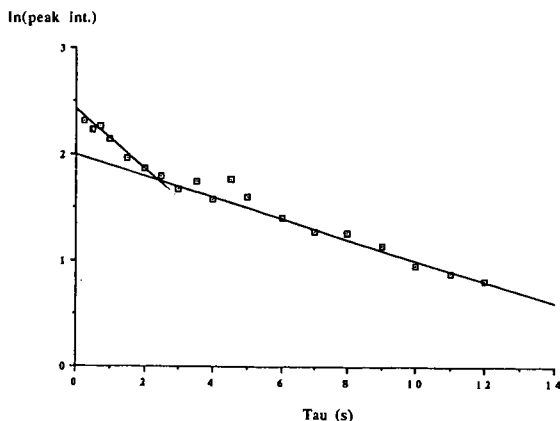


FIGURE 1 DECAY OF AROMATIC PEAK INTENSITY FOR THE TOLUENE-INSOLUBLE FRACTION IN DETERMINATION OF ^{13}C THERMAL RELAXATION TIMES

Figure 2 shows SPE spectra for the whole CTP and TI fraction. The use of TKS as an intensity standard has indicated that ca 90% of the carbon was observed by SPE in both fractions with a relaxation delay of 50 s (Table 3). As anticipated, the aromaticities are nearly 1 for both fractions but lower values (0.95-0.97 with a 1 ms contact) have been obtained by CP (Table 3).

Quaternary aromatic carbon Table 3 lists the aromaticities and fractions of quaternary carbon (C_q/C_A) derived from the SPE spectra for the whole CTP and TI fraction. Figure 3 compares the aromatic carbon intensity plots obtained from DD using SPE and CP with a 1 ms contact for the TI fraction. As for coals (8), CP grossly underestimates quaternary aromatic carbon concentrations. Although the value of 0.58 for C_q/C_A obtained with a contact time of 5 ms is significantly higher than that for 1 ms (0.40), it is still much lower than that 0.70 from SPE. The agreement between CP DD value of 0.58 for C_q/C_A and that of 0.68 for the slower relaxing carbon in the two component fit for the ^{13}C T_1 relaxation behaviour (Figure 1) is reasonably good, considering the experimental error for the latter.

As there is little aliphatic carbon and oxygen in the CTP samples (Tables 1 and 3), the errors involved in deducing the bridgehead aromatic carbon concentrations (C_{BR}/C) from the values for C_q/C_A are relatively small. The results obtained indicate that the average size of the aromatic nuclei correspond to 6/7 ring peri-condensed structures for the whole CTP and, as expected, considerably larger entities for the TI fraction

Aliphatic carbon Since the ^{13}C T_1 s of the aliphatic carbons are much shorter than those of the quaternary aromatic carbons, reasonably accurate results can thus be obtained with much shorter recycle times. Figure 4 compares the aliphatic

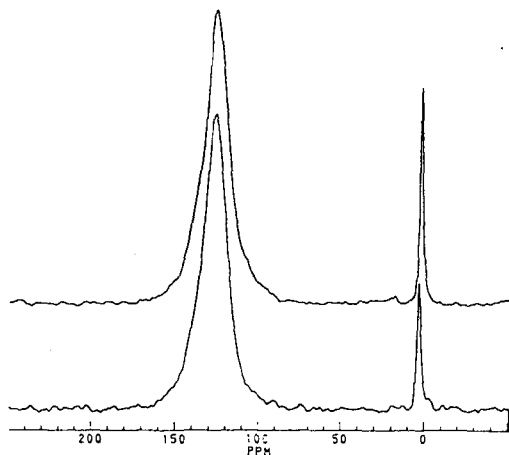


FIGURE 2 SPE ^{13}C NMR SPECTRA OF WHOLE CTP AND TOLUENE-INSOLUBLE FRACTION CONTAINING TKS

Table 3. Structural parameters for the coal tar pitch samples

Sample	Aromaticity, f_a	f_q	C_{BR}/C	% of C obs.
Whole pitch	0.98 (0.95)	0.52	0.50	93
Toluene-insolubles	>0.99 (0.97)	0.70	0.68	90

f_q = fraction of quaternary carbon of total aromatic carbon.
 C_{BR}/C = mole fraction of bridgehead aromatic carbon.

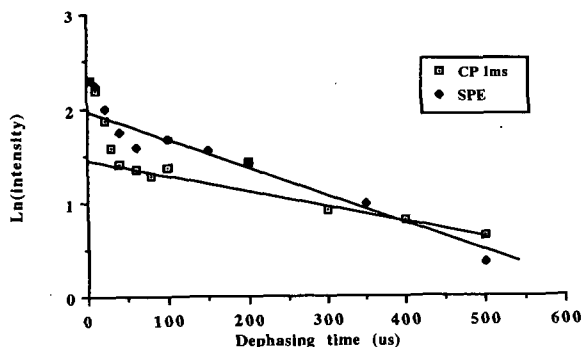


FIGURE 3 COMPARISON OF AROMATIC PEAK INTENSITIES FROM THE SPE AND CP (1 ms CONTACT) DIPOLAR DEPHASING EXPERIMENTS ON THE TOLUENE-INSOLUBLE FRACTION

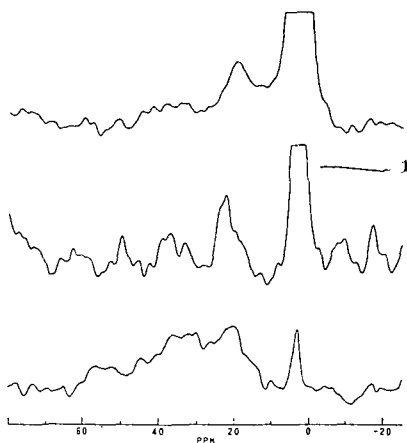


FIGURE 4 ALIPHATIC CARBON BANDS FROM SPE AND CP SPECTRA OF THE TOLUENE-INSOLUBLE FRACTION

regions from the SPE spectrum of the TI fraction obtained with a recycle delay of only 5 s with those from the CP spectra obtained with contact times of 0.5 and 2 ms. Although the signal to noise ratios are understandably low, the proportion of CH₃ (10-25 ppm) observed at the shorter contact time is only 30-40% of the aliphatic carbon due to the incomplete CP of the rotationally mobile CH₃. The proportion observed is higher at the longer contact time of 2 ms but the signal to noise ratio is less than in the SPE spectrum which indicates that CH₃ accounts for at least 60 to 70% of the aliphatic carbon.

Biomass pitch Figure 5 shows the spectra obtained by SPE with a 50 s relaxation time and by CP with a 1.5 ms contact time. Table 4 lists the relaxation parameters and the carbon aromaticity. As for the CTP, over 90% of the carbon was observed by SPE with a relaxation delay of approximately 5 times the ¹³C T₁ for quaternary aromatic carbons (ca 10 s, Table 4). The biomass pitch is structurally diverse with methoxyl groups (peak at 55 ppm, Figure 5) surviving the carbonisation which clearly indicates that tar evolves at relatively low temperatures. The carbon aromaticity of 0.60 obtained by SPE compares with that of 0.58 from CP suggesting that, as for wood and other lignocellulosic materials (13), the discrimination against aromatic carbon is not as great as for low-rank coals.

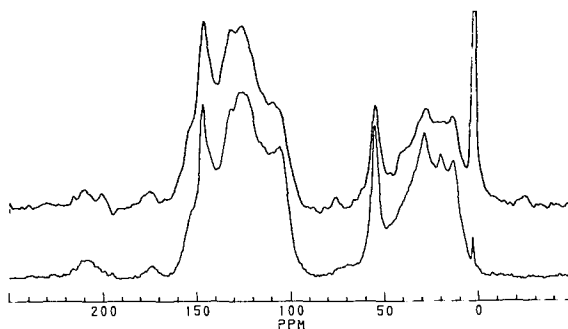


FIGURE 5 SPE AND CP (1 ms CONTACT) SPE ^{13}C NMR SPECTRA OF THE BIOMASS PITCH

Table 4. Structural and relaxation parameters for the biomass pitch.

T_1^H /ms	T_1^C aromatic /s	% C observed	Aromaticity, f_a
46 (80%)	9.8 (44%)	96	0.60
91 (20%)	0.8 (56%)		(0.58) (a)

(a) = CP value with a contact time of 1 ms.

CONCLUSIONS

^{13}C thermal relaxation times for quaternary aromatic carbons in coal tar and biomass pitches investigated are in the range 10-15 s and, provided that suitably long relaxation delays are used in SPE, over 90% of the carbon is observed. Further, the self-consistent quaternary aromatic carbon concentrations derived by SPE-DD are higher than those obtained from CP, even with long contact times. SPE has indicated that the aliphatic carbon present in the CTP TI fraction investigated is predominately methyl.

ACKNOWLEDGEMENTS

The authors thank the the Science and Engineering Research Council (Grant no. GR/F/87264) and the European Community (Contract No. CI 1-CT92-0028, DGXII-G) for financial support and C. Luengo of the Universidade Estadual de Campinas, Brazil for supplying the wood-derived pitch.

REFERENCES

1. H. Marsh and R. Menendez, *Fuel Process. Technol.*, **20**, 269 (1988).
2. Z. Weishauptova, J. Medek and M. Rada, *Fuel*, **73**, 177 (1994).
3. M. Matsumoto, M. Higuchi, T. Tomioka and H. Sunago, *Fuel*, **73**, 237 (1994).
4. P. Oliver and B.C. Gerstein, *Carbon*, **22**, 409 (1984).
5. H. Sfih, P. Tougne and A.P. Legrand, *Fuel Process. Technol.*, **20**, 43 (1987).
6. A. Grint, G.P. Proud, I.J.F. Poplett, K.D. Bartle, S.Wallace and R.S. Matthews, *Fuel*, **68**, 1490 (1989).
7. C.E. Snape, A.M. Kenwright, J. Bermejo, J. Fernandez and S.R. Moinelo, *Fuel*, **68**, 1605 (1989).
8. G.D. Love, R.V. Law and C.E. Snape, *Energy & Fuels*, **7**, 639 (1993).
9. C.E. Snape, D.E. Axelson, R.E. Botto, J.J. Delpuech, P. Tekely, B.C. Gerstein, M.Pruski, G.E. Maciel and M.A. Wilson, *Fuel*, **68**, 547 (1989) and references therein.
10. J.A. Franz, R. Garcia, J.C. Linehan, G.D. Love and C.E. Snape, *Energy & Fuels*, 1992, **6**, 598.
11. Muntean, J.V. and Stock, L.M., *Energy & Fuels*, **5**, 767 (1991).
12. D.A. Torchia,, *J. Magn. Reson.*, **30**, 613 (1978).
13. G.D. Love, C.E. Snape and M.C. Jarvis, *Biopolymers*, **32**, 1187 (1992).

CPMAS AND DDMAS ^{13}C NMR ANALYSIS OF COAL LIQUEFACTION RESIDUES

Chunshan SONG,* Lei HOU, Ajay K. SAINI, and Patrick G. HATCHER

Fuel Science Program, Department of Materials Science and Engineering
The Pennsylvania State University, University Park, PA 16802

Keywords: ^{13}C NMR, CPMAS, Coal Liquefaction, Residues

INTRODUCTION

We have shown in previous papers that spectroscopic analyses of liquefaction residues (by NMR, pyrolysis-GC-MS, and FT-IR) can provide important structural information which can be used for elucidating the chemical reactions of liquefaction (Song et al., 1992, 1993, 1994) as well as the effects of dispersed catalysts (Saini et al., 1992; Huang et al., 1993; Song et al., 1994). The present work involves solid-state ^{13}C NMR studies of residues of two subbituminous coals from their liquefaction at 300-425°C, using cross-polarization (CP), dipolar dephasing (DD) and magic-angle-spinning (MAS) techniques. A preliminary survey of some CPMAS ^{13}C NMR results for one of the two coals was presented previously (Song et al., 1993). In a companion paper, we report on the analysis of oils from liquefaction of these coals by two-dimensional HPLC and GC-MS (Saini and Song, 1994).

EXPERIMENTAL

Sample Preparation. Three types of samples were examined in this study. The first set of samples are THF-insoluble residues from temperature-programmed liquefaction (TPL) of a Montana subbituminous coal (DECS-9) in tetralin solvent at a final temperature ranging from 300°C to 425°C for 30 min (Song et al., 1992). The second set of samples are THF-insoluble residues from liquefaction of a Wyodak subbituminous coal (DECS-8) at 350°C with and without a solvent (Song et al., 1994). The coals were predried in vacuum at about 100°C for 2 h prior to liquefaction. The third set of samples are the fresh raw coals (DECS-8, DECS-9) and THF-extracted but unreacted coals. Our experience shows that trace amounts of THF always remain in the THF-extracted residues even after vacuum drying at 100°C for over 6 h, which interferes with spectroscopic analysis. We have solved the problem by washing the residue first with acetone, then with pentane, followed by vacuum drying at 100°C for 6 h prior to spectroscopic analysis. The residue samples were also subjected to elemental analysis.

Solid-State ^{13}C NMR. NMR spectra were acquired on a Chemagnetics M-100 spectrometer. The measurements were carried out at a carbon frequency of 25.035 MHz. The spectrometer performance was checked with a standard sample of hexamethylbenzene to assure the Hartman-Hahn match. In a typical analysis, about 0.4-0.6 g of a sample was packed in a 0.4 mL bullet-type rotor made of polychlorotrifluoroethylene (Kel-F). Kel-F does not have a CPMAS ^{13}C signal. The MAS speed of the rotor was about 3.5 kHz.

The CPMAS ^{13}C NMR spectra were obtained by using the combined high power proton decoupling, cross-polarization, and magic angle spinning techniques. The experimental conditions for all the samples are as follows: a cross-polarization contact time of 1 msec, a pulse delay time of 1 sec, 50 kHz of proton decoupling, sweep width of 14 kHz, and 20-30 Hz line broadening. Carbon aromaticity was determined by integrating the peaks between 95 and 165 ppm (ppm relative to tetramethylsilane). Spinning sideband intensity was distributed for aromatic carbons. Other details concerning CPMAS maybe found elsewhere (Hatcher, 1987).

Dipolar-dephasing ^{13}C NMR spectra (DDMAS) were acquired by using the pulse sequence described by Alemany et al. (1983) and Wilson et al. (1984). After the protons are spin-locked and cross-polarization is induced, a variable dephasing time T_{dd} is inserted, during which the high-power decoupler is turned off. During this period, which lasts from 5 to 180 μsec , carbon magnetization becomes influenced and diminished (dephased) by the strong dipolar interactions between ^{13}C and ^1H spins. Carbons directly bonded to hydrogens (protonated carbons) dephase much more rapidly than those without attached hydrogens (non-protonated carbons). More details about the theory and procedures of dipolar dephasing may be found elsewhere (Hatcher, 1987, 1988; Pan and Maciel, 1993). In general, protonated carbons dephase within the first 60 μsec (T_{dd}), and the signals remain after 60 μsec are due to non-protonated carbons.

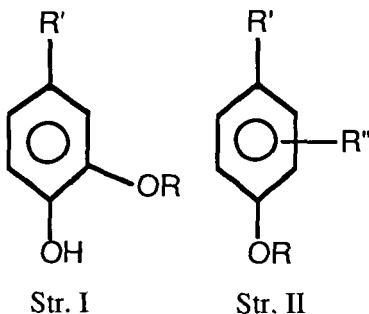
RESULTS AND DISCUSSION

Structural Characteristics of THF-extracted Coals

Figure 1 shows the CPMAS and DDMAS ^{13}C NMR spectra of THF-extracted but unreacted Montana subbituminous coal (DECS-9). In the CPMAS spectrum, there are two major bands, an aromatic bands from 95 to 165 ppm and an aliphatic band from 0 to 80 ppm. Among the aliphatic bands, methyl carbons appear at 0-25 ppm, methylene carbons resonate between 25-51 ppm, methoxyl groups around 51-67 ppm and ether groups between 67-93 ppm (Yoshida et al., 1987). The aromatic region includes two shoulders which may be attributed to catechol-like oxygen-bound carbons (centered around 142-144 ppm) and phenolic carbons (centered around 152-154 ppm). There are two other bands with lower intensities, including carboxyl groups between 170-190 ppm and ketonic carbonyl groups between 190-230 ppm.

* Corresponding author.

DDMAS ^{13}C NMR was used to examine the degree of protonation of carbons. Protonated carbons decay at a rate that is dependent on T_{dd}^2 and is often referred to as the Gaussian component of signal decay; non-protonated carbons decay at a much slower rate that is exponential with respect to T_{dd} (Alemany et al., 1983). Compared to the CPMAS spectrum, signal decay in the 95-165 ppm region was due mainly to protonated aromatic carbons (95-130 ppm). The signal intensity remaining in the aromatic region in the DDMAS spectrum in Figure 1 can be attributed to bridgehead and substituted aromatic carbons (130-148 ppm) and oxygen-bound aromatic carbons (140-165). Apparently, the shoulders that we identified as catecholic (structure I) and phenolic (structure II) carbons remain in the DDMAS structure and are clearly non-protonated carbons.



Our assignment of the peak centred at 142-144 ppm in the DDMAS spectra is different from that of Pan and Maciel (1993). They assigned the 144 ppm peak for Beulah-Zap lignite (801) to an aniline-type aromatic carbon. We have assigned this peak to the catecholic oxygen-bound aromatic carbon (shown in structure I). This is based on the NMR spectra of lignin-related model compounds and lignin (Hatcher, 1987) and the combined CPMAS NMR and pyrolysis-GC-MS studies of low-rank coals, including DECS-9 (Song et al., 1993) and DECS-8 (Saini et al., 1992) coals used in this work, as well as a lignite (Wenzel et al., 1993).

Flash pyrolysis GC-MS of lignites (Hatcher et al., 1988; Wenzel et al., 1993), DECS-9 Montana coal (Song et al., 1993), and DECS-8 Wyodak coal (Saini et al., 1992) revealed that catechol and phenol as well as their homologs are important components in the pyrolyzates of low-rank coals. Another important evidence is that as catechol observed in the pyrolysis-GC-MS diminishes, so does the catecholic peak in the CPMAS ^{13}C NMR spectra (Hatcher et al., 1988; Song et al., 1993; Wenzel et al., 1993).

Quantitative CPMAS NMR analysis of Montana coal was performed by means of curve-fitting, as described in our recent paper (Song et al., 1993). This coal has 63-64% aromatic carbons among total carbons. Combination of DDMAS and CPMAS NMR data reveals that about 34-35% of the aromatic carbons are protonated carbons; 23-24% of aromatic carbons are chemically bound to oxygen atoms; the remaining 31-33% aromatic carbons are bound primarily to other carbon atoms and secondarily to nitrogen and sulfur. The above spectroscopic results suggest that the Montana coal contains approximately two or three protonated carbons, one or two oxygen-bound carbons, and two substituted or bridgehead carbons per aromatic ring.

Compared to the Montana coal, THF-extracted Wyodak subbituminous coal (DECS-8) has a lower aromaticity (57%). However, it also has all the characteristic peaks (aliphatic, aromatic, carboxyl, carbonyl) and shoulders (phenolic, catecholic) that DECS-9 Montana coal possess (Figure 1). The DDMAS ^{13}C NMR data are not available for this sample at the present time.

Characterization of Residues from Non-Catalytic Liquefaction

Figure 2 presents the CPMAS and DDMAS ^{13}C NMR spectra of THF-insoluble residue from non-catalytic TPL of a Montana subbituminous coal (DECS-9) in the presence of tetralin solvent at a final temperature of 350°C for 30 min. Details of TPL procedures and results may be found elsewhere (Song and Schobert, 1992). Comparative examination of DDMAS data indicates at least three trends. First, relative to the THF-extracted unreacted coal, non-protonated carbons contribute more to the aromatic band in the residue from 350°C run. Second, the catecholic peak almost disappeared after 30 min at 350°C. Third, phenolic peak does not diminish as much as the catecholic peak upon reaction at 350°C, as can be seen by comparing the two DDMAS spectra (Figures 1 and 2).

Figure 3 shows the CPMAS and DDMAS ^{13}C NMR spectra of THF-insoluble residue from non-catalytic reaction of a vacuum-dried Wyodak subbituminous coal (DECS-8) in the absence of any solvent at 350°C for 30 min under 6.9 MPa H_2 . Since no donor solvent or catalyst was used, the coal conversion is very low, only about 12.5 wt%. More liquefaction results of this coal are described elsewhere (Song et al., 1994). The characteristics of both CPMAS and DDMAS spectra of this sample resemble those of the corresponding spectra for residue from Montana coal (Figure 2), although the two samples were derived from different coals under different conditions.

The reaction temperature has the most significant impact on the spectral characteristics of the liquefaction residues. We have performed both DDMAS and CPMAS ^{13}C NMR analysis of the THF-insoluble residues from TPL reactions of Montana coal (DECS-9) at 300, 350°C, 375, 400 and 425°C for 30 min. Catechol-like structures were found to be thermally sensitive and diminish gradually with increasing temperature up to 350°C. The catecholic shoulder at 142-144 ppm disappears from the residue of 375°C run. Carboxyl (165-190 ppm) and carbonyl (190-230) peaks diminish significantly after 375°C and they disappear in the spectrum of residue from 400°C run. Phenolic structures diminish with increasing temperature up to 425°C. These results clearly indicate that there are thermally reactive oxygen functional groups in coal and their reactions can take place at temperatures as low as 300-375°C.

As shown in Figure 4, the carbon aromaticity of residues increased monotonically with increasing reaction temperature after 300°C. Comparison of the curve for H/C atomic ratio and that for carbon aromaticity

indicates that THF extraction of unreacted coal and that reacted at 300°C, removed more aliphatic materials. However, the conversion level at 300°C in tetralin is below 10 wt% (dmff). The H/C ratio of the residues decreased significantly with increasing temperature up to 425°C. The aromaticity of the residues increased with increasing coal conversion, being consistent with the observations by two other groups on residues from liquefaction (Fatemi-Badi et al., 1991; Franco et al., 1991). The increase in carbon aromaticity is driven primarily by temperature, and secondarily by the adduction of aromatic solvent molecules (Song et al., 1993, 1994). Another interesting observation is that, while the total aliphatic carbons decrease, the percentage methyl carbons relative to total aliphatic carbons increases with increasing temperature up to 425°C.

DDMAS analysis (Figure 5) shows that the degree of protonation of aromatic carbons in the residues decreased from 35% (for THF-extracted but unreacted Montana coal) to 13% for residue from the non-catalytic run at final reaction temperature of 375°C. General trends observed from DDMAS experiments for residues from DECS-9 are as follows. The degree of protonation of aromatic carbons in the residue decreases with increasing coal conversion. In other words, the higher the coal conversion into THF-soluble products, the more non-protonated aromatic carbons in the THF-insoluble residues. The higher content of non-protonated carbons among total aromatic carbons could originate from either higher degree of condensation or higher extent of substitution. Since the aromaticity increases and atomic H/C ratio decreases with increasing temperature, the decrease in the relative content of protonated aromatic carbon (or the increase of non-protonated aromatic carbons) is due mainly to the increased degree of condensation. This means that there are more bridgehead aromatic carbons or more condensed-ring aromatic structures in the residues from runs at higher temperatures.

As discussed above, there exists good correlation between carbon distribution and reaction temperature above 300°C. We have attempted mathematical correlation of the NMR data for the residue with reaction temperature (Song et al., 1993). Figure 6 shows that the changes in the aromatic, aliphatic, and oxygen-bound carbons of the residues can be related to the liquefaction temperature by a linear correlation. A general expression is given below:

$$C_i = \alpha f_i + \beta T \quad \text{for specific carbon type } i \quad (1)$$

where T is reaction temperature (°C), f_i and C_i represent the content of specific carbons (%) in the original coal and residue, respectively, and α and β are constants. The specific correlations for aromatic C (C_{ar}), aliphatic C (C_{al}), and oxygen-bound carbons (C_{O-C}) are given in Figure 6. We have quantitatively analyzed the NMR spectra of 26 residues from liquefaction of DECS-9 coal under various conditions with and without solvents (Song et al., 1993). The results show that equation 1 holds for all the cases with good linear correlation.

REFERENCES

- Alemany, L.B.; Grant, D.M.; Alger, T.D.; Pugmire, R.J. *J. Am. Chem. Soc.*, 1983, 105, 6697.
 Franco, D.V.; Gelan, J.M.; Martens, H.J.; Vanderzande, D.-J.-M. *Fuel*, 1991, 70, 811-817.
 Hatcher, P.G. *Org. Geochem.*, 1987, 11 (1), 31-39.
 Hatcher, P.G. *Energy & Fuels*, 1988, 2 (1), 48-58.
 Hatcher, P.G.; Lerch III, H.E.; Kotra, R.K.; Verheyen, T.V. *Fuel*, 1988, 67, 1069-1075.
 Hatcher, P.G.; Wilson, M.A.; Vassallo, A.M.; Lerch III, H.E. *Int. J. Coal Geol.*, 1989, 13, 99-126.
 Huang, L.; Song, C.; Schobert, H.H. *Am. Chem. Soc. Div. Fuel Chem. Prepr.*, 1993, 38 (3), 1093-1099.
 Saini, A. K.; Song, C.; Schobert, H. H.; Hatcher, P. G. *Am. Chem. Soc. Div. Fuel Chem. Prepr.*, 1992, 37 (3), 1235-1242.
 Saini, A. K.; Song, C. *Am. Chem. Soc. Div. Fuel Chem. Prepr.*, 1994, 37 (3-4), in press.
 Pan, V.H.; Maciel, G.E. *Fuel*, 1993, 72 (4), 451-468.
 Song, C.; Schobert, H.H.; Hatcher, P.G. *Energy & Fuels*, 1992, 6 (3), 326-328.
 Song, C.; Schobert, H.H. *Am. Chem. Soc. Div. Fuel Chem. Prepr.*, 1992, 37 (2), 976-983.
 Song, C.; Hou, L.; Saini, A.K.; Hatcher, P.G.; Schobert, H.H. *Fuel Processing Technol.*, 1993, 34 (3), 249-276.
 Song, C.; Saini, A.K.; Schobert, H.H. *Energy & Fuels*, 1994, 8 (2), 301-312.
 Fatemi-Badi, S.M.; Swanson, A.J.; Sethi, N.K.; Roginski, R.T. *Am. Chem. Soc. Div. Fuel Chem. Prepr.*, 1991, 36 (2), 470-480.
 Wenzel, K.; Hatcher, P. G.; Cody, G. D.; Song, C. *Am. Chem. Soc. Div. Fuel Chem. Prepr.*, 1993, 38 (2), 571-576.
 Wilson, M.A.; Pugmire, R.J.; Karas, J.; Alemany, L.B.; Woolfenden, W.R.; Grant, D.M. *Anal. Chem.*, 1984, 56, 933-943.
 Yoshida, T.; Maekawa, Y., *Fuel Processing Technol.* 1987, 15, 385-395.

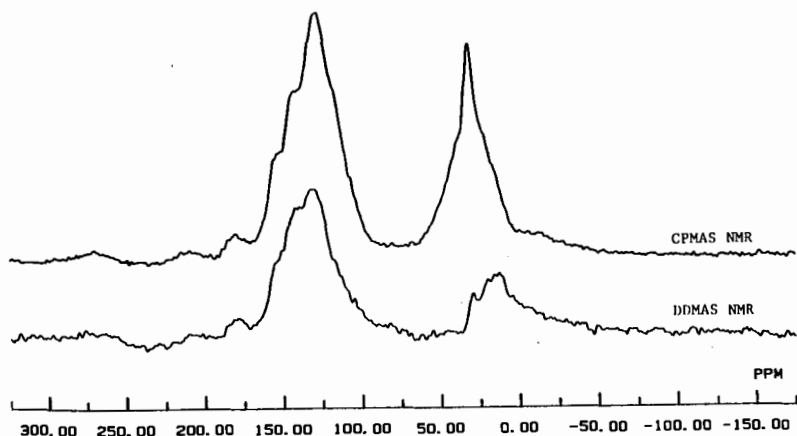


Figure 1. CPMAS and DDMA5 ^{13}C NMR spectra of THF-extracted but unreacted Montana subbituminous coal (DECS-9). For DDMA5, $T_{dd} = 60 \mu\text{s}$.

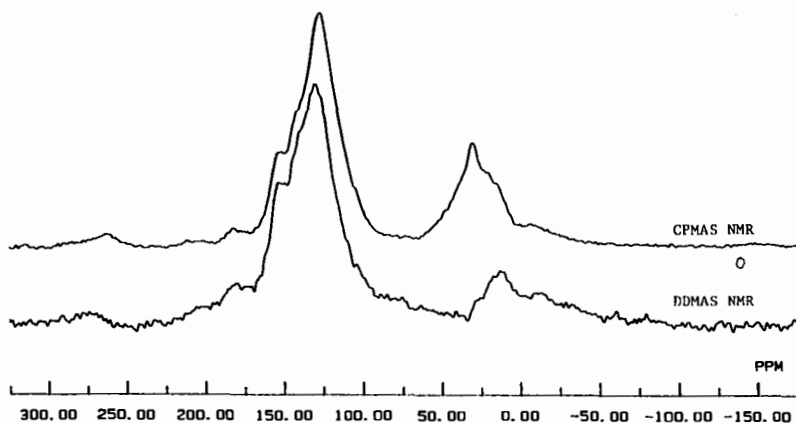


Figure 2. CPMAS and DDMA5 ^{13}C NMR spectra of residue from TPL of Montana coal in the presence of tetralin at a final temperature of 350°C for 30 min. For DDMA5, $T_{dd} = 60 \mu\text{s}$.

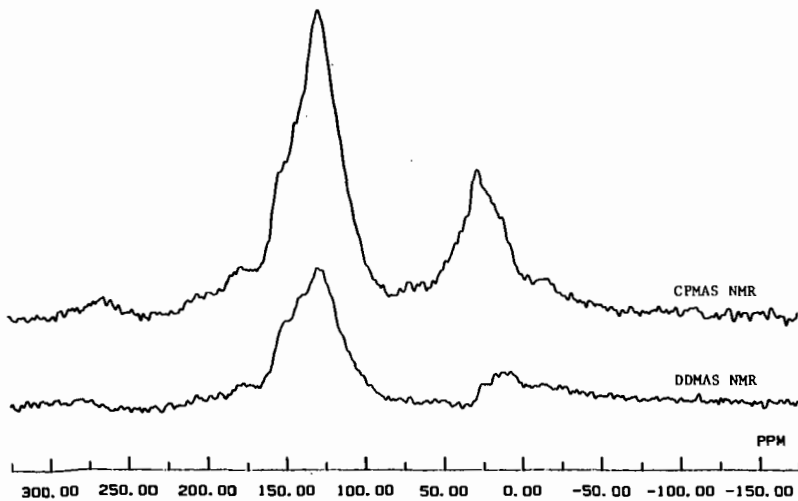


Figure 3. CPMAS and DDMA5 ^{13}C NMR spectra of residue from liquefaction of Wyodak coal (DECS-8, vacuum-dried) without any solvent at 350°C for 30 min. For DDMA5, $T_{dd} = 60 \mu\text{s}$.

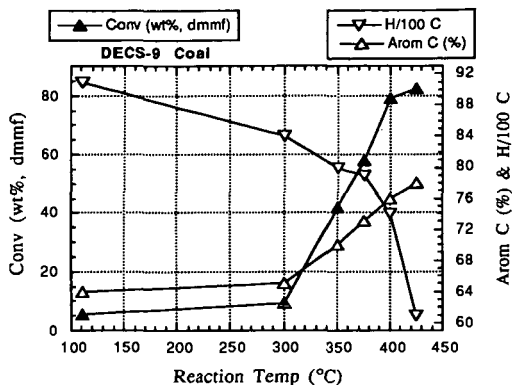


Figure 4. Conversion of Montana coal and changes in aromaticity (Arom C, %) and No. of H atoms/100 C in the residues versus final temperature of liquefaction (TPL) in tetralin.

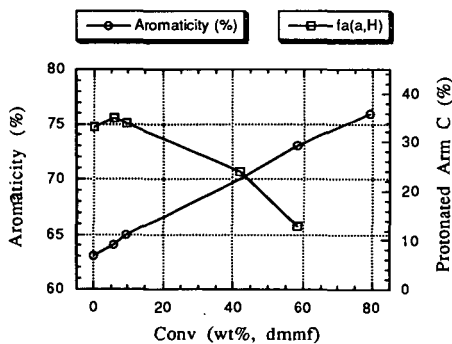


Figure 5. Change of aromaticity and percentage degree of protonation of aromatic carbons [fa(a,H)] in the residues versus conversion of DECS-9 Montana coal in TPL with tetralin.

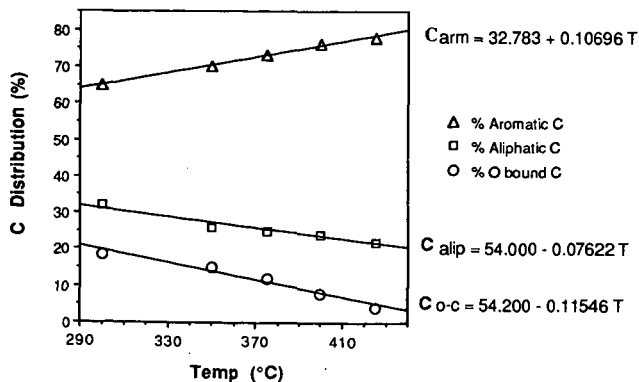


Figure 6. Linear correlation of contents of aromatic, aliphatic, and total oxygen-bound carbons in residues from DECS-9 Montana coal with final temperature of TPL in tetralin.

SCOPE AND LIMITATION OF RUTHENIUM ION CATALYZED OXIDATION OF COAL AS AN ANALYTICAL TOOL FOR AN ALIPHATIC PORTION OF COAL ORGANIC MATERIALS

Satoru Murata, Ken-ichi U-esaka, Hirohiko Ino-ue, and Masakatsu Nomura*
Department of Applied Chemistry, Faculty of Engineering, Osaka University,
Suita, Osaka 565, Japan

Keywords: Ruthenium tetroxide, Oxidation of coal, Aliphatic portion of coal

Introduction

We have been investigating a chemical structure of Japanese bituminous Akabira coal by Curie-point pyrolysis GC/MS coupled with CP/MAS ^{13}C NMR and proposed a unit chemical structure of the coal on the basis of these results.¹ In that paper, we had pointed out more precise and quantitative evaluation of chemical bonds connecting aromatic rings should be clarified in order to evaluate more precise chemical structures of coal organic materials (COM). As for this, Stock *et al.*, investigated ruthenium ion catalyzed oxidation (RICO) of coal.² Ruthenium tetroxide is well known to have a property to attack selectively sp^2 carbons of organic substrates: for example, in this oxidation arylalkanes and diarylalkanes could be converted to aliphatic monocarboxylic and dicarboxylic acids, respectively. One of the most critical points of this reaction is believed to be the difficulty in attaining quantitative analyses of lower carboxylic acids because they are main products, showing high volatility. Stock *et al.* and Strausz *et al.* had applied the isotope dilution method² and esterification with phenacyl bromide³ for the quantitative analysis, respectively. The former, however, needs preparation of deuterium-labeled carboxylic acids and the later has a slow rate of conversion of the carboxylic acids to their phenacyl esters.

In this paper, we have examined quantitative determination of carboxylic acids resulted from RICO reaction and proposed the method to accomplish this, applying this for RICO reaction of Illinois #6 (American subbituminous), Akabira (Japanese bituminous), and Zao Zhuang (Chinese bituminous) coals.

Experimental Section

Reagents, Samples, and Instruments.

As to Illinois #6 coal, Argonne premium coal sample was used. Whole coals employed in this paper were pulverized under 100 mesh and dried at 100°C *in vacuo* (5 mmHg) for 10 h prior to use. Solvents were distilled according to conventional methods. Other reagents were commercially available and used without further purification.

Procedure for RICO Reaction of Coal.

RuCl_3 (40 mg) and coal (1 g) were added to a 100 ml flask containing MeCN (20 ml), CCl_4 (20 ml), and H_2O (30 ml), the mixture being stirred magnetically for 1 h. NaIO_4 (10 g) was added gradually and the resulting mixture was stirred at 40°C for 24 h. After the end of the reaction, the mixture was filtered to remove an inorganic residue. The filtrate was analyzed with the following two methods; (i) For analysis of lower carboxylic acids ($\leq\text{C}_6$), aqueous NaOH solution (5 %, 100 ml) and ether (100 ml) were added to the filtrate and the aqueous phase was separated. This aqueous solution was diluted to 1000 ml by using deionized water and 5 ml portion of this solution was analyzed by a DIONEX 2000i/sp ion chromatograph (HPICE-AS-1 column). (ii) For analysis of higher carboxylic acids ($\text{C}_7\leq$), diluted hydrochloric acid (5 %, 100 ml) were added to the filtrate and the resulting solution was extracted with 100 ml of ether, twice. The ethereal solution was dried over sodium sulfate. After evaporation of ether, carboxylic acids produced were esterified with diazomethane and analyzed with a Shimadzu GC-8APF (CBP-1 capillary column, ϕ 0.50 mm x 25 m) and a Shimadzu QP-2000A GC-MS (CBP-1 capillary column, ϕ 0.25 mm x 25 m).

Results and Discussion

Problems in RICO Reaction of Coal.

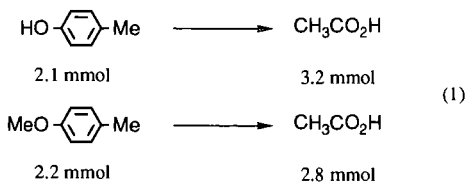
At first, we have examined availability of ion chromatography to analyze a mixture of lower carboxylic acids. Figure 1 shows ion chromatograms of a model mixture containing succinic, formic, acetic, propionic, butyric, and valeric acids

and RICO products of Akabira coal, this suggesting that peak separation is relatively good and analysis of these carboxylic acids is not disturbed by the presence of Γ and IO_x ions contained in the reaction mixture.

We have discussed the possible factors affecting the results of RICO reaction; (i) evolution of acetic acid from hydrolysis of MeCN, (ii) oxidation rate of COM, and (iii) further decomposition of carboxylic acids produced with $\text{RuCl}_3\text{-NaIO}_4$. As to the first possibility, Strausz *et al.* had pointed out that EtCN should be used in place of MeCN for analysis of methyl groups attached to aromatic moieties.³ In fact, treatment of mixture of MeCN, CCl_4 , and H_2O with $\text{RuCl}_3\text{-NaIO}_4$ at 40°C for 24 h was found to afford acetic acid along with small amount of formic acid. These results suggest that, in this solvent system, reliable yields of carboxylic acids having more than three carbons (propionic acid or higher) could be obtained, however, yield of acetic acid is unreliable because of contamination of the decomposition product from the solvent system. Subsequently, we decided to employ EtCN instead of MeCN, as Strausz *et al.* pointed out. Treatment of a mixture of EtCN, CCl_4 , and H_2O with $\text{RuCl}_3\text{-NaIO}_4$ afforded formic, acetic, propionic, and butyric acids, however, yield of acetic acid from EtCN was less than that from MeCN, this suggesting that EtCN is preferable than MeCN for analysis of acetic acid.

Table 1 summarizes the results of treatment of a mixture of lower carboxylic acids with $\text{RuCl}_3\text{-NaIO}_4$ in the two solvent systems (MeCN or EtCN with $\text{CCl}_4\text{-H}_2\text{O}$). In the case of MeCN, 1.4 mmol excess of acetic acid was observed along with 0.74 mmol of formic acid. On the other hands, in the case using EtCN, excess amounts of acetic acid observed reduced to 0.77 mmol. On the basis of these results, we employed two tertiary solvent systems; one containing EtCN for analysis of acetic acid from α -methyl groups and another containing MeCN for analysis of carboxylic acids with more than three carbons (propionic acid or higher).

RICO reaction was carried out using coal model compounds in the solvent system containing EtCN. The reaction of *p*-cresol and *p*-methylanisole proceeded almost completely, while excess acetic acids (1.1 and 0.6 mmol) were produced. These results suggest that evolution of acetic acid from hydrolysis of EtCN was 0.8 ± 0.2 mmol, this value showing good agreement with the value in Table 1. These results also suggested a reactivity of oxygen containing compounds is relatively high. Since coal usually has these functional groups, it is supposed that the reactivity of coal should be high.



In order to get more precise information about the conversion rate of coal under above reaction conditions, we have carried out the following experiments; after the end of RICO reaction of Akabira coal, the resulting reaction mixture was filtered, the filter cake being washed thoroughly with water and CH_2Cl_2 . The residue was found almost completely to be dissolved in water and CH_2Cl_2 , this suggesting that the coal was converted to soluble products almost completely.

RICO Reaction of Three Coals.

Illinois #6 (C 76.6 wt%, daf), Akabira (82.3 %), and Zao Zhuang coals (86.6 %) were employed in this study. As described in the former section, the ion chromatograph was used for analysis of lower carboxylic acids ($\leq\text{C}_6$) and GC and GC-MS were used for higher carboxylic acids ($\text{C}_7\leq$) after esterification with diazomethane. In the case of the analysis of acetic acid produced, EtCN was used as a co-solvent.

Figure 2 shows gas chromatograms for RICO reaction products of Akabira coal, this indicating that Akabira coal has a wide range of alkyl side chains from C_7 to

C₃₀. Figure 3 shows the plot of yield of whole monocarboxylic acids against carbon numbers. From Figure 3, it is clear that yields of carboxylic acids decreased monotonically from acetic acid to valeric acid, this suggesting that methyl group is dominant substituents of aromatic moieties. This is parallel with the findings reported so far. As to yields of lower carboxylic acids, three coals showed very similar distribution of carboxylic acids, indicating aliphatic substitution of aromatic moieties ranging from methyl to hexyl groups are very similar to each other. These results showed a good agreement with the results reported by Stock *et al.*² On the other hands, yields of higher carboxylic acids are different among three coals: a lower rank coal has longer alkyl side chains attached to aromatic moieties than those of higher rank coal.

Since this RICO reaction has some limitations, a precise information about all parts of aliphatic functional groups in COM can be hardly obtained only based on this reaction. However, we have to evaluate this RICO reaction to be able to afford us very useful information about aliphatic portions of COM by the combination use of ¹³C NMR.

Acknowledgment.

The authors greatly acknowledge the analytical assistance provided by Dr. S. Nishida and Mr. N. Shimo-irisa (KN Lab analysis).

References

- (1) Nomura, M.; Matsubayashi, K.; Ida, T.; Murata, S. *Fuel Process. Technol.*, 1992, 31, 169.
- (2) Stock, L. M.; Tse, K.-T. *Fuel*, 1983, 62, 974; Stock, L. M.; Wang, S.-H. *Fuel*, 1985, 64, 1713; Stock, L. M.; Wang, S.-H. *Fuel*, 1986, 65, 1551; Stock, L. M.; Wang, S.-H. *Fuel*, 1987, 66, 921; Stock, L. M.; Wang, S.-H. *Energy Fuels*, 1989, 3, 535.
- (3) Mojelesky, T. W.; Ignasiak, T. M.; Frakman, Z.; McIntyre, D. D.; Lown, E. M.; Montgomery, D. S.; Strausz, O. P. *Energy Fuels*, 1992, 6, 83.

Table 1. Treatment of Free Lower Carboxylic Acid with RuCl₃-NaIO₄ in RCN-CCl₄-H₂O Mixed Solvent^a

	MeCN			EtCN		
	Used amount (mmol)	Observed amount (mmol) ^b	Difference (mmol)	Used amount (mmol)	Observed amount (mmol) ^b	Difference (mmol)
Formic acid	-	0.74	+0.74	-	0.083	+0.083
Acetic acid	1.74	3.11	+1.37	0.87	1.64	+0.77
Propionic acid	0.64	0.50	-0.14	0.68	0.92	+0.24
<i>n</i> -Butyric acid	0.49	0.48	-0.01	0.59	1.31	+0.72
<i>n</i> -Valeric acid	0.19	0.16	-0.03	0.50	0.47	-0.03

^aTreatment of carboxylic acids with RuCl₃ (40 mg) and NaIO₄ (10 g) were carried out in the solvent system containing RCN (20 ml), CCl₄ (20 ml), and H₂O (30 ml) at 40 °C for 24 h. ^bDetermined by an ion chromatograph.

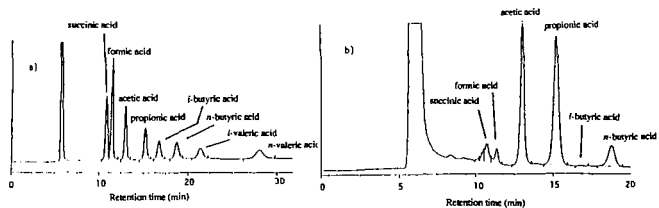


Figure 1. Ion chromatograms of model mixture of lower carboxylic acids (a) and the reaction products from the oxidation of Akabira coal (b)

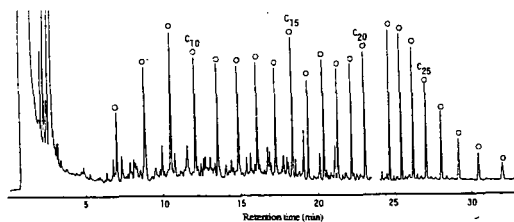


Figure 2. A gas chromatogram for carboxylic acid methyl esters from the oxidation reaction of Akabira coal

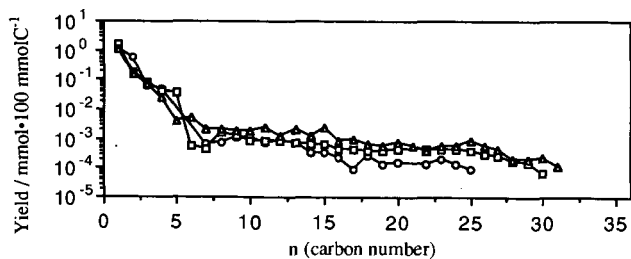


Figure 3. Yields of fatty monoacids, $C_nH_{(2n+1)}CO_2H$, from oxidation of the coals; Illinois No. 6 (Δ), Akabira (\square), and Zao Zhuang coals (\circ)

Absolute Hydrogen Determination in Coal-Derived Heavy Distillate Samples* R. J. Kottenstette, D. A. Schneider and D. A. Loy, Dept. 6212 and 1812, Sandia National Laboratories, P.O.Box 5800, Albuquerque, NM 87185.

Keywords: Hydrogen Analysis, Proton NMR, Heavy Distillate

Introduction

Coal liquefaction involves the use of recycle oils to mix slurry feed materials, and transfer hydrogen to coal as it is digested at high temperatures. Hydrogen donating abilities of recycle oils can be measured using Proton Nuclear Magnetic Resonance ($^1\text{H-NMR}$) Spectroscopy [1], liquefaction testing [2] and dehydrogenation tests [3]. This paper will describe the absolute determination of total organic elemental hydrogen by $^1\text{H-NMR}$ of small (less than one gram) heavy distillate samples produced for research purposes. A comparison will be made between a conventional combustion method and the NMR spectroscopic method.

Organic elemental hydrogen analysis is routinely performed with an automated analyzer having a high temperature combustion zone that is connected to a detector which measures the response of the product water. This technique has its historical roots in the experiments of Lavoisier [4] who in the 1770's burned alcohol and other combustible organic compounds in oxygen to gravimetrically determine the product water and carbon dioxide. Quantitative recovery and measurement of the combustion products were demonstrated by Berzelius and Liebig in the early 1800's. The work of Pregl [5] at the turn of this century advanced this technique to a high degree with the introduction and perfection of microchemical techniques (sample sizes in the milligram range). With the advent of instrumental electronics, automated microanalysis gradually replaced the gravimetric techniques mainly because of increased analysis speed. Modern automated organic elemental analysis consists of combusting the sample in the presence of a solid oxidant and sweeping the products into a thermal conductivity or infrared detector [4,5]. An alternative technique for the detection of hydrogen is to react the product water with carbonyldiimidazole to generate a quantitative amount of carbon dioxide which is measured by a coulometric titration [6].

The development of Proton Nuclear Magnetic Resonance Spectroscopy has led to the description and qualitative classification of hydrogen in organic compounds. These techniques have been especially helpful in describing hydrogen as it is classified into aliphatic, aromatic and hydroaromatic groupings [1,2,3]. In addition, low resolution proton $^1\text{H-NMR}$ has been successfully used to determine absolute amounts of hydrogen in a variety of petroleum fractions [7,8]. Our technique involves simple integration of high resolution $^1\text{H-NMR}$ spectra with careful attention given to sample preparation and spectral integration.

Experimental

Materials

Heavy distillate samples from Run 262 at the Wilsonville Advanced Coal Liquefaction Pilot Plant were supplied from CONSOL inc. The samples came from the V1074 stream and had an approximate boiling range of 650°F to 1050°F. The samples were hydrotreated in a laboratory scale trickle-bed reactor at 365°C. 1,2,3,6,7,8 hexahdropyrene (H_6Py) and deuterated chloroform (99.96%D) were purchased from Aldrich, naphthyl dibenzyl methane (NBM) was acquired from TCI America, acetanilide was obtained from Perkin Elmer and paraffin oil was purchased from LECO corporation.

Procedure

Combustion Analysis - Hydrogen amounts were determined with a Perkin Elmer model 2400 CHN analyzer. The combustion temperature was set at 925°C and the reduction tube was set at 640°C. Since the heavy distillate samples are viscous, the "standard" tin capsules could be used to contain the samples. Careful attention was paid to sample size since larger samples (>3mg) often lead to incomplete combustion or an "overload" condition which gives erratic hydrogen results. The analyzer is conditioned before sample analysis by running successive external standard samples until the hydrogen output stabilizes (usually one to two samples). The conditioning samples always show a lower than expected hydrogen value if they are preceded by a blank determination. External standards for the combustion technique include acetanilide, paraffin oil, and NBM.

Proton NMR - A Bruker AM 300 FT-NMR spectrometer was used to determine hydrogen mass percents. Heavy distillate samples were prepared in CDCl_3 at a concentration of 30.0 mg per 1.0 mL of solvent. External standard samples (H_6Py) were prepared at concentrations ranging from 0.5 mg to 45.0 mg per 1.0 mL of solvent to generate a calibration curve. All samples were weighed in 20 mL sample vials; CDCl_3 was introduced with a syringe. Solutions were immediately capped, mixed thoroughly, and transferred to 5 mm NMR tubes with Pasteur pipettes. Spectra were acquired with a total time of 2.36 seconds between 20 degree RF pulses. At low external standard concentrations (0.5 mg-30 mg), 512 scans per sample were acquired to improve signal to noise ratios. It was found that the number of scans could be reduced from 512 to 64 for distillate samples and more concentrated external samples (30 mg to 45 mg). H_6Py standard samples of 30.0, 37.7, and 45.0 mg/mL were prepared and analyzed daily for distillate analyses. CDCl_3 acts as a de facto internal standard having a chemical shift of 7.27 ppm; the samples are integrated between 10.5 and 0.5 ppm. Before integrating the spectra, the baseline curvature is corrected using a spline-fit algorithm incorporated in the Bruker software. Area counts due to the CDCl_3 of approximately 0.2 are considered negligible compared to the output for a 30 mg H_6Py standard (arbitrarily set to give 100.0 area counts). NBM was also analyzed to check the accuracy of the method.

Results and Discussion

Previous tests in our laboratory showed that heavy distillate samples acquired less than 1 wt% additional hydrogen during catalytic hydrogenation even under the most favorable of conditions. Therefore, determining hydrogen concentration changes on the order of 0.3 to 1.0 wt% has become necessary. Analyses for hydrogen in our laboratory (using the CHN analyzer) have been deemed acceptable if the precision of the analysis was $\pm 0.3\text{wt}\%$. This was not acceptable when trying to detect the small hydrogen increases in the hydrotreated distillates.

Figure 1 shows a linearity plot of area (detector response) vs. absolute hydrogen content of a wide variety of model compounds and a known heavy distillate. The data in Figure 1 shows the calibration curve constrained through the origin. This curve illustrates that a one-point calibration (such as is commonly used in automated CHN analyses) would underestimate the hydrogen in samples such as acetanilide (6.71% H) and overestimate the amount of hydrogen in paraffin oil (13.63% H). A one point calibration becomes especially inaccurate if the standard has a hydrogen content much different than the sample to be analyzed. Since the recommended sample weight for the combustion analysis should fall in the narrow range between one and three milligrams, the difficulty in establishing a linear calibration curve is compounded. One solution to this dilemma is to plot the raw data against a wide range of known hydrogen standards. This is the method illustrated in Figure 2, in which the calibration curve is not constrained through the origin. This linear regression curve-fit has a correlation coefficient of 0.994 and provides a more reliable basis for analysis of samples within the range of the calibration curve (hydrogen content between 6.71% and 13.63%).

Figure 3 shows a four point calibration curve of area vs. hydrogen content for different amounts of hexahydropyrene in deuterated chloroform as analyzed with the ^1H -NMR technique. This curve has excellent linearity over its range giving a linear regression correlation coefficient of 0.9999. The ^1H -NMR technique requires only one type of standard at different concentrations rather than multiple standards for the combustion technique. The X-axis in Figure 3 is an order of magnitude larger than the corresponding axis for the combustion technique since a typical sample weight for the ^1H -NMR analysis is ten times larger (30 mg vs. >3 mg) than for the microcombustion technique. The Y-axis presents the integrated area in arbitrary units with the 30mg/mL H_6Py standard assigned a value of 100.0.

Table 1 shows the analytical results and uncertainties for a series of heavy distillate samples and model compounds typically used in coal liquefaction research. Hydrogen concentration is presented as the average of four runs for the combustion analyses and the average of three determinations for the ^1H -NMR analyses. The theoretical hydrogen content is shown for the two model compounds, H_6Py ($\text{C}_{16}\text{H}_{16}$) and NBM ($\text{C}_{22}\text{H}_{25}$). The distillate samples were taken at different times "on-stream" with the highest hydrogen content being for the sample taken after one hour when the catalyst was the freshest. Hydrogen content decreases with time on-stream until at ten hours the reaction temperature was raised by 10°C to increase the rate of hydrogenation. Indeed this sample showed a slight increase of 0.1 wt% hydrogen. In general the absolute hydrogen analyses for the two methods are remarkably close with the largest difference between the averages being no more than 0.16%. The standard deviations are larger for the ^1H -NMR determinations in general with the exception of the H_6Py sample which gave a very low (0.05%) standard deviation. Figure 4 is a parity plot comparing the results from the two

techniques. Again the correlation coefficient from a linear regression gave a good linear fit, thus the two techniques compare well, at least in the range of hydrogen concentrations studied.

Figure 5 shows an analysis of hydrogen distribution according to three broad categories. Alkyl protons are defined as alkyl α , alkyl β , and gamma having $^1\text{H-NMR}$ chemical shifts of 2.5-2.0, 1.4-1.0, and 1.0-0.5 ppm respectively. Condensed aromatic and uncondensed aromatic hydrocarbons have chemical shifts of 10.5-7.15 and 7.15-4.7 ppm, respectively. Hydroaromatic hydrogens are defined as cyclic α and cyclic β protons with proton shifts of 4.7-2.5 and 2.0-1.4 ppm respectively. Results in Figure 5 illustrate the additional benefit of the $^1\text{H-NMR}$ technique. The $^1\text{H-NMR}$ spectrum can quantitatively analyze the hydrogen species in a heavy distillate sample (not possible with combustion elemental analyses). These proton distributions can then be used to evaluate the quality of a liquid (in our case for hydrogen donation purposes).

Conclusion

Elemental hydrogen determinations giving sample repeatability of less than 0.1 wt% at the 10 wt% level have not been demonstrated with either the combustion or the $^1\text{H-NMR}$ technique. However, excellent correlation has been achieved between the combustion method and the $^1\text{H-NMR}$ method, giving results for model compounds which are quite good (see Table 1). A refinement of the combustion analysis has been shown by improving the calibration procedure from the typically used single point calibration. Small differences in hydrogen content were noted for a series of hydrotreated heavy distillate samples. In addition the absolute determination of hydrogen by $^1\text{H-NMR}$ can also yield information about the relative amounts of aromatic, alkyl and hydroaromatic protons. The $^1\text{H-NMR}$ technique can also be applied to evaluate absolute hydrogen content when a rapid combustion technique is not immediately available.

Acknowledgments

We would like to thank Ed Huffman and Sue Zeller of Huffman Laboratories for their helpful discussions about combustion and detection techniques.

References

- 1) J. Delpuech, D. Nicole, M. Le Roux, P. Chiche and S. Pregerman. *Fuel*, 1986, Vol.65, p1600.
- 2) R. A. Winschel, G. A. Robbins, and F. P. Burke. *Fuel*, 1986, Vol.65, p 526.
- 3) J.W. Tierney and I. Wender, *Coal Liquefaction Process Streams Characterization*, February, 1994. DOE/PC 89883-87.
- 4) T.S. Ma and R.C. Rittner, *Modern Organic Elemental Analysis*. New York, Marcel Dekker, 1979.
- 5) G. Ingram, *Methods of Organic Elemental Microanalysis*. New York, Reinhold, 1962.
- 6) M. Houde, J. Champy. *Microchemical Journal*, 1979, Vol. 24, p 300.
- 7) P. T. Ford, N.J. Friswell, and I. J. Richmond. *Analytical Chemistry*, 1977, Vol.49, No.4, p 594.
- 8) M. Bouquet. *Fuel*, 1985, Vol. 64, p 226.

* This work was supported by the U. S. Department of Energy at Sandia National Laboratories under contract DE-AC04-94AL85000.

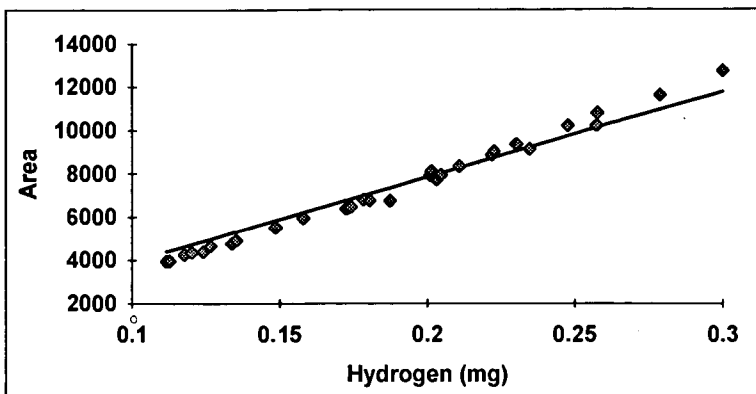


Figure 1. Calibration Curve for Combustion Elemental Hydrogen Analysis (forced through zero, $r^2=0.971$)

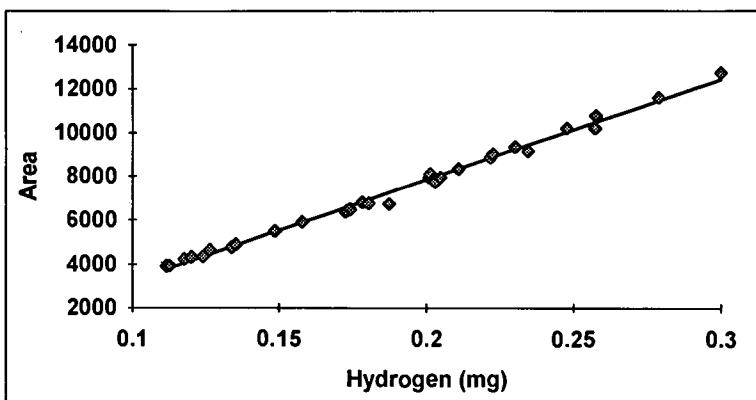


Figure 2. Calibration Curve for Combustion Elemental Hydrogen Analysis ($r^2 = 0.994$)

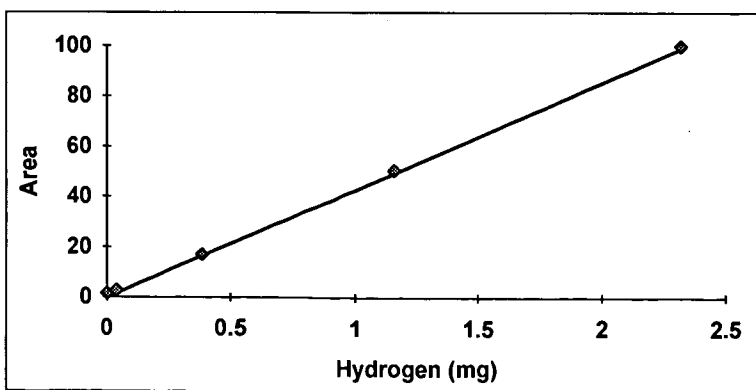


Figure 3. Calibration Curve for Proton NMR Hydrogen Analysis using Hexahydroindole ($r^2 = 0.999$)

Table 1. Comparison of Combustion and NMR Hydrogen Data for Flow Reactor Product (Heavy Distillate)

Sample	%H Theory	%H Combustion	Std. Dev.	%H NMR	Std. Dev.
V1074	NA	9.66	0.23	9.68	0.12
Reactor Feed	NA	8.57	0.11	8.42	0.21
1 Hour	NA	9.33	0.06	9.34	0.37
2.5 Hour	NA	8.97	0.11	9.04	0.27
7 Hour	NA	8.81	0.06	8.94	0.30
10 Hour (+10°C)	NA	8.92	0.14	9.04	0.20
H6Py*	7.74	7.74	0.17	7.75	0.05
NBM**	6.87	6.98	0.10	6.83	NA

* 1,2,3,6,7,8 Hexahdropyrene. ** Naphthyl Dibenzyl Methane

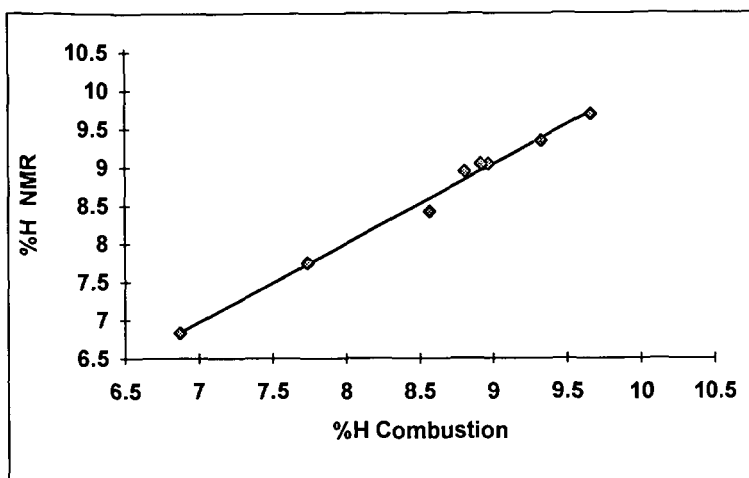


Figure 4. Comparison of Combustion Analysis with NMR Analysis ($r^2 = 0.993$)

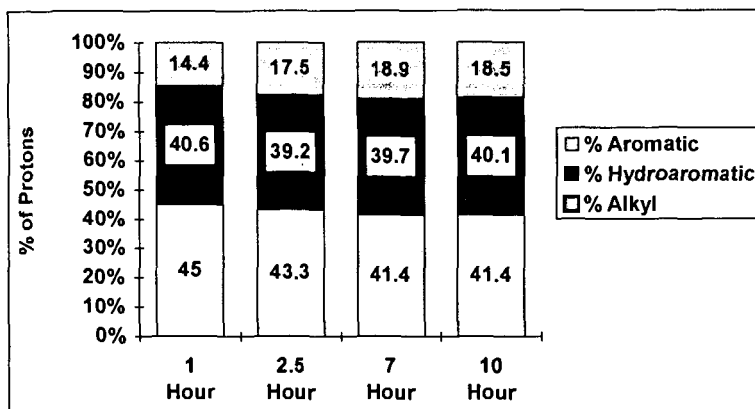


Figure 5. Hydrogen Distribution in Heavy Distillate Sampled at Intervals from Flow Reactor (Proton NMR)

TWO-DIMENSIONAL HPLC AND GC-MS OF OILS FROM CATALYTIC COAL LIQUEFACTION

Ajay K. SAINI and Chunshan SONG*

Fuel Science Program, Department of Materials Science and Engineering
The Pennsylvania State University, University Park, PA 16802

Keywords: Normal-phase, HPLC, GC-MS, Oils, Coal Liquefaction

ABSTRACT

We have employed normal-phase HPLC with photo diode array detector and GC-MS techniques to characterize the oils (hexane soluble fraction) from the catalytic and non-catalytic liquefaction of Wyodak subbituminous coal at 400 °C under 6.9 MPa H₂ pressure. The use of a dispersed Mo catalyst afforded much higher oil yield than the non-catalytic run. HPLC reveals that the oils from the catalytic runs contain more phenolic compounds and more of heavier components as compared to the oils from non-catalytic run. On the other hand, GC-MS shows that there is a significant amount of long-chain alkanes in the oils, ranging from C₁₁ to C₃₅. The analytical results from the two techniques appear to be complementary to each other. The oils contain some heavier components which are detectable by HPLC but undetectable by GC-MS. GC-MS of HPLC fractions of the oils from the catalytic run confirmed the presence of significant amount of phenols and indanols.

INTRODUCTION

Catalytic coal liquefaction is a potential route to alternate liquid transportation fuels and aromatic chemicals (Song and Schobert, 1993). However, the characteristics of the liquefaction products must be clarified before effective implementation. Certain coal-derived aromatic compounds can be used to make high-value chemicals through shape-selective catalysis (Song and Kirby, 1993, 1994; Song and Moffatt, 1993, 1994; Schmidt and Song, 1994). The non-fuel use of coal liquids could improve the economics of liquefaction significantly, although the majority of the coal liquids may be used for transportation fuels (Song and Schobert, 1993; Derbyshire et al., 1994).

The present work aims at clarifying the compositional characteristics and molecular components of oils from catalytic liquefaction of Wyodak subbituminous coal using a dispersed Mo catalyst. This paper reports on the oil analysis using normal-phase high-performance liquid chromatography (HPLC) with photo diode array (PDA) detector which allows continuous two-dimensional scanning analysis of HPLC elutes over UV wavelength range.

While reversed-phase HPLC is popular for analysis of a variety of samples that are soluble in water or polar organic solvents (Poole & Poole, 1991; Wise et al., 1993), normal-phase HPLC can be used for analyzing components dissolved in non-polar organic mixtures (Snyder et al., 1988). Reversed-phase HPLC is characterized by strong interactions between the polar mobile phase and various sample molecules. However, coal-derived oils are not soluble in the common solvent systems (such as water-acetonitrile) for reversed-phase HPLC. In normal-phase HPLC, sample-adsorbent (stationary phase) or solvent-adsorbent interactions are strong but sample-solvent interactions are relatively weak. Neutral organic solvent (hexane) and weakly polar solvent (methylene chloride) can be used for normal-phase HPLC, which are also good solvents for coal-derived oils. Some bonded-phase HPLC columns for normal-phase HPLC have become commercially available recently. The conventional monochromator UV detector has limited the amount of information that can be extracted from HPLC, since one particular wavelength may not be suitable for analyzing all the compounds in the complex mixtures (Snyder et al., 1988; Fetzer et al., 1993). PDA detector represent a recent development in the HPLC detection system, which allows sample analysis over UV range. Recently PDA has been demonstrated to be very useful in the analysis of PAHs in heavy liquids either by reversed-phase (Liu et al., 1992) or normal-phase HPLC (Clifford et al., 1994).

EXPERIMENTAL

Reagents and Materials. All the oils were derived from liquefaction of Wyodak subbituminous coal, which is one of the U.S. Department of Energy Coal Samples (DECS-8) maintained in the DOE/Penn State Sample Bank. Ammonium tetrathiomolybdate (ATTM) was dispersed as a catalyst precursor on to coal (1 wt% Mo on dmmf basis) by incipient wetness impregnation from its aqueous solution. ATTM is expected to generate molybdenum sulfide particles on coal surface upon thermal decomposition at ≥ 325 °C (Artok et al., 1993). The impregnated or the raw coal samples were dried in a vacuum oven at 100 °C for 2 h before use. The liquefaction was carried out in 25 mL tubing bomb reactors at 400°C for 30 min (plus 3 min heat up) under an initial H₂ pressure of 6.9 MPa. The oils are hexane-soluble fraction of liquefaction products. Detailed results of liquefaction may be found elsewhere (Song et al., 1993).

Various reagents were used as standards for confirmation of identification of HPLC and GC-MS peaks. The following reagents were purchased from Aldrich: phenol (99+%), 1,2,3,4-tetrahydro-1-naphthol (97%), tetralin (99%), 1-methylnaphthalene (98%), 9,10-dihydrophenanthrene (94%), and 1-naphthol (99+%). Sixteen polycyclic aromatic hydrocarbons were purchased from Supelco as a mixture defined as EPA Mixture 610. This mixture contains the following components: naphthalene,

* Corresponding author.

acenaphthylene, acenaphthene, fluorene, phenanthrene, anthracene, fluoranthrene, pyrene, benzo(a)fluoranthene, chrysene, benzo(b)fluoranthene, benzo(k)fluoranthene, benzo(a)pyrene, dibenzo(a,h)anthracene, benzo(g,h,i)perylene, and indeno(1,2,3,c,d)pyrene.

High Performance Liquid Chromatography (HPLC). The Waters HPLC system consists of U6K Universal Injector, 600E Powerline Multi-Solvent Delivery Module, and 991 Photodiode Array (PDA) Detector. The 600 Powerline Module serves as a system controller for setting up all solvent gradient conditions, injection and detection parameters and wavelength ranges. The PDA detector is capable of continuous monitoring and acquisition of all UV/VIS wavelengths from 190 to 800 nm. Through the use of computer, the 991 PDA operates exclusively with Millennium 2010 Chromatography Manager software system, which allows fully automated data acquisition, processing, and reporting as well as 3-D graphics. The resolution of the PDA detection is 4.7 nm.

The column used for HPLC was a Hypersil PAH-2 purchased from Keystone Scientific, Inc., which is a commercially available column (150 x 4.6 mm i.d.) made by Shandon Scientific, Inc., U.K. The Hypersil PAH-2 has been developed using tetrachlorophthalimidopropyl bonded silica. This type of column can be used for analyzing the polyaromatic compounds dissolved in organic mixtures such as crude oils and coal liquids. Classical n-alkyl bonded phases are not suitable for analyzing such non-polar mixtures.

For HPLC analysis, the oils were diluted in 50%-50% hexane-methylene chloride solution (approximate concentration: 1 mg/mL) and filtered through 0.2 µm membrane filter (Supeco Iso-Disc P-32) attached to a syringe. This assures that the solution to be analyzed is free of suspended micron-sized particles. For each HPLC analysis, about 10-20 µL of a sample solution was injected and the solvent elution was controlled by the gradient program, as shown in Table 1. Gradient elution was used: hold at 100% n-hexane for 20 min, from 100% hexane to 50% hexane-50% methylene chloride between 20 to 80 min, and to 100% methylene chloride between 80 to 100 min, followed by a 20 min hold at 100% methylene chloride. The flow rate of the mobile phase was 0.8 mL/min. The data acquisition of all the oils and standards were made in the UV wavelength range of 200 to 400 nm at the rate of 30 scans/minute. All the HPLC analyses were conducted at ambient temperature. HPLC fractions were collected for some representative samples and analyzed by GC-MS.

Gas Chromatography-Mass Spectrometry (GC-MS). The HPLC fractions of oil were analyzed on a HP 58901 GC coupled with an HP 5971A Mass Selective Detector (MSD). The column used for capillary GC was J&W DB-5 column: 30 m x 0.25 mm i.d. fused silica capillary column coated with 5% phenyl-95% methyl polysiloxane with a 0.25 µm film thickness. More analytical details may be found elsewhere (Song et al., 1994). In a typical GC-MS run, about 1 µL of the diluted methylene chloride solution of the sample was injected through the split/splitless injector in the splitless mode, with a 5 min delay of ionization to cut off the solvent. The GC oven in GC-MS was temperature-programmed as follows: 5 min isothermal holding at 40°C, subsequent heat-up to 280°C at 4°C/min, followed by isothermal holding at 280°C for 30 min.

RESULTS AND DISCUSSION

HPLC of Oils

Figures 1 and 2 show the 3-dimensional HPLC plots for oils from non-catalytic and catalytic runs, respectively, where the signal intensity (Z axis) is plotted against the UV wavelength (X, 247-390 nm) and retention time (Y). The use of a dispersed molybdenum sulfide catalyst increased oil yield from 10 to 46 wt% (based on dmmf coal). Apparently, the dispersed catalyst not only improved coal conversion, but also altered the compositional features of oils, as can be seen from the 3-D HPLC plots. The 3-D plots indicate that oils from the catalytic run contain more components that have either larger aromatic ring-size or are more polar, as compared to the non-catalytic runs.

To assist in the peak assignments, we performed HPLC analysis of two standard mixtures. Figure 3 shows 3-D plot for a standard containing 16 PAHs. The UV spectra of some peaks eluted before 20 min in the PAH mixture are in the similar wavelength range as those peaks in the real sample of oil from catalytic coal liquefaction. However, it becomes clear that the intense peaks in the 30-65 min range in the oil from catalytic runs (Figure 2) are not due to condensed PAHs (Figure 3). Figure 4 shows a maxiplot (maximum UV absorbance corresponding to each retention time unit) for the PAH standard mixture, in which the peaks were identified based on the information from the column supplier (Keystone Scientific, 1994).

As oxygen compounds are also possible products, we also analyzed the HPLC profiles of several pure polar compounds. Figure 5 gives a maxiplot for the phenolic mixture containing phenol, 1-naphthol, 1,2,3,4-tetrahydro-1-naphthol, and 1-indanol as well as aromatic hydrocarbons including tetralin, 1-methylnaphthalene, and 9,10-dihydrophenanthrene. The results with phenolic standards are very useful in understanding the differences between oils from non-catalytic and catalytic runs. Some major peaks around 60 min in the 3D-plot in Figure 2 have UV spectra similar to those of phenolic compounds.

The sample retention in normal-phase HPLC is governed by adsorption to the stationary phase. As PAHs are electron-donors, the chemically bonded electron-acceptor stationary phase (PAH-2 phase) allows the selective retention of PAHs in non-polar mobile phases. It is interesting to note that all the phenolic compounds interact so strongly with the tetrachlorophthalimidopropyl bonded-phase that their retention times (Figure 5) are longer than those of all the 16 PAHs (Figure 4). These results also indicate that, for HPLC analysis using PAH-2 column, one should be very careful in determining the ring size of aromatic compounds solely based on normal-phase HPLC. The most illustrative example is that the retention time of phenol, a single-ring compound, is even longer than that of a six-ring PAH, indeno(1,2,3,c,d)pyrene.

The HPLC results seem to imply that, as compared to the oils from non-catalytic run (Figure 1), the

oils from the catalytic runs (Figure 2) contain more phenolic compounds and more of heavier components. At first glance, these HPLC results are surprising, as a good catalyst was used in the liquefaction. The present HPLC results, however, are in agreement with our earlier work on GPC. We have analyzed the molecular size distribution of coal-derived oils using HPLC operating in the GPC mode with polystyrene gel column (Song et al., 1988, 1989). The GPC results suggested that the oils from catalytic runs have more components with larger molecular sizes.

GC-MS of HPLC Fractions

To clarify the molecular components and to identify the HPLC peaks, we have collected eleven HPLC fractions of the oils derived from catalytic liquefaction. Figure 6 shows the maxplot together with the number and retention time ranges of individual HPLC fractions. We have analyzed all the HPLC fractions using GC-MS. The results are summarized below.

GC-MS shows that all the HPLC peaks and fractions represent a mixture rather than a single component. Fraction 1 (2-3.5 min) is a co-elute of monoaromatic compounds with long-chain alkanes, ranging from C₁₁ to C₃₅. The aromatic compounds include alkylbenzenes, indanes, and tetralins. The HPLC peak intensity for this fraction does not include long-chain alkanes. Fraction 2 (3.5-6.0 min) consists of naphthalene, methyl-naphthalene, and alkylbiphenyls (or acenaphthenes). Fraction 3 (6-8.0 min) corresponds to a small peak in the HPLC and contains C₂-naphthalenes and other two-ring compounds. In Fraction 4 (8-10.5 min) we detected phenanthrene and a C₄-alkyl-substituted phenanthrene. Fraction 5 (10-13.5) contains many three-ring compounds, phenanthrene and its derivatives. Fraction 6 (14-18 min) seems to give a very noisy GC-MS total ion chromatogram (TIC), but some compounds in this fraction are three-ring compounds. Fraction 7 (14-18 min) contains four-ring compounds including fluoranthene (m/z: 202) and pyrene (m/z: 202). Fraction 8 (21-30 min) contains several peaks with same molecular ion of m/z 216, and are probably methylfluoranthene and methylpyrene.

We detected significant amount of phenolic compounds in the fractions between HPLC retention time of 30 to 60 min. Beginning with fraction 9 (30-38 min), phenols and indanols were observed. Fraction 10 (38-45 min) contains mainly C₁-, C₂-, C₃- and C₄-phenols. Fraction 11 (50-60 min) is the dominant phenolic fraction. It contains phenol, C₁-, C₂-, C₃-phenols and indanol, C₁- and C₂-indanols. These GC-MS results in combination with HPLC results clearly revealed that the oils from catalytic liquefaction of Wyodak subbituminous coal using a dispersed molybdenum sulfide catalyst contain more phenolic compounds (30-65 min range in HPLC) and more heavier components (70-110 min range in HPLC), as compared to oils from the non-catalytic run at 400°C for 30 min under 6.9 MPa H₂. The HPLC retention times for peaks with this sample are not exactly the same to those for the PAH and phenolic standards (due to some difference in instrumental conditions).

In addition, the fact that a catalytic run gives more phenolic compounds also provides further evidence that the initial reaction involves the cleavage of O-C bonds in coal. The stabilization of the radicals from these bond cleavages by hydrogen transfer can produce phenolic compounds, otherwise these highly reactive radicals would seek self-stabilization through retrogressive cross-linking reactions. The use of a dispersed Mo catalyst facilitates the transfer of hydrogen to radicals.

It should be mentioned that Clifford et al. (1994) analyzed several coal liquefaction process streams (oils) by normal-phase HPLC. They detected many polyaromatic compounds but did not observe oxygen compounds in their samples. The samples they analyzed represent highly 'upgraded' products, because they were derived from two-stage catalytic liquefaction of coals in Wilsonville pilot plant and HRI pilot plant. The present samples, however, were derived from primary (one-stage) liquefaction of Wyodak subbituminous coal under mild conditions (400°C, 30 min).

ACKNOWLEDGMENTS

We wish to thank Prof. Harold Schobert for his encouragement. This work was supported by the U.S. Department of Energy under contract No. DE-AC22-91PC91042.

REFERENCES

- Artok, L.; Davis, A.; Mitchell, G.D.; Schobert, H.H. *Energy & Fuels*, 1993, 7, 67.
- Clifford, D.J.; McKinney, D.E.; Hou, L.; Hatcher, P.G. *Coal Liquefaction Process Streams Characterization and Evaluation*. Topical Report. High Performance Liquid Chromatography (HPLC) of Coal Liquefaction Process Streams Using Normal-Phase Separation with UV Diode Array Detection. DOE/PC 89883-85, January 1994, 47 p.
- Derbyshire, F.; Jagtoyen, M.; Fei, Y. Q.; Kimber, G. *Am. Chem. Soc. Div. Fuel Chem. Prepr.*, 1994, 39 (1), 113.
- Fetzer, J.C.; Biggs, W.R. *J. Chromatogr.*, 1993, 642, 319.
- Liu, Y.; Eser, S.; Hatcher, P.G. *Am. Chem. Soc. Div. Fuel Chem. Prepr.*, 1992, 37, 1227.
- Poole, C.F.; Poole, S.K. *Chromatography Today*. Elsevier: Amsterdam, 1991, 1026 p.
- Schmitz, A.; Song, C. *Am. Chem. Soc. Div. Fuel Chem. Prepr.*, 1994, 39 (3-4), in press.
- Snyder, L.R.; Glajch, J.L.; Kirkland, J.J. *Practical HPLC Method Development*. John Wiley & Sons: New York, 1988, 260 p.
- Song, C.; Hanaoka, K.; Ono, T.; Nomura, M. *Bull. Chem. Soc. Japan*, 1988, 61, 3788.
- Song, C.; Hanaoka, K.; Nomura, M. *Fuel*, 1989, 68, 287.
- Song, C.; Kirby, S. *Am. Chem. Soc. Div. Petrol. Chem. Prepr.*, 1993, 38 (4), 784.
- Song, C.; Moffatt, K. *Am. Chem. Soc. Div. Petrol. Chem. Prepr.*, 1993, 38 (4), 779.
- Song, C.; Schobert, H. H. *Fuel Processing Technol.*, 1993, 34, 157.
- Song, C.; Saini, A.K.; Schobert, H. H. *Am. Chem. Soc. Div. Fuel Chem. Prepr.*, 1993, 38 (3), 1031.
- Song, C.; Lai, W.-C.; Schobert, H. H. *Ind. Eng. Chem. Res.*, 1994, 33, 534.
- Song, C.; Moffatt, K. *Microporous Materials*, Elsevier, 1994, in press.
- Song, C.; Kirby, S. *Microporous Materials*, Elsevier, 1994, in press.
- Wise, S.A.; Sander, L.C.; May, W.E. *J. Chromatogr.*, 1993, 642, 329.

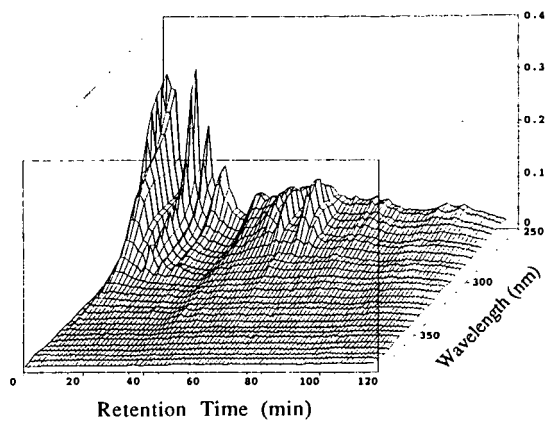


Figure 1. 3-D HPLC plot of oils from non-catalytic liquefaction of Wyodak subbituminous coal.

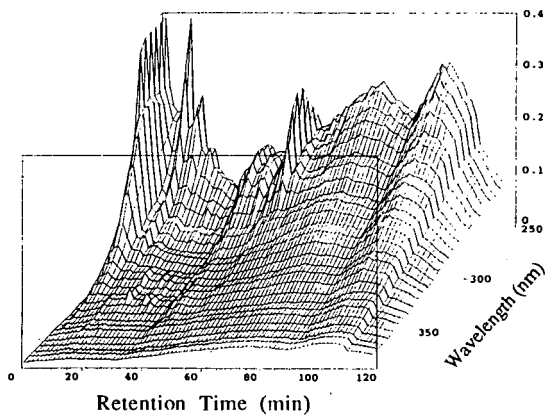


Figure 2. 3-D HPLC plot of oils from catalytic liquefaction of Wyodak subbituminous coal.

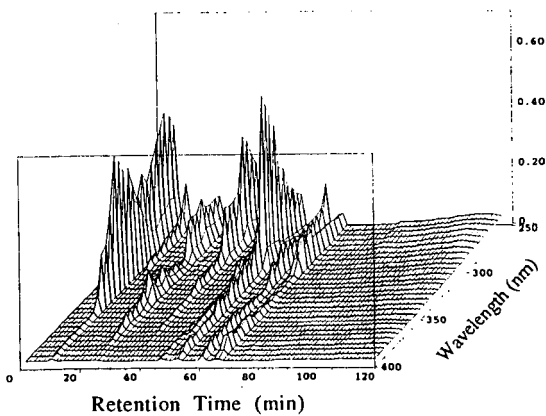


Figure 3. 3-D HPLC plot of a mixture of 16 polynuclear aromatic hydrocarbons (PAHs).

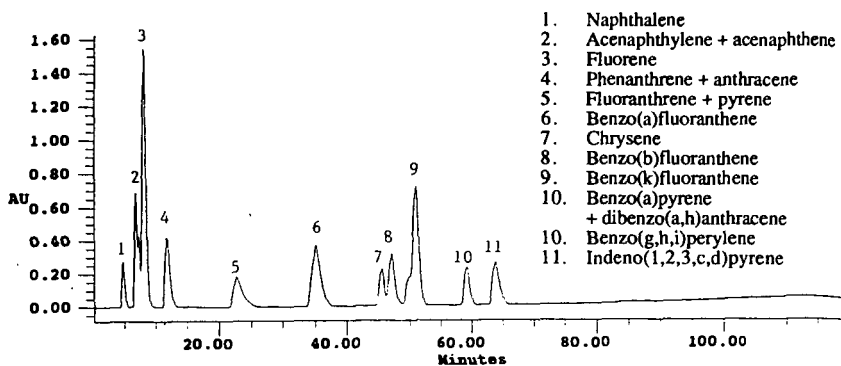


Figure 4. HPLC maxplot of PAH standard containing 16 PAHs.

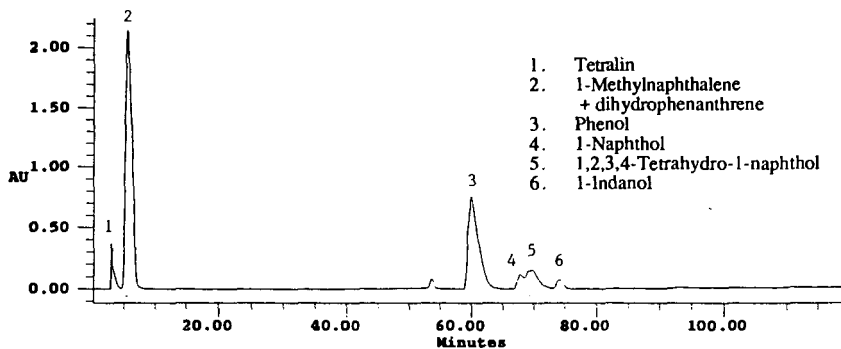


Figure 5. HPLC maxplot of phenolic standard mixture.

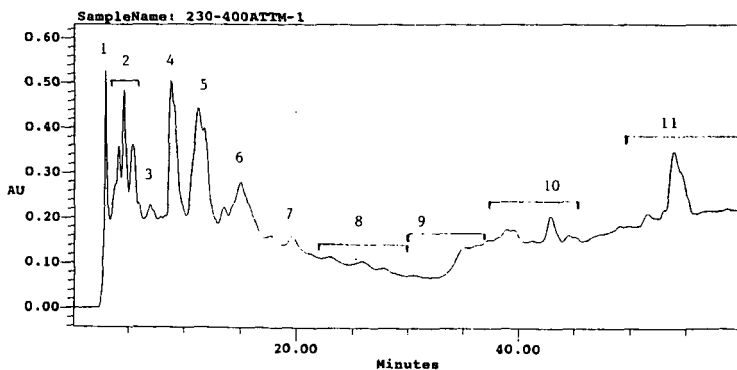


Figure 6. Expanded HPLC maxplot of oils from catalytic liquefaction at 400°C for 30 min. The number and accompanying lines indicate the retention time range of HPLC fractions collected.

USE OF HYDROLYSIS-MS TO PROBE THE HYDROCRACKING OF DIPHENYLALKANE LINKAGES IN THE SOLID STATE

S.D. Brown ⁽¹⁾, O. Sirkecioglu ⁽¹⁾, K. Ismail ⁽¹⁾, J. Andresen ⁽¹⁾, C.E. Snape ⁽¹⁾, A.C. Buchanan III ⁽²⁾ and P.F. Britt ⁽²⁾

- (1) University of Strathclyde, Department of Pure & Applied Chemistry, Glasgow G1 1XL, UK
(2) Chemistry and Analytical Sciences Division, Oak Ridge National Laboratory, Oak Ridge, Tennessee 37831, USA

Keywords: hydrolysis, resites, silica-immobilised substrates

INTRODUCTION

Diphenylalkanes have been extensively used as model substrates to probe the free radical mechanisms involved in C-C bond cleavage reactions during coal liquefaction ⁽¹⁾. However, the fact that the macromolecular structure in coals is undoubtedly subject to highly restricted motion suggests intuitively that free radical pathways are likely to be somewhat different from those encountered in the vapour phase. Indeed, this has been confirmed by the use of silica-immobilised substrates where bimolecular reaction steps are significantly perturbed for diphenylalkanes compared to the corresponding vapour phase reactions ⁽²⁻⁵⁾. For pyrolysis studies, these model substrates have the inherent advantage that they do not soften and so remain in the reactor. Thus, immobilised substrates have considerable potential for modeling coal pyrolysis phenomena, particularly the effects of high hydrogen pressures (hydrolysis). Indeed, for immobilised benzene, the Si-O-C bond linking the substrate to the surface is reasonably stable and does not cleave until above 500°C (peak maximum at 550°C) with 150 bar hydrogen pressure ⁽⁶⁾. For immobilised diphenylmethane (DPM), it was demonstrated previously that the use of 150 bar hydrogen pressure and a sulphided Mo catalyst both reduced the peak evolution temperatures for benzene and toluene clearly demonstrating their separate contributions to promoting C-C bond cleavage ⁽⁶⁾.

An alternative class of materials to immobilised substrates that should prove equally as suitable for modeling pyrolysis phenomena are cured phenol-formaldehyde resins. These offer the option of incorporating a wide variety of hydrocarbon and heteroatomic moieties into the basic phenolic macromolecular structure. A series of co-resites were recently prepared from phenol and, as the second component, a series of sulphur-containing precursors, namely 2-hydroxydibenzothioephene, *p*-hydroxydiphenylsulphide, 4-hydroxyphenylbenzylsulphide and 4-hydroxythioanisole ⁽⁷⁾. These precursors have also been used previously for the preparation of silica-immobilised substrates ⁽⁸⁾ which, together with the resites have been used as calibrants in temperature programmed reduction ⁽⁷⁻⁹⁾. To investigate the hydrocracking of diphenylalkane linkages in the solid state with the additional aim of elucidating how the nature of a particular substrate might influence the reaction pathways, hydrolysis experiments with on-line mass spectrometric analysis have been conducted on silica-immobilised substrates, phenolic resites and a polystyrene-divinylbenzene network using hydrogen pressures of 5 and 150 bar.

EXPERIMENTAL

Substrates and their synthesis The diphenylmethane co-resites were prepared using the procedure described by Bar and Aizenshtat ⁽¹⁰⁾ which was used previously for the sulphur-containing resites ⁽⁷⁾. A total phenol to formaldehyde mole ratio of 1:2.5 was used with sodium hydroxide as catalyst for the condensation reaction, a mole ratio of 0.1 with respect to phenol being employed. The mole ratio of phenol to the monohydroxydiphenylalkanes (diphenylethane and propane) was 3:1 to ensure that a reasonably high degree of crosslinking was achieved in the initial resoles. DSC indicated that co-resoles prepared with a mole ratio of only 1:1 melted to a considerable extent in the temperature range,

250-280°C. The co-resites were cured in an oven purged with nitrogen gas at a temperature of 200°C. Solid state ^{13}C NMR was used to monitor the conversion of the ether/alcohol functional groups to methylene bridges during curing. Cross polarisation/magic-angle spinning (CP/MAS) spectra were obtained using a Bruker MSL100 instrument operating at 25 MHz for carbon.

The silica-immobilised samples were prepared from the appropriate phenol as previously described (2-5). The loadings of the diphenylmethane (DPM) and diphenylethane (DPE) substrates investigated here are summarised below. These were determined by hydrolysing the substrates with base and conducting GC analysis of the resultant phenols which were silylated.

	Loading, mmol g ⁻¹
Diphenylmethane, normal	0.45
Dideuterated diphenylmethane (PhCD ₂ Ph)	0.31
Co-attached diphenylmethane/tetralin	0.28/0.18
Diphenylethane	0.60

The polystyrene-divinylbenzene (PS-DVB) sample used, XAD-4 is commercially available.

Hydropyrolysis-MS Details on the high pressure system have been reported previously (7,8,11). Hydrogen pressures of 5 and 150 bar were used with a heating rate of 5°C/min over the range 100-600°C. Typically, between 0.2 and 0.3 g of the resite (particle size range of ca 0.1-1.0 mm) was mixed with 2-3 g sand. The volatile species evolved were detected on-line using a quadrupole mass spectrometer (VG Sensorlab, 0-300 a.m.u).

RESULTS AND DISCUSSION

C₁-linkages Figure 1 shows the evolution of benzene, toluene and cresol at 150 bar pressure from a normal phenol resite not containing a second constituent. The benzene evolving at high temperature (T_{MAX} of 550°C) is considered to arise mainly from the hydrodeoxygenation of phenol, cresols and xylenols. The cresol profile and, to a lesser extent, that for m/z 91 (this probably comprises fragment ions of 108) contain peaks at ca 550°C which are attributed to the primary cleavage of the methylene bridges. Figure 2 compares the benzene evolution profiles at 150 bar pressure from the immobilised DPM substrates. As found previously (6), the profiles can be resolved into two broad components. The higher temperature one (530-600°C) is consistent with that anticipated for cleavage of the SiO-C bond in surface-immobilised benzene. Toluene is similarly formed following the prior hydrogenolysis of the C-C linkages in diphenylmethane according to the reaction scheme:



The T_{MAX} of 480-500°C of the lower component at is very similar to that for the resite suggesting that the additional free radical chemistry that occurs in the resite does not significantly promote the cleavage of the methylene bridges at high hydrogen pressure.

The similar intensities of the m/z 78 and 79 intensities indicates that, as anticipated, extensive scrambling of the methylene deuteriums has occurred. The co-attachment of tetralin had little effect on the benzene and toluene evolution profiles both at low and high pressure (Figure 2). The greater m/z 78 intensity observed for the co-attached DPM is probably attributable to the likely contributions from tetralin breakdown products. No naphthalene was detected indicating that hydrogen transfer had not occurred to a significant extent.

C₂-linkages Figures 3 and 4 show the benzene and toluene profiles from the immobilised DPE at low and high pressure and Figure 4 compares the toluene evolution profiles for the immobilised DPE and DPE-containing resite at 150 bar. Given that the relative response factor of benzene to toluene is ca 3.1, the toluene concentration is much the higher at low pressure. This is consistent with

all the low pressure isothermal work on DPE (both free and immobilised) (1,2) where there is little evidence of cleaving the aryl-C bonds. At high pressure, this is clearly no longer the case with benzene concentration being considerably higher (ca 30% of that for toluene, Figures 3 and 4). Increasing the hydrogen pressure has also given rise to a slightly lower T_{MAX} for benzene and toluene (430 cf 450°C) and, as for DPM, resulted in much more benzene evolving above 500°C indicating the role of hydrogen pressure in circumventing char-forming reaction pathways.

By comparison with Figure 2, the contribution below 480°C in the profile for the resite can be ascribed to cleavage of the DPE linkage. Although the high temperature contributions from the remainder of the resite dominate the trace, the low temperature region matches fairly closely that for the immobilised DPE with an initial T_{MAX} occurring at ca 430°C.

C₃-linkages Figure 5 shows the virtually identical toluene and ethyl benzene evolution profiles from the PS-DVB at 5 and 150 bar pressure. The concentration of styrene evolving at low pressure was comparable to that of ethylbenzene. At low pressure, a sharp T_{MAX} occurs at 450°C with smaller amounts of toluene and ethylbenzene evolving at higher temperatures from secondary reactions. At high pressure, the evolution profiles are considerably broader. The volatiles begin to evolve at 320°C but the broad peak in the temperature range is the superposition of more than one distinct reaction pathway. Further, much greater quantities evolve above 470°C which again is indicative of the role of hydrogen pressure in circumventing char-forming reaction pathways.

Figure 6 compares the evolution profile of toluene from the PS-DVB and DPP-containing resite. The traces are very similar indicating again that, with high hydrogen pressures, the primary scission of the C-C bonds in diphenylalkanes is fairly independent of the nature of the substrate.

CONCLUSIONS

The results have indicated increasing the hydrogen pressure reduces the extent of retrogressive chemistry for all the model substrates investigated. The primary pyrolytic event at high hydrogen pressure, as characterised by the evolution of benzene, toluene and ethylbenzene/styrene, occurs at virtually the same temperature for a given alkane linkage in the different substrates used. The C₂ and C₃ linkages investigated are cleaved at ca 50-100°C lower than their C₁ counterparts. The pyrolysis of immobilised diphenylmethane appears to be largely unaffected by the co-attachment of tetralin.

ACKNOWLEDGEMENTS

The research was supported at (i) the University of Strathclyde by the Science & Engineering Research Council (Grant No. GR/J/08997) and the Department of Trade & Industry and at (ii) Oak Ridge National Laboratory by the Division of Chemical Sciences, Office of Basic Energy Systems, US DoE (Contract No. DE-AC05-84OR21400 with Martin Marietta Energy Systems, Inc.).

REFERENCES

1. M.L. Poustma, Energy & Fuels, 1990, 4(2), 113 and references therein.
2. A.C. Buchanan III, T.D.J. Dunstan, E.C. Douglas and M.L. Poustma, J. Am. Chem. Soc., 1986, 108, 7703.
3. A.C. Buchanan III and C.A. Biggs, J. Org. Chem., 1989, 54, 517.
4. A.C. Buchanan III, P.F. Britt and M.L. Poustma, Prepr. Am. Chem. Soc. Div. Fuel Chem., 1990, 35(1), 217.
5. P.F. Britt and A.C. Buchanan III, J. Org. Chem., 1991, 56, 6132.
6. S.C. Mitchell, C.J. Lafferty, R. Garcia, K. Ismail, C.E. Snape, A.C. Buchanan III, P.F. Britt and E. Klavetter, Energy & Fuels, 1993, 7, 331.
7. K. Ismail, G.D. Love, S.C. Mitchell, S.D. Brown and C.E. Snape, Prepr. Amer. Chem. Soc. Div. Fuel Chem., 1994, 39(2), 1691.
8. S.C. Mitchell, C.J. Lafferty, R. Garcia, K. Ismail, C.E. Snape, A.C. Buchanan III, P.F. Britt and E. Klavetter, Prepr. Amer. Chem. Soc. Div. Fuel Chem., 1992, 37(4), 551.

9. K. Ismail, R. Garcia, S.C. Mitchell, C.E. Snape, A.C. Buchanan III, P.F. Britt, D. Franco and J. Yperman, Proc.1993 Int.Conf. on Coal Science, Banff, September 1993.
10. H. Bar and Z. Aizenshtat, J. Anal. Appl. Pyrolysis, **19**, 1991, 265.
11. C.J. Lafferty, S.C. Mitchell, R. Garcia and C.E. Snape, Fuel, 1993, **72**, 367.

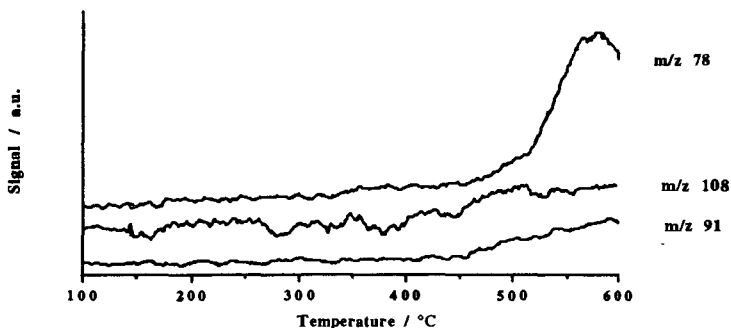


Figure 1. Hydropyrolysis evolution profiles of benzene, toluene and cresol from the normal phenolic resite under 150 bar H₂

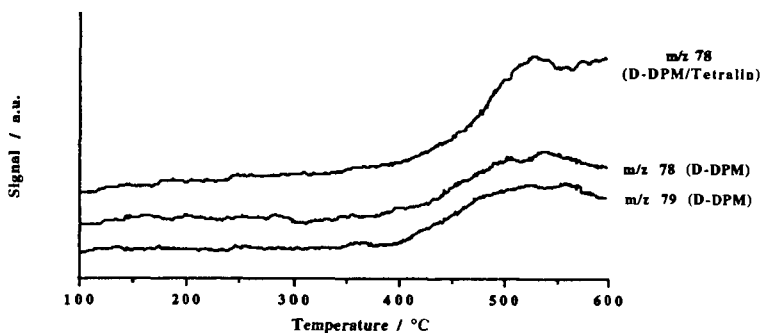


Figure 2. Evolution profiles of benzene from silica-immobilised di-deuterated diphenylmethane and silica-immobilised di-deuterated diphenylmethane with co-attached tetralin under 150 bar H₂

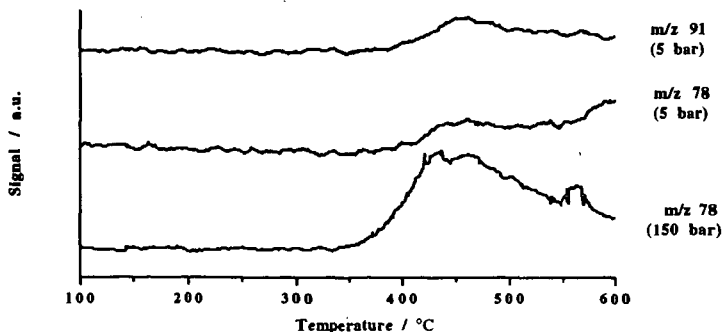


Figure 3. Hydropyrolysis-m.s. profiles of silica-immobilised diphenylethane under 5 and 150 bar H₂

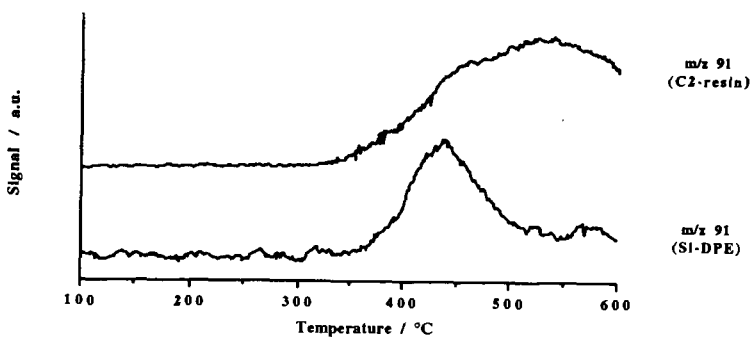


Figure 4. Toluene evolution profiles from the diphenylethane phenolic resite and the silica-immobilised diphenylethane under 150 bar H₂

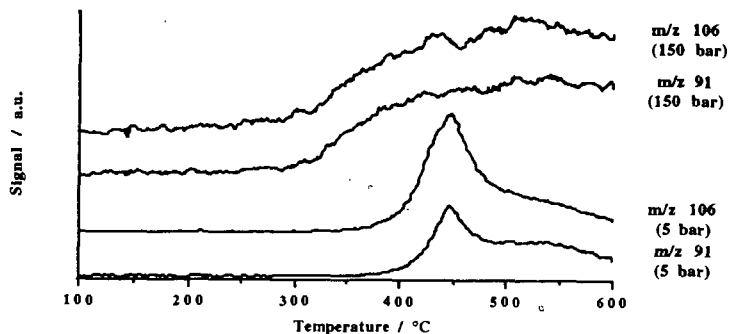


Figure 5. Evolution profiles of toluene and ethylbenzene from the PS-DVB under 5 and 150 bar H₂

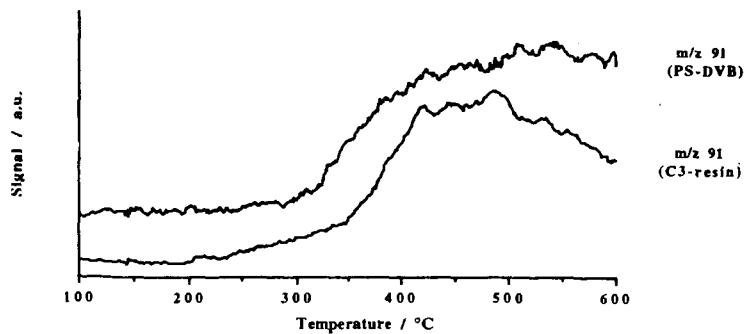


Figure 6. A comparison of the toluene evolution profiles from the PS-DVB and the diphenylpropane phenolic resite under 150 bar H₂

A CRITICAL SURVEY OF THE VALUE OF MICROWAVE HEATING FOR THE ACCELERATION OF REACTIONS OF -OH GROUPS IN COAL, AND THE RELATIONSHIP TO NEW ANALYTICAL METHODS FOR -OH DETERMINATION

Parisa Monsef-Mirzai, Harminder Manak and William R. McWhinnie
Department of Chemical Engineering & Applied Chemistry,
Aston University, Aston Triangle, Birmingham B4 7ET

Keywords: Microwave, -OH derivitisation, MASNMR.

INTRODUCTION

Research continues into coal utilisation by means which involve chemical reactions, particularly for the production of liquid products. Most of the new processes are based on hydroliquefaction, and for assessment of the suitability of particular coals for this purpose it is desirable to have detailed knowledge of their chemical constitution and reactivity. In respect of the use of coals as chemical feedstocks, as in hydroliquefaction, new classification systems might be desirable based on chemical parameters rather than on carbonisation properties as at present, and here the various functional groups attached to the coal hydrocarbon skeleton would be of great importance.

Functional groups in coals derive from the 'heteroatoms' O, N and S, and of these oxygen is by far the most important, varying regularly with coal rank between about 1 and 15% in British coals. Although -COOH and -CH₃ groups occur in coals of very low rank, oxygen in British coals is distributed between hydroxyl, carbonyl and ether-type groups. The hydroxyl groups, which certainly include phenolic groups, are the most important, and probably provide active reaction sites during hydroliquefaction.

Hydroxyl groups may be detected with reasonable certainty by spectroscopic methods, and can be measured by conversion into derivatives, e.g. by acetylation. Subsequent steps such as hydrolysis, distillation and titration of the recovered acetic acid afford data on -OH content. All such methods are based on heterogeneous reaction processes and there may be residual doubt as to whether the reactions have progressed to equilibrium. Indeed, a method dependent scatter of results is seen in the literature.

The ability of microwave heating to greatly accelerate chemical reactions is now well established.¹ The reaction mixture is typically contained in a microwave transparent Teflon bomb and the rate acceleration is achieved via an Arrhenius effect due to the superheating of the solvent. For this to be possible, it is necessary that the solvent is polar since non-polar materials will not interact with the microwave field. Following testing of a wide range of polar solvents we have found that acetonitrile is the best choice. This is because it superheats rapidly and extracts the minimum amount of the more labile components of coal under the experimental conditions employed. GC/MS analysis of the limited amount of material extracted reveals that oxygen containing materials constitute a negligible quantity of the extract. When the appropriate reagents are sufficiently soluble in acetonitrile, mixed solvents may be used as long as one is a microwave "receptor" e.g. acetonitrile/toluene. For polar reagents, e.g. transition metal salts, water is very appropriate. Of particular interest is that the method is excellent for the acceleration of a range of heterogeneous reactions.² In this presentation we outline the applications of microwave heating for driving coal -OH derivitisation reactions. We point out both advantages and drawbacks of the method.

Methodology

A known weight (0.5 - 1.0 g) of coal (90 < 212 > mm) is mixed with reagents (total liquid volume ≤ 10 cm³) in a Teflon bomb. The Teflon bomb is placed in the microwave oven (even a domestic model may be used) and subjected to bursts of microwave energy until it is judged, usually on the basis of FTIR, that the reaction has reached equilibrium. The time required proves to be a function of the coal used, the reagents, and the solvent. These observations may be understood in terms of variation of porosity of the coal, differing steric demands of the reagents, and differing degrees of superheating of the polar solvents.

Acetylation

Acetylation³ can be achieved in two ways: (a) With ketene, CH₂=CO, a small highly reactive gas molecule which can move easily, penetrate the porous coal structure and thus give the maximum probability of complete reaction with coal -OH groups, but the substance is very toxic and long reaction times are required due to loss of reagent via ketene polymers formed on the coal preventing further reaction with hydroxyl groups. Therefore after every ten hours reaction, the ketene polymers should be removed by extraction with toluene then, after drying and weighing the coal, this procedure continues until a constant acetyl content is obtained. (b) With reagents such as acetic anhydride/pyridine, acetic anhydride/conc. H₂SO₄; acetic anhydride/(CF₃CO)₂O; CH₃COOH/CF₃COOH. Blom *et al.*⁴ have pointed out that acetylation of coal proceeds slowly due to steric hindrance of the -OH groups, thus long reaction times are needed for reproducible data to be obtained. Likewise the hydrolysis step may need several days refluxing with barium hydroxide prior to distillation and titration of the acetic acid. It has been shown that³ microwave heating certainly accelerates both the acetylation using the conventional reagents and hydrolysis reactions, and that greater conversions are achieved than by using the same reagents in prolonged reactions on the bench top. For example, seven days hydrolysis on the bench top produces barium silicate, which has been formed from etching the glass with weak barium hydroxide, as an undesirable side

product, but such problems are totally avoided in the microwave method. Thus not only is the microwave method more reliable in driving the reactions to equilibrium but the saving in time can also avoid unwanted reactions which are a function of the very long reaction times associated with conventional procedures.

Silylation

Even if microwave heating is used to accelerate the derivitisation and hydrolysis stages, the acetylation process is a multi-step procedure. We have developed a method based on silylation which is a "one pot" process since the silylated coal is analysed directly by quantitative ^{29}Si MASNMR methods. A range of silylation reagents is available but not all are equally effective for use in the microwave method. For studies of coals, N-(trimethylsilyl)imidazole was the preferred reagent when used in acetonitrile solution. Even with this reagent a side reaction with more tenaciously held moisture occurred to give Me_3SiOH but fortunately the presence of this material did not interfere with the analysis. A wider range of reagents could be used for the silylation of simple substituted phenols, "model compounds", although a 1:1:1 mixture of N,O-bis(trimethylsilyl)acetamide, N-(trimethylsilyl)imidazole, and trimethylchlorosilane was optimal under conditions of microwave heating.

Remarkable acceleration of reactions was achieved e.g. from 24 hours (bench) to 35 minutes (microwave) for Creswell coal, and the ultimate -OH analytical data were in excellent (Creswell) or satisfactory (e.g. Cortonwood) agreement with the definitive ketene data.⁵ (Table 1a and 1b).

The analytical method for silicon requires knowledge of the spin lattice relaxation times T_1 of silylated coals (~8s) and of appropriate standard compounds (~25s). The method requires a pulse delay of $5T_1$ (maximum) seconds between pulses, thus the accumulation time for quantitative spectra with good signal to noise ratios may be considerable. However, despite this, the time taken from commencement of analysis to result may truly be described as "rapid" in comparison with other methods.

Stannylation

Tri-n-butyltin is a much more sterically demanding reagent than is Me_3Si -. It is not surprising therefore that even under microwave acceleration, stannylation of 2,6-di-t-butylphenol does not occur, whereas, by contrast, reaction with 2,6-dimethylphenol occurs readily. The less sterically demanding (smaller cone angle) Me_3Sn - group will react with more hindered phenols e.g. 2,6-diphenylphenol; the product, 2,6- $\text{Ph}_2\text{C}_6\text{H}_4\text{OSnMe}_3$, having been confirmed by single crystal X-ray crystallography.

The use of the triorganotin chlorides, R_3SnCl (R=Me, n-Bu) was not effective for coal since microwave accelerated loss of reagent *via* side reactions, and loss due to volatility, occurred. More effective was the use of the oxides $(\text{R}_3\text{SnO})_2\text{O}$. The point illustrated is that microwave heating may accelerate both analytically desirable and undesirable reactions.

To date a range of coals and coal macerals has been successfully stannylated using TBTO (i.e. bis-tri-n-butyltin oxide) in conjunction with acetonitrile, usually mixed with toluene, in microwave driven experiments. Quantitative methods of analysis based on ^{119}Sn MASNMR are under development and it is hoped that the more sterically demanding n- Bu_3Sn - will show a lower apparent -OH content for a given coal than that determined with Me_3Si -, thus enabling the proportion of more hindered -OH groups to be established.

To date preliminary qualitative ^{119}Sn MASNMR data indicate chemical shifts similar to those observed for 2,6-di-substituted-stannylated phenols in which the 2,6-substituents are of small steric demand. Thus it does appear possible that the density of -OH sites of differing degrees of steric hindrance might be mapped out by treatment of the same coal with a range of reagents of differing steric demand.

Phosphorylation

Both ^{29}Si (4.71%) and ^{119}Sn (8.45%) are of relatively low natural abundance thus the development of quantitative MASNMR methods to include phosphorus is attractive given the 100% abundance of ^{31}P and its excellence as an NMR probe.⁶ In the event the microwave acceleration of phosphorylation reactions with phosphorus(III) reagents, e.g. $\text{P}(\text{OEt})_2\text{Cl}$, produced complex mixtures both when the substrate was coal or model compounds. In addition to direct phosphorylation of -OH, four side reactions were noted:

- | | | | | |
|-------|--|--------|---|------|
| (i) | oxidation | P(III) | → | P(V) |
| (ii) | hydrolysis | P-Cl | → | P-OH |
| (iii) | solvolysis | P-OEt | → | P-OH |
| (iv) | $\text{ROH} + \text{EtO-P} \rightarrow \text{ROP} + \text{EtOH}$ | | | |

This rendered quantitative study impossible. Naturally, more vigorous control of reaction conditions (exclusion of oxygen and moisture) would allow greater success but this departs from the objective of devising a simple, one pot method for coal -OH determination. Ironically, there is qualitative evidence that phosphorylation could be better than silylation for identifying subtle differences in -OH environments. Indeed when coal is the substrate there is

evidence for the occurrence of all reactions (i) — (iv) above. From the spectrum of ^{31}P chemical shifts, it may be deduced that a rich variety of phosphorus environment results from the reaction of coal with reagents of the class $\text{P}(\text{OR})_2\text{Cl}$. In fact the oxidation reaction is very rapid and regardless of the initial reagent being $\text{P}(\text{III})$ or $\text{P}(\text{V})$, any $-\text{OH}$ groups on the coal which are phosphorylated contain $\text{P}(\text{V})$. An oxidation and hydrolysis of a product reagent such as $\text{P}(\text{OEt})_2\text{Cl}$ is $\text{OP}(\text{OEt})_2(\text{OH})$ and this material adheres strongly to the coal suggesting that it originates primarily from reaction with any tenaciously held coal moisture (all coal samples are dried at 105°C under N_2 over one or more hours). Thus whilst the system is not without interest chemically, the analytical usefulness is limited. It may however be noted, as mentioned above, that preliminary qualitative studies of tri-*n*-butylstannylated coals give chemical shifts consistent with stannylation of weakly hindered $-\text{OH}$ groups.

Ion Exchange

It may be noted that the ability of microwave heating to accelerate the ion exchange of clay minerals² may also be exploited in coal science to afford transition metal exchanged $-\text{OH}$ groups (e.g. Ni^{2+}) which are suitable for preliminary study by EXAFS to provide some information about average $-\text{OH}$ environments.

Attempts may be made to exchange the weakly acidic sites directly, or alternatively, prior conversion to the potassium derivative may be employed. Selection of salts of copper(II) can lead to complex chemistry and ill defined products. With nickel(II) and cobalt(II) cleaner reactions could be obtained. Thus microwave derivitisation has once again proved useful in developing materials for physical study by a method (EXAFS) which may give information about the average environment of $-\text{OH}$ groups in a given coal.

Conclusions

Microwave heating will not necessarily accelerate only a reaction of particular analytical interest, the rates of side reactions may also be accelerated. If the method is to be used to derivitise $-\text{OH}$ groups it is desirable to select reagents with either no or with a minimum of side reactions. If that condition can be fulfilled, as it usually is if the reagent is selected from group 14, in our view microwave heating is now the preferred method for such derivitisation reactions.

References

1. Mingos, D.M.P., and Baghurst, D.R., *Chem. Soc. Rev.*, 1991 **20**, 1.
2. Bond, S.P., Gelder, A., Homer, J., Perry, M.R., and McWhinnie, W.R., *J. Mater. Chem.*, 1991, **1**, 327.
3. Monsef-Mirzai, P., Lawson, G.J., and Bailey, N.T., *Fuel*, 1990, **69**, 533.
4. Blom, L., Edelhansen, L., and Van Knevelen, D.W., *Fuel*, 1957, **36**, 135.
5. Monsef-Mirzai, P., Lawson, G.J., Bailey, N.T., and Ikejani, A.O.O., *Fuel*, 1992, **71**, 45.
6. Wroblewski, A.E., Reinartz, K., and Verkade, J.G., *Energy and Fuels*, 1991, **5**, 786.

Table 1 (a)
Quantitative ^{29}Si MASNMR
determination of $\text{OOH}/\text{O}_{\text{Total}}$

$\text{OOH}/\text{O}_{\text{Total}}$ Quantitative ^{29}Si MASNMR				
Coals	%C	%O	$\text{OOH}/\text{O}_{\text{Total}}$ % by Silylation	Reaction Time
Gedling	81.6	9.4	41	2h
Ollerton	82.6	7.5	55	2h
Linby	83.0	8.7	61	2h
Creswell	84.5	5.9	91	35 mins.
			92	2h
Cortonwood	87.2	3.9	84	3h
Cwm	90.3	2.9	—	5h
Cynheidre	95.2	0.9	—	5h

Table 1(b)
Acetylation data from ketene and from conventional
reagents used in the microwave oven for comparison

$\text{OOH}/\text{O}_{\text{Total}}$ % by Acetylation					
Ketene	Reaction Time	$(\text{CH}_3\text{CO})_2\text{O}/$ H_2SO_4	$(\text{CH}_3\text{CO})_2\text{O}/$ Py	$\text{CH}_3\text{COOH}/$ $(\text{CF}_3\text{CO})_2\text{O}$	$(\text{CH}_3\text{CO})_2\text{O}/$ $(\text{CF}_3\text{CO})_2\text{O}$
73	100h	53	49	47	43
59	100h	50	49	40	37
75	140h	48	50	37	33
90	125h	62 (1h)	63 (1h)	61 (1h)	54 (1h)
		72 (2h)	65 (2h)	64 (2h)	54 (2h)
77	114h	83	50	78	69
55	120h	60	1.6	52	55
17	48h	117	2.5	11	23

THE APPLICATION OF PIXE/PIGE ANALYSIS TO LIQUEFACTION STUDIES

C.J. Lafferty¹, C. Eloi², R.K. Anderson¹ and J.D. Robertson^{1,2}

¹Center for Applied Energy Research and ²Department of Chemistry, University of Kentucky, Lexington, KY 40511-8433.

Keywords: liquefaction, ash analysis, PIXE, PIGE.

Introduction

Proposed 'full-scale' direct coal liquefaction pilot plants all incorporate a combustion/gasification stage to recover the thermal content of the insoluble organic matter derived from the primary dissolution of the coal in process solvent. This step will result in the production of an ash which will have to be either sold as a value-added-product or most likely stored in a designated landfill, with the ongoing costs of leachate treatment added to the overall plant economics. At present, ash derived from coal burning power plants is exempt from federal regulations regarding the long-term disposal of hazardous materials. However a recent US Supreme Court ruling determined that ash produced from municipal incinerators must be treated as hazardous waste¹, increasing overall disposal costs by an estimated factor as high as 10, presenting a potentially severe economic impact upon proposed liquefaction plants. It is therefore imperative that data be obtained regarding both the composition and leaching properties of combusted liquefaction residues in order to more accurately estimate the long term processing costs of this material. Additionally, a need exists to follow the distribution and effective use of dispersed catalysts during liquefaction, as well as catalyst recovery, recycle and rejection from the system, which are especially important should more expensive catalytic systems be contemplated.

Elemental analysis with a high energy charged-particle beam is a powerful analytical tool that has moved out of the realm of the specialized 'nuclear' laboratory and found widespread use amongst researchers in many different areas. We are currently using simultaneous particle-induced X-ray and gamma-ray emission analysis (PIXE/PIGE) to investigate the fate of major, minor and trace metal species during the direct liquefaction of a sub-bituminous coal. In addition, PIXE/PIGE is being used to follow the fate of these species during the combustion of liquefaction residues.

Particle-Induced X-ray Emission Analysis (PIXE)

PIXE as an analytical procedure is a relatively recent innovation, being first reported in 1970 by workers at the Lund Institute of Technology². Because the most common particle used for this purpose is the proton, the acronym has also come to mean proton-induced x-ray emission. PIXE, like other x-ray spectroscopic techniques used for elemental analysis, utilizes the x rays that are emitted from the atoms in a sample when that sample is exposed to an excitation source. The use of a proton beam as an excitation source offers several advantages over other x-ray techniques. Among these are; (1) a higher rate of data accumulation across the entire periodic table and (2) better overall sensitivities, especially for the lower atomic number elements. In the case of electron excitation, the better sensitivity is due to a lower bremsstrahlung background and, in the case of x-ray fluorescence analysis (XRF), the enhanced sensitivity is due to the lack of a background continuum across the entire spectrum. Of course, the chief disadvantage of PIXE is that it requires the use of a particle accelerator.

Particle-Induced γ -ray Emission Analysis (PIGE)

PIGE is based on the detection of prompt γ rays that are emitted following a charged-particle-induced nuclear reaction. The energy of the γ ray is indicative of the isotope present and the intensity of the γ ray is a measure of the concentration of the isotope. This technique is generally combined with PIXE to provide trace level concentration data for the light elements lithium through chlorine. Because it is based upon specific nuclear reactions, the sensitivity of PIGE varies greatly from isotope to isotope. For most light elements, the sensitivity is in the order of 1 to 100 μg per gram. A comprehensive review of the theory and analytical applications of PIGE can be found in the text by Bird and Williams³.

2. Ashing of Samples.

In order to simulate combustion, samples of the starting coal and the liquefaction resids were ashed in a LECO MAC 400 proximate analyzer at 750°C in air.

3. PIXE/PIGE analysis.

The PIXE/PIGE measurements were performed at the University of Kentucky 7.5 MV Van de Graaf accelerator⁷. The samples were irradiated for 15 minutes with an external 2.5 MeV proton beam in 1 atm. of He. The X rays are detected with a retractable Si(Li) detector with a FWHM resolution of 165 eV at 5.90 keV (Mn K α). A 10 μ m thick critical absorber Cr foil is used to reduce the intensity of the Fe X rays, and a 350 μ m thick Mylar film is used to reduce the bremsstrahlung background. The γ rays are detected with a HpGe detector, 20% relative efficiency, with a FWHM resolution of 2.4 keV at 1274 keV. A detailed description of the IBA facility and the PIXE/PIGE analysis procedure has been previously published⁸. The system was calibrated using standard coals obtained from the US National Institute of Standards and Technology (1632a and 1632b) as well as a NIST standard coal ash (1633). Previous work has confirmed the validity of results obtained using these standards for the analysis of coals and related ashes⁹.

Results

Table 1 shows the product yields determined for the liquefaction experiments, which are typical for the experimental conditions and catalysts used. Total conversions measured at 415°C for each of the iron catalyzed runs were significantly higher than the conversions measured for the non-catalyzed runs carried out at 440°C.

Table 2. lists the metal retention indices calculated for each of the liquefaction resids as well as initial composition of the feed coal. Note that a retention index of 100 implies that 100% of the metal originally present in the feed coal was retained in the resid. The retention indices obtained for molybdenum, nickel and zinc were all several orders of magnitude above those calculated from the original coal composition. This was attributed to contamination of the sample with anti-seize compound used to protect the threads of the micro-autoclave during liquefaction. This compound was found to consist of molybdenum disulfide, nickel powder and zinc oxide, which correlates with the enrichments measured. This problem has been corrected in subsequent experiments, however the data to be discussed in this paper will focus on other metals. It is of interest to note that the retention indices measured for sodium, potassium, calcium and titanium were all reduced in the catalyst impregnated resid. samples suggesting the transformation of some of these metals into an oil soluble form during liquefaction.

It is to be noted that the three catalyst-promoted resid samples all show a large increase in iron retention over the parent coal due to the iron impregnation prior to liquefaction. The most efficient form of iron impregnation appears to be the method used in run R3-208-3, super fine iron oxide addition, with 92% of the added iron being detected in the resid sample. The other two methods of iron addition, iron oxide addition and $\text{Fe}_2(\text{SO}_4)_3 \cdot 5\text{H}_2\text{O}$ impregnation showed iron retentions of 75% and 50% of theoretical, suggesting that iron partitioning amongst the liquefaction products may differ as a function of catalyst precursor. Further work is currently underway to examine this hypothesis. The resid samples also showed a high degree of retention for sodium, strontium, aluminum, titanium and manganese.

Table 3. lists the metal retention indices measured for each of the combusted resid samples. Whilst the ashing temperature (750°C) was significantly lower than the temperatures that would be typically found in the combustor/gasifier systems proposed for full scale liquefaction facilities, it does, however, demonstrate the likelihood of the metallic species from the catalyst enriched resids being retained within the resulting ash.

As expected the samples resulting from the Fe catalyst promoted liquefaction runs again show a high degree of enrichment in iron over the feed coal, whilst high percentages of strontium, aluminum, titanium and manganese are also retained in the ash. The retention of these metals in the combustor ash would have important consequences on the composition of leachate generated from a storage landfill containing combustor/gasifier ash. Future work will be directed

Comparison With Other Analytical Techniques

Conventionally, analyses of minor and trace elements in coal and coal liquefaction and combustion residues have been carried out by Atomic Absorption (AA) and Inductively Coupled Plasma Atomic Emission (ICP-AE) spectroscopy, or by instrumental methods such as XRF or Neutron Activation Analysis (NAA). While the sensitivity of PIXE and PIGE for most elements is below that of AAS, ICP-AES, and NAA, it is important to keep in mind that there is no need to use a higher sensitivity than required by the analytical situation.

In comparison to PIXE/PIGE, the main disadvantage of AAS and ICP-AES is the complicated and time consuming sample preparation procedure required prior to analysis. These steps usually involve wet or dry ashing of the coal, and dissolution of the ash via acid digestion or fusion. During these procedures, great care must be taken to ensure that volatile elements such as As and Pb are not lost and that sample contamination is avoided. The other principal drawback of AAS and ICP-AES is the possibility of chemical matrix interferences.

While NAA has greater sensitivities for most metals (e.g. Hg, Cd, Sb) than PIXE in coal and coal ash, pre- or post- irradiation chemical separations are often required in order to achieve maximum sensitivities. Moreover, NAA cannot be used to determine some of the environmentally significant elements such as Pb, Tl and Sn. Finally, PIXE/PIGE can provide a rapid multielemental analysis (20 to 30 elements) in 15 to 20 minutes, whereas a complete multielemental analysis by NAA may require multiple irradiations and up to 3 months of a delayed counting period.

The principal advantage of applying PIXE/PIGE to these particular resid samples is that the technique requires only a small amount sample (≈ 100 mg) for a complete metal analysis to be performed. Other traditional techniques require several grams of sample in order that ashing and acid digestion be carried to produce sufficient solution for a complete metal analysis.

Experimental Procedure

1. Coal Liquefaction Samples.

To provide liquefaction residues for this study, experiments were performed using Wyodak coal supplied by CONSOL, Inc. from the Black Thunder mine in Wright, Wyoming. Four runs were made without added catalyst at temperatures to 440°C, and reaction times to thirty minutes using tetralin as solvent. In addition, to gauge the impact that typical catalysts may have on the composition of these residues, three runs were made at 415°C for 30 minutes with different Fe catalyst precursors.

The three precursors used included $\text{Fe}_2(\text{SO}_4)_3 \cdot 5\text{H}_2\text{O}$ impregnated on the coal feed in an aqueous solution, without base precipitation (FeIII);⁴ Superfine Iron Oxide (SFIO), a finely divided 30 Å iron oxide supplied by MACH I, Inc.,⁵ and iron oxide (IO) used as a catalyst at the Advanced Coal Liquefaction Research and Development Facility at Wilsonville in Run 262, supplied by Kerr-McGee⁶. Additional information on these materials and methods of preparation is available in the literature cited.

In a typical liquefaction experiment, 3 g of coal, ground to -200 mesh, was added to 50 ml microautoclaves with 5.4 g tetralin. When Fe was added, dimethyl disulfide was also added in an amount sufficient to convert the Fe to pyrrhotite. The reactor was pressurized with hydrogen to 6.89 MPa (cold pressure), and agitated in a heated, air fluidized sand bath at 400 cpm. The reactor was cooled in a second sand bath, and gas products were collected and analyzed by gas chromatography. The other products were removed from the reactor with THF and extracted in a Soxhlet apparatus. The THF solubles were subsequently separated into pentane soluble (Oils) and pentane insoluble (PA+A) fractions. Total THF conversion was determined from the amount of insoluble material that remained (resid). Any added Fe was subtracted from the residue sample weight at its equivalent weight of pyrrhotite. Oils are calculated by difference, and as a result, water produced during liquefaction, as well as any experimental error, is included in this fraction. All product yields are stated on an maf coal basis.

towards obtaining larger quantities of combusted resids in order to evaluate the leaching characteristics of these materials via standard procedures.

Conclusions

The results reported in this paper have demonstrated the advantages of using PIXE/PIGE as an approach for following the distribution of metal species during liquefaction. Further employment of this technique will facilitate a greater understanding of catalyst utilization, recovery and recycle during coal liquefaction, as well as emerging solid waste disposal concerns.

Acknowledgements

Support for this work was provided by the University of Kentucky Center for Applied Energy Research and the University of Kentucky Graduate School. Preparation of the liquefaction resid samples was carried out under DOE contract DE AC22-91PC91040.

**Table 3. Metal Retention Indices for Combusted Resid. Ash
(% Metal retained in Ash.)**

	R2-154-2	R2-154-1	R3-152-1	R3-80-1	R3-258-2	R3-208-3	R3-342-2
F	71	111	75	105	0	48	10
Na	83	88	64	86	67	56	61
Al	80	97	64	80	59	75	61
K	172	238	92	239	167	124	176
Ca	62	72	62	58	65	49	47
Ti	55	62	55	50	52	45	40
Mn	80	101	71	65	95	93	133
Fe	69	82	67	67	238	328	321
Ni	8160	17313	3397	26649	14598	3722	10866
Zn	3447	175	1698	6939	5033	107	4457
Rb	0	45	45	38	85	0	70
Sr	63	73	60	61	65	50	49
Zr	44	43	21	26	25	55	37
Mo	11421	25813	5172	28395	15408	3963	17125
Ag	44	123	143	158	46	43	0
Ba	40	64	56	40	50	43	44

References

1. American Chemical Society, *Chemical and Engineering News*, May 9, 1994, p 21.
2. T.B. Johansson, K.R. Akselsson and S. A. E. Johansson, *Nucl. Instr. Meth. Phys. Res.* 84, 141 (1970).
3. *Ion Beams for Metal Analysis*, J.R. Bird and J.S. Williams, Eds. (Academic Press, San Diego, CA, 1989).
4. H.F. Ni, R.K. Anderson, E.N. Givens and J.M. Stencel, *Prep. Pap.- Am. Chem. Soc., Div. Fuel Chem.* 1993, 38 (3), 1107.
5. J. Zhao, F.E. Huggins, Z. Feng, F. Lu, N. Shah and G.P. Huffman, *Journal of Catalysis*, 1993, 143, pp 499-509.
6. R. K. Anderson, E. N. Givens and F.J. Derbyshire, *Prep. Pap.-Am. Chem. Soc., Div. Fuel Chem.* 1993, 38 (2), 495.
7. J.M. Savage, A.S. Wong and J.D. Robertson, *J. of Trace and Microprobe Tech.* 10(2-3) (1992) 151-168.
8. A.S. Wong, E.A. Lurding J.D. Robertson and H. Francis, *J. of Trace and Microprobe Tech.* 10(2-3) (1992) 169-182.
9. A.S. Wong and J.D. Robertson, *Proc. Tenth Annual Pittsburgh Coal Conference*, 1122 (1993).

Table 1. Product Yields for Liquefaction Experiments.^a

Catalyst Added	none	none	none	none	FeIII	SFIO	IO
Rxn temperature, °C	415	415	440	440	415	415	415
Rxn time, min	15	30	15	30	30	30	30
Added Fe, wt% maf Coal	none	none	none	none	0.8	1.2	1.2
S/Added Fe, m/m	none	none	none	none	1.6	3.0	3.0
Products, wt% maf Coal							
HC Gases	0.4	0.7	0.9	1.3	0.8	1.5	1.3
CO+CO ₂	4.2	4.4	5.0	5.8	4.9	6.0	4.4
Oils	21	28	39	45	36	37	39
PA+A	40	43	36	28	42	40	39
IOM	34	24	19	20	16	16	16
THF Conv.	66	76	81	80	84	84	84
Run numbers	R2-154-2	R2-154-1	R3-152-1	R3-80-1	R3-258-2	R3-208-3	R3-342-2

a. 3.0 g Black Thunder coal in 5.4 g tetralin, using 6.89 MPa H₂ (cold).

**Table 2. Metal Retention Indices for Liquefaction Resids.
(% Metal Retained in Resid.)**

	A.R. Coal (ppm)	R2-154-2	R2-154-1	R3-152-1	R3-80-1	R3-258-2	R3-208-3	R3-342-2
F	58	128	143	231	116	125	121	96
Na	319	98	91	84	68	67	65	68
Al	6703	81	111	95	74	65	99	78
K	351	78	113	134	50	82	64	79
Ca	12843	67	61	56	54	39	35	36
Ti	623	80	66	58	54	38	44	39
Mn	44	109	108	71	69	76	63	124
Fe	3807	82	81	81	64	207	379	315
Ni	2	7897	14415	26323	2476	10367	3069	11079
Zn	17	2806	6295	7733	1719	3945	1003	4055
Rb	9	98	108	86	48	93	90	95
Sr	2	82	85	76	65	67	61	55
Zr	243	43	57	46	32	30	45	40
Mo	N.D.	10781	27874	31960	5457	15120	5195	19191
Ag	16	41	112	128	194	0	52	0
Ba	779	64	59	56	44	62	71	54

X-RAY CHARACTERIZATION OF THE CRYSTALLINE INORGANIC SPECIES AND THE ORGANIC MATRIX IN WILSONVILLE RECYCLE RESID FROM RUN # 259.

David L. Wertz and Charles B. Smithhart*
Department of Chemistry & Biochemistry
and
Center for Coal Product Research
University of Southern Mississippi
Hattiesburg, MS 39406-5043 USA

Key Phrases: Pyrrhotite 11-C, hard and soft x-ray fluorescence, x-ray diffraction and absorption.

INTRODUCTION.

Products recovered from the two-stage direct liquefaction of a Pittsburgh seam coal (and several other coals) produced at the Wilsonville facility have been studied extensively as part of a global project sponsored by the U.S. Department of Energy.¹

An x-ray scattering-diffraction-fluorescence spectral study of the resids produced from processing Illinois # 6 coal at the Wilsonville facility has recently appeared. The effect(s) of the two-stage catalytic processes on the poly-cyclic aromatic character in the resids (as indirectly measured by the diffuse scattering caused by its graphitic layer stacking) and on the crystalline inorganic materials are reported.

Presented below are our preliminary finding from an x-ray study of the recycle resid produced during run # 259 at the Wilsonville facility. This study is a continuation of the group's efforts to utilize x-ray characterization methods to better understand the molecular structuring in coals and how various processes (such as liquefaction) affect that structuring.

EXPERIMENTAL.

Each sample was received (from Brandes) as a fine powder and was analyzed "as received."¹

Diffraction Experiments. A carefully weighed amount (ca. 0.5 grams) of each sample was deposited onto the sample holder (1.0 mm depth) and mounted into our θ - 2θ x-ray diffractometer. The sample was irradiated with copper x rays. Scattered x-ray intensities were accumulated by measuring the CuK_α wavelength (made monochromatic by use of a graphite crystal at $\Delta 2\theta \approx 0.01^\circ$ from $2\theta = 10.00^\circ$ to $2\theta = 90.00^\circ$ for 2 second intervals using the conventional step-scan procedure.³

Absorption Experiments. A carefully weighed amount of each sample (ca. 0.1 or 0.5 grams) was deposited onto the aluminum sample holder (which served as the substrate). The intensity of the (311) peak of the aluminum was measured both in the presence of and in the absence of the resid sample.⁴ For the recycle resid, an aluminum sample holder with depth of 1.0 mm was used. For its tetrahydrofuran insoluble fraction, a sample holder of 0.1 mm depth was used.

X-Ray Fluorescence Spectral Experiments. Approximately 1 gram of each resid was pressed into a pellet and then mounted into our wavelength dispersive x-ray spectrometer. Using chromium as the exciting radiation, both a soft x-ray spectrum (using a MOXTEK multi-layer as the monochromator) and a hard x-ray spectrum (using graphite as the monochromator) were obtained using the normal step-scan procedure.

RESULTS AND DISCUSSION.

X-Ray Fluorescence Experiments. The soft and hard x-ray spectra of the recycle resid and its THF-insoluble fraction are presented in Figures One and Two. After irradiation with the Cr x rays, large secondary x-ray peaks due to iron and calcium are observed, along with smaller peaks due to titanium, potassium, sulfur, and silicon are

observed in both spectra.

Mass Absorption Experiments. Shown in Figure Three are the intensities of the (311) diffraction peak from the aluminum sampleholder in the absence of and in the presence of the recycle resid sample. The mass absorption coefficient of each resid was calculated by:

$$\mu = [T \sin \theta / 2m] \ln[A_s/A_p] \quad (1)$$

In eq. 1, T is the irradiate surface area, $\theta = 0.52\theta$ for the (311) peak, and A_s and A_p are the areas measured under the (311) peak of aluminum in the absence of and in the presence of the finely powdered resid samples. The mass absorption coefficient of each sample is presented in Table I.

X-Ray Diffractograms. The measured secondary x-ray intensity, $I(2\theta)$ was converted to the absorption corrected intensity by:

$$I'(2\theta) = \mu m I(2\theta) / \{1 - \exp(-2\mu m / T \sin \theta)\} \quad (2)$$

The absorption corrected diffractograms of the recycle resid and its THF-fraction are shown in Figure Four. The absorption corrected diffractograms have been utilized throughout the remainder of this manuscript because peaks $I'(2\theta)$ are proportional to the abundances of the various analytes in the complicated resid matrices.

The diffraction peaks due to the crystalline mineral components present in the resid (B) and its THF-insoluble component (A) are shown in Figure Six. That the mineral peak intensities are much higher in the THF-insoluble fractions is consistent with its significantly higher ash content and its significantly higher x-ray mass absorption coefficient and substantiates that extraction by tetrahydrofuran increases the relative abundances of the crystalline minerals by preferentially removing carbonaceous materials from the resid.

Huffman, Huggins, et al.⁶ have recently reported that pyrrhotite ($Fe_{1-x}S$) is formed by reaction with H_2S during direct coal liquefaction processes using iron-based catalysts, with iron oxide(s) present only in the case of insufficient sulfur.⁶ Our best current correlation to date of the diffraction peaks with the crystalline components present in these samples involves pyrrhotite 11-T as well as α -quartz and other minerals but not iron oxide(s).⁷

REFERENCES

- * DOE EPSCoR Fellow. Funding of EPSCoR Fellowship is acknowledged.
- 1. Brandes, S. D., R. A. Winschel, and F. P. Burke, *Am. Chem. Soc., Div. Fuel Chem.*, 1991 (36) 1172; 1992 (37) 1243.
- 2. Wertz, D. L., C. B. Smithhart, M. L. Steele, and S. Caston, *J. Coal. Quality*, 1993 (12) 36.
- 3. Wertz, D. L., *Energy Fuel*, 1990 (4) 442.
- 4. Wertz, D. L., C. B. Smithhart, and S. L. Wertz, *Adv. X-Ray Anal.*, 1990 (33) 475.
- 5. Wertz, D. L. and M. Bissell, *Energy Fuel*, 1994 in press.
- 6. Huffman, G. P., F. E. Huggins, et al., *Energy Fuel*, 1993 (7) 285.
- 7. Joint Committee of Powder Diffraction Systems; International Centre for Diffraction Data, 1991. # 29-726.

TABLE I. MASS ABSORPTION COEFFICIENT CALCULATIONS.

SAMPLE	MASS (g)	A_s (CPS)	A_p (CPS)	μ cm ₂ /g
recycle resid	0.3351	26,130	2,303	13.8
THF-insoluble	0.1036	23,886	1,215	54.8

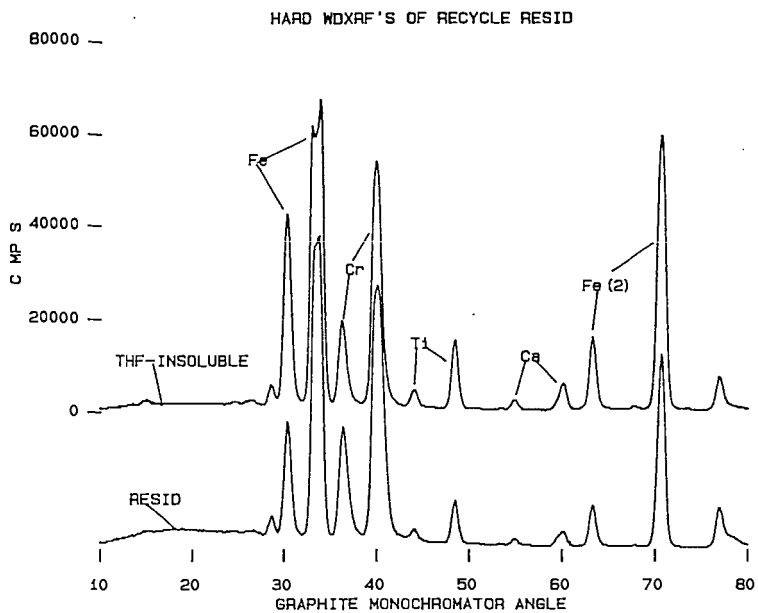


FIGURE ONE. Hard x-ray spectra of the recycle resid and its THF-insoluble fraction.

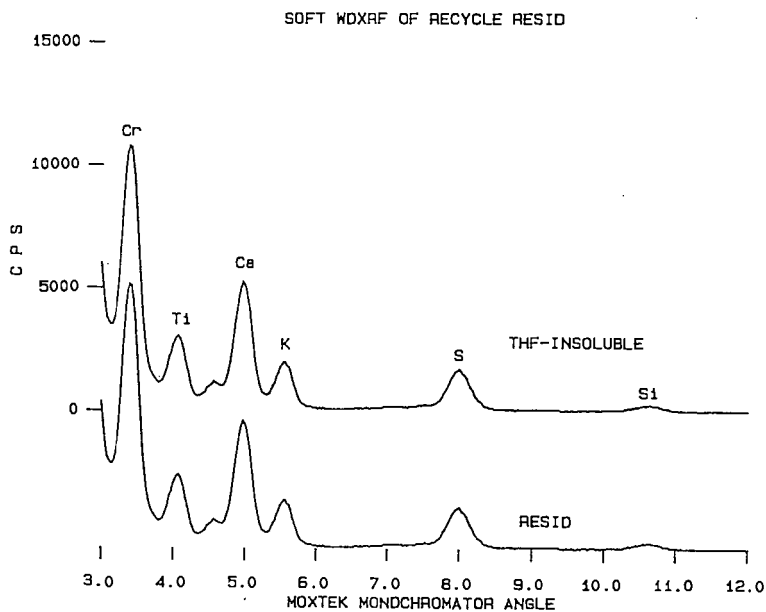


FIGURE TWO. Soft x-ray spectra of the recycle resid and its THF-insoluble fraction.

DIFFRACTION FROM Al (311) PEAK

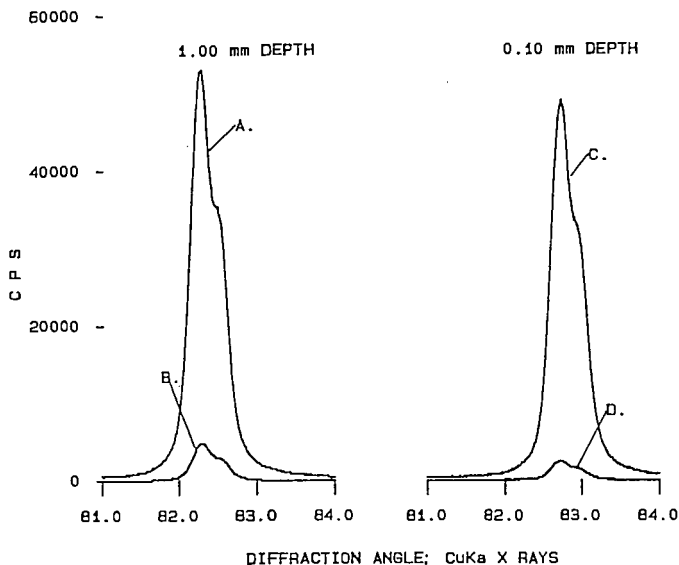


FIGURE THREE. Diffraction from the (311) of the aluminum sample holders. (A) Diffraction intensity from the sample holder with 1.00 mm depth, and (B) intensity from the sample holder with 0.3351 g of the recycle resid deposited onto it. (C) Diffraction intensity from the (311) peak of the aluminum sample holder with 0.10 mm depth, and (D) intensity from the sample holder with 0.1036 g deposited onto it.

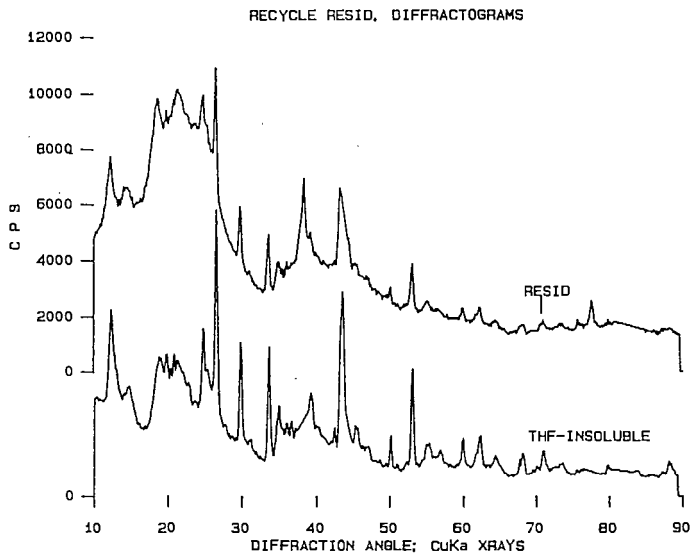


FIGURE FOUR. Absorption corrected diffractograms of the recycle resid and its THF-insoluble fraction.

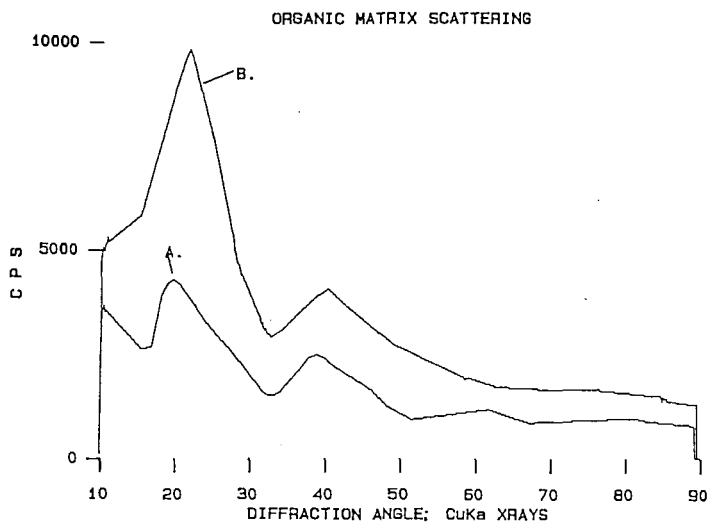


FIGURE FIVE. The diffuse scattering from the recycle resid (B) and its THF-insoluble fraction (A).

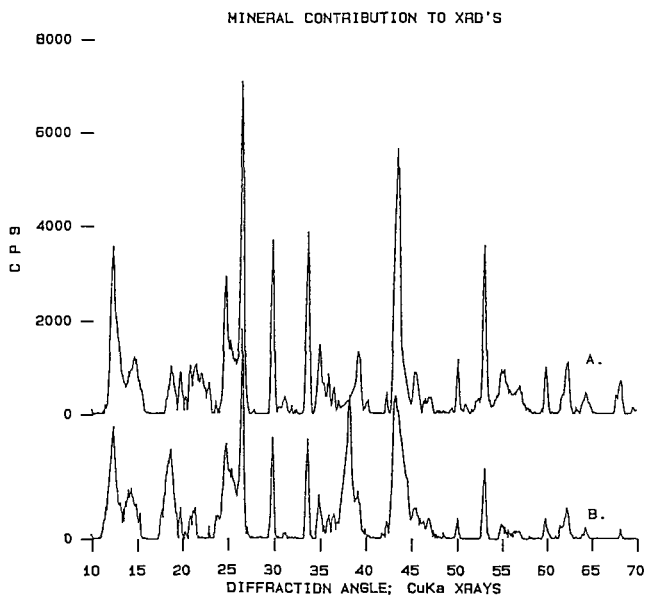


FIGURE SIX. Conventional diffraction from the crystalline materials in its THF-insoluble fraction (A) and the recycle resid.

NITROGEN XANES STUDIES OF ARGONNE COALS

S. Mitra-Kirtley¹
O. C. Mullins²
J. van Elp³
S. P. Cramer^{3,4}

¹ Dept. of Physics and Applied Optics, Rose-Hulman Institute of Technology, Terre Haute, IN 47803

² Schlumberger-Doll Research, Old Quarry Road, Ridgefield, CT 06877

³ Lawrence Berkeley Lab, Berkeley, CA 94720

⁴ Dept. of Applied Science, University of California, Davis, , Davis, CA 95616

Keywords: XANES, nitrogen, coals

ABSTRACT

All the major forms of nitrogen in a group of Argonne coals are detected and quantified by X-ray Absorption Near-Edge Structure (XANES) studies; these forms are pyridine, pyridone, and pyrrole. In addition, there is evidence of aromatic and quarternary amines in small amounts, and virtually no saturated amines. Pyridone is found to be abundant in the low rank coals; with maturation of coals, the pyridone forms become transformed into pyridine forms. The quarternary nitrogen has been analyzed as a potential contribution to coal spectra. This compound has a distinctive peak in the nitrogen XANES spectra allowing contribution of quarternary nitrogen in the coal spectra to be determined. By this method we have found that coals generally have at most small quantities of quarternary nitrogen.

INTRODUCTION

Important natural resources such as coal often contain heteroatoms such as sulfur and nitrogen; these heteroatoms pose serious threats to the environment, as well as to effective utilization of the resources. Elucidation of the chemical structures of the heteroatom containing compounds in coals aids in the removal of the compounds, and also in understanding the complex maturation processes of these fossil fuels.

X-ray Absorption Near-Edge Structure (XANES) spectroscopy has been very versatile in direct and non-destructive studies of fossil fuel samples. Sulfur XANES studies have been performed successfully on coals(1-6), and petroleum asphaltenes(7-9). XANES studies showed that both coals and petroleum asphaltenes contain saturated and aromatic forms of sulfur; thiophenic (aromatic) is the most dominant form, followed by sulfidic (saturated) form. There are small amounts of oxidized forms in coals and asphaltenes, and unlike asphaltenes, some coals have inorganic sulfide structures present in them.

Nitrogen XANES studies have also been successfully performed on coals(10,11) petroleum asphaltenes(12), and organic parts of source rocks such as kerogens and bitumens(13). Several nitrogen model compounds have been studied to analyze the fossil fuel spectra; they are pyridine, pyridone, pyrrole, aromatic amine, porphyrin, and saturated amine. It is found that most of the nitrogen is found in aromatic forms in these fossil fuel samples, with negligible quantities of saturated forms. Pyrrolic and pyridinic are the most common forms of nitrogen in these samples. In low rank coals, considerable amounts of pyridone are also found, whereas in the high rank coals the pyridone structures are mostly replaced by pyridine structures. In addition, coals also have small quantities of aromatic amines. Some quantities of porphyrin and smaller quantities of saturated amines are present in the kerogens and bitumens in addition to the other nitrogen structures mentioned above.

Other methods which have been used in the past to elucidate the nitrogen chemical structures of fossil-fuels have been mostly destructive and indirect. Chromatographic and extraction methods have been problematic either due to high molecular weights or they are not powerful enough to study the entire sample. Several spectroscopic studies have been performed; however, they suffered mostly from resolution difficulties. X-ray Photoelectron Spectroscopy (XPS) studies on coals(14-16) and coal-related materials(17) have been informative. Earlier XPS studies on

coals(15) have shown the presence of pyridine and pyrrole; a more recent study(16) has also shown the presence of quarternary nitrogen. XPS experiments clearly could not resolve signatures arising from oxygen containing pyridone or the aromatic and saturated amine structures in coals.

In this report, preliminary XANES studies of quarternary nitrogen (pyridinium) are presented as a potential contributor to coal spectra. Several analogues of pyridinium compounds have been studied. It is found that these structures have a distinct sharp π^* resonance at 401.8 eV, and is invariant among the different analogues. The pyridinium resonance is between the pyridine and the pyridone resonances, and is distinguishable from those from other structures. The coal spectra do not show any prominent sharp feature at the pyridinium π^* energy, and at most show only small quantities of these structures. The pyridone percentage far exceeds the quarternary percentage, and the inverse connection between the pyridone and pyridine percentages is still more prominent.

EXPERIMENTAL SETUP

Nitrogen x-ray data on all the coal and model samples have been obtained at the soft x-ray beam line U4B, designed and constructed by AT&T Bell Labs(18), at the National Synchrotron Light Source at Brookhaven National Laboratory. U4B is equipped with a grating monochromator with a grating of 600 lines/mm. The sample chamber was maintained at pressures of 10^9 to 10^{10} torr by means of a turbo-molecular pump and a cryopump. The samples were mounted on pieces of nitrogen-free 3M tape and positioned on a sample holder by a load-lock system. A multichannel Ge fluorescent detector(19) was used with a 2- μ s shaping time. The energy resolution was about 140-400 meV.

The coal samples were provided by Dr. Karl Vorres from Argonne Premium Coal Sample Bank at Argonne National Laboratory(20). The coal sample suite consisted of eight samples; these samples belonged to varying ranks, starting from lignite to low-volatile bituminous. The samples were: a low-volatile bituminous coal from Pocahontas #3, VA (POC); a medium-volatile bituminous coal from Upper Freeport, PA (UF), four high-volatile bituminous coals from Pittsburgh #8, PA (PITT), Lewiston-Stockton, WV (WV), Blind Canyon, UT (UT), and Illinois #6, IL (IL), and a subbituminous from Wyodak-Anderson, WY (WY), and a lignite from Beulah-Zap, ND (ND).

The nitrogen model samples were obtained from Aldrich Chemical Company. The pyridine samples were acridine, 4,7-diphenyl-1,10-phenanthroline, phenanthridine, di-p-tolylpyridine, and 4-polyvinylpyridine-costyrene; the pyridinium samples were pyridinium dichromate, 1-ethyl-4-(methoxycarbonyl) pyridinium iodide, and pyridinium 3-nitrobenzenesulfonate; the pyridone samples were 6-(2,2-diphenyl-2-hydroxyethyl)-2(1H)-pyridone, 2-hydroxyquinoline, 1-hydroxyisoquinoline, 1-methyl-4-pentadecyl-2(1H)-quinoline; the pyrrole samples were tetrahydrocarbazole, 2-phenylindole, 9-vinylarbazole, and carbazole; the aromatic amine samples were 2-aminofluorene, and 2,7-diaminofluorene, and the saturated samples were 1,3,5-tribenzylhexahydro-1,3,5-triazine, and diaminododecane. All the coal and the nitrogen model XANES spectra were calibrated with respect to the first π^* resonance of zinc octaethylporphyrin at 399.72 eV.

RESULTS AND DISCUSSIONS

The XANES spectra of the coals show similar features with three well-resolved resonance regions(11). The feature at 401.8 eV is relatively insignificant compared to the major resonances; it occurs at the red tail-end of the second broad resonance region between 402 and 405 eV. The major resonances are much more intense; of these, the first resonance at 399.7eV varies in intensity among the different ranked coals. The lowest rank coal has a less intense resonance at 399.7eV while the same resonance in the higher rank coals is much more intense. The second resonance region, upon close inspection, shows the presence of three resonances, at \sim 402eV, \sim 403.5eV, and at \sim 405 eV. The intensity of the 402 eV also varies significantly among coals of different ranks; it is more prominent in the low rank coals than in the high rank coals. The feature at 405eV is also comparatively insignificant, and is merely a valley with varying depth, with no strong trend as a function of coal rank. All the coal spectra show a prominent resonance at 408eV.

XANES studies of different nitrogen model compounds have been performed in order to analyze the coal spectra. In the present report, spectra of six groups of model compounds have been associated with the coal spectra; they are pyridine, pyridinium, pyridone, pyrrole, aromatic amine and saturated amine. In our previous work(11) we have analyzed all the above nitrogen structures except for pyridinium. The pyridinium π^* resonances are sharp, and invariant; they are well grouped together at around 401.8 eV, consistent with our earlier results(11) of the different π^* resonances of pyridine analogues (at 399.7 eV), pyridone analogues (at 402 eV), pyrrole analogues (at 403.5 eV), and aromatic amines (at 405eV). The pyridinium π^* resonances occur at a higher energy than the pyridine π^* resonances; this is consistent with the observation in the case of sulfur structures(5), where the π^* resonances are blue shifted with more positive oxidation numbers. The π^* resonances of pyridone, on the other hand, are generally at higher energies than pyridinium resonances. Perhaps with more number of analogues a small overlap may be observed between the pyridone and pyridinium resonances. The pyrroles have higher energy π^* resonances compared to pyridine; we have explained this due to the difference of the orbital location of the lone pair of electrons at the nitrogen site. The fact that each different nitrogen structure has a characteristic π^* absorption feature distinct from that of another structure helps in the analysis of coal spectra which may contain several different nitrogen structures.

The coal spectra do not show any prominent absorption resonance at the pyridinium signature (401.8 eV). The coal spectra show only a wing at this absorption energy which is at least in part due to the pyridone resonance occurring at a higher energy. This, therefore, shows that there is at most a small amount of pyridinium present in the coals. This is consistent with the XPS results(16) which show presence of small amounts of quarternary nitrogen in these coals. In contrast, XANES results show that pyridine and pyrrole are the two major nitrogen structures in coal, consistent with XPS studies(16). XANES data also show signatures arising from pyridone, aromatic amine and saturated amine. To the best of our knowledge, unlike XANES methodology, XPS technique can not resolve features arising from pyridone, aromatic and saturated amines; XANES and XPS can therefore be considered as complimentary techniques.

Previous results(11) show that the low rank coals have a significant pyridone percentage and a low pyridine percentage; on the other hand, the opposite is true with the higher rank coals. This suggests that with maturation of coal, pyridone structures lose their oxygen content, and become transformed into pyridine. The variation of the intensity of the pyridine and the pyridone peaks as a function of coal rank is much more drastic than the small pyridinium content in the different coals.

CONCLUSIONS

XANES methodology is an excellent tool for studying heteroatom structures in coals. Nitrogen occurs mostly in aromatic forms in the coals; pyridine and pyrrole are the two most common nitrogen structures; low rank coals have a high percentage of pyridone and a small percentage of pyridine, and the opposite is true with the high rank coals. This leads to the conclusion that as coals mature, oxygen is driven away, and pyridone structures are converted into pyridine structures. XANES data do not show any prominent resonance at the quarternary nitrogen π^* energy, and low rank coals have inore significant amounts of pyridone than quarternary nitrogen structures.

REFERENCES

1. C. E. Spiro, J. Wong, F. W. Lytle, R. B. Greegor, D. Maylotte, and S. Lampson, *Science*, **226**, 48 (1984).
2. G. P. Huffman, F. E. Huggins, N. Shah, D. Bhattacharya, R. J. Pugmire, G. Davis, F. W. Lytle, and R. B. Greegor, *Processing and Utilization of High Sulfur CoalsII*, Y. P. Chugh et al eds. (Elsevier, amsterdam, 1987), p.3
3. M. L. Gorbaty, G. N. George, and S. R. Kelemen, *Am. Chem. Soc. Div., Fuel Div. Che. Prepr.*, **34**, 738, (1989)
4. G. P. Huffman, F. E. Huggins, S. Mitra-Kirtley, N. Shah, R. Pugmire, B. Davis, F. W. Lytle, and R. B. Greegor, *Energy and Fuels*, **3**, 200, (1989)

5. G. P. Huffman, S. Mitra-Kirtley, F. E. Huggins, N. Shah, S. Vaidya, and F. Lu, *Energy and Fuels*, **5**, 574, (1991)
6. M. L. Gorbaty, G. N. George, and S. R. Kelemen, *Fuel*, **69**, 1065, (1990)
7. G. N. George, and M. L. Gorbaty, *J. Am. Chem. Soc.*, **111**, 3182, (1989)
8. S. R. Kelemen, G. N. George, and M. L. Gorbaty, *Fuel*, **69**, 939, (1989)
9. G. S. Waldo, O. C. Mullins, J. E. Penner-Hahn, and S. P. Cramer, *Fuel*, **71**, 53, (1992)
10. S. Mitra-Kirtley, O. C. Mullins, J. van Elp, and S. P. Cramer, *Fuel*, **72**, 133, (1993)
11. O. C. Mullins, S. Mitra-Kirtley, J. van Elp, and S. P. Cramer, *Applied Spectroscopy*, **47**(8), 1268, (1993)
12. S. Mitra-Kirtley, O. C. Mullins, J. van Elp, S. George, J. Chen, and S. P. Cramer, *J. Am. Chem. Soc.*, **115**, 252, (1993)
13. S. Mitra-Kirtley, O. C. Mullins, J. F. Branthaver, and S. P. Cramer, *Energy and Fuels*, **7**(6), 1128, (1993)
14. P. Burchill, *Proc. of the International Conf. on Coal Science*, J. A. Moujlin et al eds., (Elsevier, Amsterdam, 1987)
15. P. Burchill, and L. S. Welch, *Fuel*, **68**, 100, (1989)
16. S. R. Kelemen, M. L. Gorbaty, S. N. Vaughn, P. J. Kwiatek, *Prepr. Paper, Am. Chem. Soc., Fuel Div. Chem.*, **38**(2), 384, (1993)
17. S. Wallace, K. D. Bartle, and D. L. Perry, *Fuel*, **68**, 1451, (1989)
18. C. T. Chen, *Nucl. Instrum. Methods Phys. Res., Sect. A*, **256**, 595, (1987); C. T. Chen, and F. Sette, *Rev. Sci. Instrum.*, **60**, 1616, (1989)
19. S. P. Cramer, O. Tench, M. Yocum, H. Kraner, L. Rogers, V. Radeka, O. C. Mullins, and S. Rescia, *X-ray Absorption Fine Structure, Proc. of the 6th International XAFS Conf.*, S. S. Hasnain ed. (Ellis Horwood, Chichester, 1991), p. 640
20. K. S. Vorres, *Energy and Fuels*, **4**, 420, (1990)

Comparison of Element-Specific Capillary Chromatography Detectors for the Identification of Heteroatomic Species in Coal Liquids

S.C. Mitchell, K.D. Bartle, K.M.L. Holden
School of Chemistry, University of Leeds
Leeds, LS2 9JT, UK.

C.E. Snape
Department of Pure & Applied Chemistry, Univ. of Strathclyde,
Glasgow, G1 1XL, UK.

S. Moinelo and R. Garcia
Instituto Nacional del Carbon
Apartado 73, 33080 Oviedo, Spain.

Keywords: Gas chromatography, element-selective detection, polycyclic aromatic compounds, atomic emission detection

Abstract

A series of heteroatom-rich coal and coal-derived liquids have been analysed using gas chromatography (GC) in combination with three different element-selective detectors. Selected chromatograms, including a supercritical extract (Mequinenza lignite) and aromatic fractions isolated from coal tar pitch samples are presented. In each case a series of sulphur- and/or nitrogen-containing compounds have been identified using either flame photometric detection (GC/FID/FPD) or nitrogen-phosphorous detection (GC/FID/NPD) and the information compared with that obtained from a GC coupled to an atomic emission detector (GC-AED). Preliminary results have demonstrated the relative response characteristics of each detector and their respective ability to acquire qualitative and quantitative information in interfering background matrices. Further, due to the unique capabilities of GC-AED, a number of dual heteroatomic (sulphur-oxygen and nitrogen-oxygen) compounds have been identified.

Introduction

Polycyclic aromatic compounds (PAC) predominate in coal liquids as well as in other heavy oils derived from fossil fuels. While the polycyclic aromatic hydrocarbons (PAH) are usually the most abundant PAC, nitrogen-, sulphur-, and oxygen-containing compounds are also present in significant concentrations and their impact on processing and the environment/human health are well documented⁽¹⁻³⁾. Numerous characterisation studies have been conducted into the nature of aromatic and heterocyclic compounds present in such materials and many researchers have derived information from pyrolysis products, solvent extracts and liquefaction products⁽⁴⁻⁶⁾. Most of the recent work has focussed on the development of techniques for both separation and detection of compound or element-rich fractions. The principal methods employed to date include capillary column gas chromatography^(7,8), liquid chromatography⁽⁹⁾, element-selective detection⁽¹⁰⁻¹⁶⁾, high resolution mass spectrometry⁽¹⁷⁻²⁰⁾ and X-ray techniques⁽²¹⁾.

For the identification of heteroatomic species, the most successful approach has been the use of capillary column gas chromatography in combination with gas chromatography/mass spectrometry⁽²²⁻²⁴⁾. However, interpretation is complicated due to the properties of aromatic heterocycles being very similar to those of aromatic hydrocarbons⁽²⁾ and prior fractionation or enrichment of target compounds into compound classes is considered an essential step for their unambiguous identification^(12,13).

The use of element-selective detection in gas chromatography, for simplifying the analysis of complex hydrocarbon mixtures, is now relatively commonplace⁽²⁵⁾; but their application, particularly in the determination of trace concentrations of polycyclic

aromatic compounds, requires that due care and consideration be exercised. Flame photometric detector (FPD), has been extensively used for qualitative analysis of sulphur compounds but suffers from many inherent problems including a non-linear response (approx. quadratic) and compound dependency which makes quantitative analysis difficult and time-consuming. Moreover, quenching of the signal by coeluting hydrocarbons can considerably reduce sensitivity⁽²⁶⁾. For nitrogen compounds, the nitrogen-phosphorous detector (NPD), with a specificity (N/C) of 10^3 - 10^5 and a linear response over several orders of magnitude (see Table 1) is well suited to handling trace analysis in complex hydrocarbon mixtures⁽²⁷⁾. The relatively recent introduction of atomic emission detection (AED), as a commercially available analytical tool has received comparatively little attention⁽²⁸⁻³⁰⁾. GC-AED offers highly selective, simultaneous, multi-elemental detection and claims to suffer from none of the enigmas associated with other element-selective detectors. Based on a microwave induced plasma (MIP) and employing a moveable photodiode array (PDA) in a flat focal plane spectrometer, the AED is capable of monitoring a broad range of elements at considerably lower levels than most classical GC detectors⁽²⁷⁾. Detector response is linear and compound independent, with the possibility of empirical and molecular formula determination.

GC analysis

HP5890 Series II Gas chromatographs were used for AED and NPD analysis. A Perkin-Elmer 8500 gas chromatograph was used for FPD analysis. The GC-AED system also comprised an HP7637A Autosampler interfaced to an HP5291A AED Chemstation.

Samples were analysed by GC-AED and GC/FID/FPD using a 25m BPX-5 or equivalent column with 0.5 μ m film thickness and 0.32mm i.d. For NPD analysis a 25m SE-54 column with 0.25 μ m film thickness and 0.25mm i.d. was used. GC and AED parameters are given below:

GC parameters

Detector	FPD	NPD	AED
Injection port temperature ($^{\circ}$ C)	300	300	350
Injection mode	split (1:80)	split (1:80)	splitless
Column-detector coupling	on-line	on-line	coupled to cavity
Injection volume	1 μ l	1 μ l	0.2 or 1 μ l
Carrier gas	Helium	Hydrogen	Helium*
Oven program	Initial temp: 50 $^{\circ}$ C; Ramp rate: 4 $^{\circ}$ C/min to 280 $^{\circ}$ C; Hold: 20 min		

* High purity Helium (99.999999%) as recommended⁽²⁸⁾

AED parameters

Element	Wavelength(nm)	Scavenger gas
C	193.0	H ₂ /O ₂
S	181.4	H ₂ /O ₂
N	174.3	H ₂ /O ₂
O	777.3	H ₂ /N ₂ /CH ₄

Spectrometer purge flow: Nitrogen @ 2l/min
 Transfer line temperature: 350 $^{\circ}$ C Cavity temperature: 350 $^{\circ}$ C

Results and Discussion

The following examples illustrate the role of element-specific detectors in characterising heteroatomic species in coal liquids and demonstrate the unique capabilities of GC-AED for identifying dual or multiple heteroatom compounds in such materials. Further, from the chromatographic data accumulated to date it is anticipated that a comprehensive comparison of NPD and FPD with AED will be possible. Detailed qualitative and quantitative information is currently being obtained by a combination of literature retention time data and model compound data. Gas

chromatography-mass spectrometry (GC-MS) and GC-AED will provide structural characterisation.

From the selected chromatograms; Figure 1a,b shows the sulphur response of GC-AED and GC/FPD chromatograms respectively from the analysis of a supercritical gas extract of Mequinenza lignite. For both detectors, the chromatograms are very similar in general appearance (i.e. no. of peaks observed) and both display a series of alkyl substituted thiophenes, benzothiophenes and dibenzothiophenes. Taking into consideration sampling variations and the higher injector temperature employed in the GC-AED system the only remarkable difference is the relative peak intensities observed by both detectors. This can be accounted for by the compound dependency of the FPD and the possibility of quenching effects due to the high hydrocarbon presence.

Figure 2a,b compares the AED and NPD traces respectively for a nitrogen-rich, heat treated, coal tar pitch aromatic fraction. As anticipated from detector response characteristics for nitrogen-containing species the chromatograms are almost identical with carbazole, substituted carbazoles, benzoacridine and benzocarbazoles being observed. The NPD has the advantage of a significantly greater selectivity over carbon (see Table 1) and consequently splitless GC injections using concentrated solutions were used for AED analysis. This results in what appears to be an instrument induced effect for the high boiling heterocyclics where peak splitting and a general distortion of peak shape occurs. Similar observations have been made for sulphur and oxygen containing PACs.

The unique capabilities of the GC-AED as a multi-element detector are demonstrated by the identification of dual heteroatom compounds present in both the supercritical gas extract and the coal tar pitch sample. Figures 3a,b show segments of the C,S,O and C, N, O, chromatograms obtained for Mequinenza lignite and heat treated pitch respectively. By correlating characteristic emission wavelength responses with retention time data, the presence of oxygen-sulphur and nitrogen-sulphur compounds have been unambiguously identified. Further confirmation is obtained using a "snapshot" facility which is a selected segment of the emission spectrum showing specific elemental emission wavelengths. The exact nature of these dual heteroatom species is as yet uncertain. Figure 4 provides further evidence of the multi-element character of GC-AED where the aromatic fraction from an untreated coal tar pitch has been analysed by GC-AED for C, S, N, O (Figure 4a) and the corresponding GC/FID/NPD is shown in Figure 4b. In both cases the carbon/FID channel provides mainly evidence of nitrogen-containing species but due to the high selectivity for both sulphur and oxygen over carbon for AED (see Table 1) the presence of both sulphur and oxygen compounds (and possibly further multiple heteroatomic species) can be confirmed

References

- (1) Karr, C., Jr., Ed. "Analytical Methods for Coal and Coal Products", Academic Press: New York, 1978.
- (2) White, C.M., In: "Handbook of Polycyclic Aromatic Hydrocarbons", Bjorseth, A., Ed.; Marcel Dekker: New York, 1981: pp525-616.
- (3) Nishioka, M., Campbell, R.M., West, W.R., Smith, P.A., Booth, G.M., Lee, M.L., *Anal. Chem.*, 1985, 57, 1868-1871 and references therein.
- (4) Davidson, R.E., "Organic sulphur in coal", IEA Report No. IEACR/60, IEA Coal Research, London, UK, 1993 and references therein.
- (5) Davidson, R.E., "Nitrogen in coal", IEA Perspectives Report No. IEAPER/08, IEA Coal Research, London, UK, 1994 and references therein.
- (6) Orr, W.L., White, C.M., Eds. "Geochemistry of Sulphur in Fossil Fuels", ACS Symposium Series, 0097-6156; 429, American Chemical Society, 1989.
- (7) Later, D.W., In: Polycyclic aromatic hydrocarbons. Volume 2, New York, USA, Marcel Dekker Inc., pp265-350 (1985)
- (8) Hardy, R.H., Davis, B.H., *Fuel Science and Technology International*, 7 (4), 399-421 (1989).
- (9) White, C.M., Douglas, L.J., Perry, M.B., Schmidt, C.E., *Energy & Fuels*, 1 (2), 22-226, 1987.

- (10) Kong, R.C., Lee, M.L., Iwao, M., Tominga, Y., Pratap, R., Thompson, R.D., Castle, R.N., *Fuel*, 1984, 63, 707-713.
- (11) Willey, C., Iwao, Castle, R.N., Lee, M.L., *Anal. Chem.*, 1981, 53, 400-407.
- (12) Nishioka, M., Campbell, R.M., Lee, M.L., Castle, R.N., *Fuel*, 1986, 65, 270.
- (13) Nishioka, M. Lee, M.L., Castle, R.N., *Fuel*, 1986, 65, 390.
- (14) Nishioka, M., Lee, M.L., Kudo, H., Muchiri, R.R., Baldwin, L.J., Pakray, S., Stewart, J.G., Castle, R., *Anal. Chem.*, 1985, 57, 1327-1330.
- (15) Burchill, P., Herod, A.A., Pritchard, *Fuel*, 1983, 62, 11-19.
- (16) Nelson, P.F., Kelly, M.D., Wornat, M.J., *Fuel*, 70 (3), 403-407 (1991).
- (17) Winans, R.E., Neill, P.H., in "Geochemistry of Sulphur in Fossil Fuels", Symposium Series 429, American Chemical Society, 1989, pp.249-260.
- (18) Sinninghe Damste, J.S., de Leeuw, J.W., *Fuel Process Technol.*, 1992, 30, 109.
- (19) Cerny, J., Mitera, J., Vavrecka, P., *Fuel*, 68 (5), 596-600 (1989).
- (20) White, C.M., Douglas, L.J., Anderson, A.A., Schmidt, C.E., Gray, R.J., in: "Geochemistry of Sulphur in Fossil Fuels", Symposium Series 429, American Chemical Society, 1989, pp.261-286.
- (21) Bartle, K.D., Perry, D.L., Wallace, S., *Fuel Processing Technol.*, 15, 351-361, 1987.
- (22) Sinninghe Damste, J.S., Eglinton, T.L., de Leeuw, J.W., Schenck, P.A., *Geochimica et Cosmochimica Acta*, 53 (4), 873-889 (1989).
- (23) Sinninghe Damste, J.S.S., de las Herras, F.X.C., de Leeud, J.W., *Journal of Chromatography*, 607 (2), 361-376, 1992.
- (24) Eglinton, T.I., Sinninghe Damste, J.S.S., Kohnen, M.E.L., de Leeuw, J.W., Larter, S.R., Patience, R.L., in: "Geochemistry of Sulphur in Fossil Fuels", Symposium Series 429, American Chemical Society, 1989, pp.528-565.
- (25) Dreschel, M., "Selective Gas Chromatography Detectors", p.133. Elsevier Science Publishing, Amsterdam, 1986.
- (26) Farwell, S.O., Baringa, C.J., *J. Chromatogr. Sci.*, 24, 483 (1988).
- (27) Patterson, P.L., In: "Detectors for Capillary Chromatography", Hill, H.H., McMinn, D.G., Eds. Chap. 7, pp.139-168, Chemical Analysis Series, Volume 121, John Wiley & Son, Inc., 1992.
- (28) Quimby, B.D., Sullivan, J.D., *Anal. Chem.* 62, 1027 (1991).
- (29) Sullivan, J.D., Quimby, B.D., *Anal. Chem.*, 62, 1034 (1990).
- (31) Wylie, P.L., Quimby, B.D., *J. High Resol. Chromatogr.*, 12, 813 (1989)
- (32) Uden, P.C., *Chromatogr. Forum*, 1(4), 17 (1986).

Table 1: Detector response characteristics¹

	FPD	Detectors NPD	AED
Minimum detectable levels (pgS/sec) (pgN/sec)	2-50	0.05	(1-2) (50)
Selectivity (S/C) (N/C)	10 ⁴ -10 ⁵	7*10 ⁴	(8*10 ⁴) (2*10 ⁴)
Linear response	No (quadratic)	Yes	Yes
Linear dynamic range	1-5*10 ²	10 ⁵	(1*10 ⁴) (2*10 ⁴)

¹Values taken from literature⁽²⁶⁾

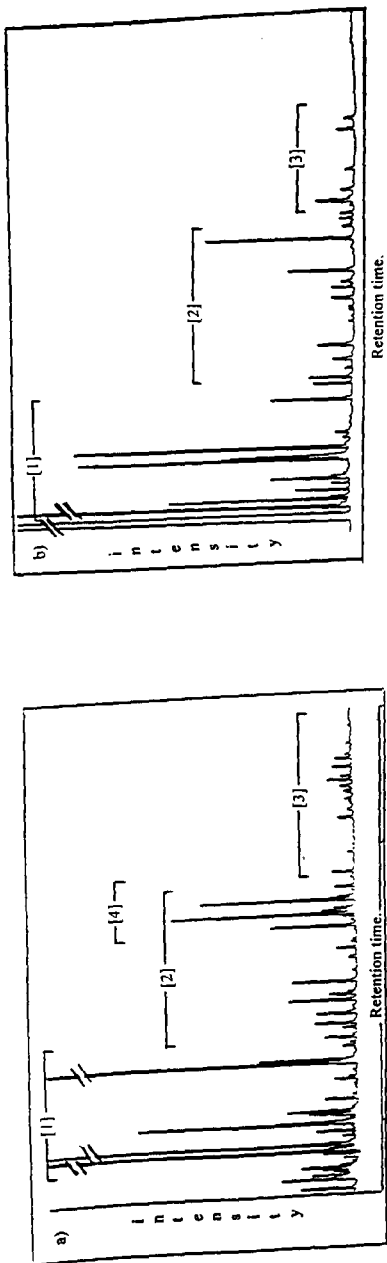


Figure 1. A supercritical gas extract of Mequinenza lignite: a) AED sulphur 181nm channel and b) FPD sulphur response. General assignments: [1] substituted thiophenes; [2] benzothiophenes and [3] dibenzothiophenes. [4] See Figure 3a) for an enlargement of this region.

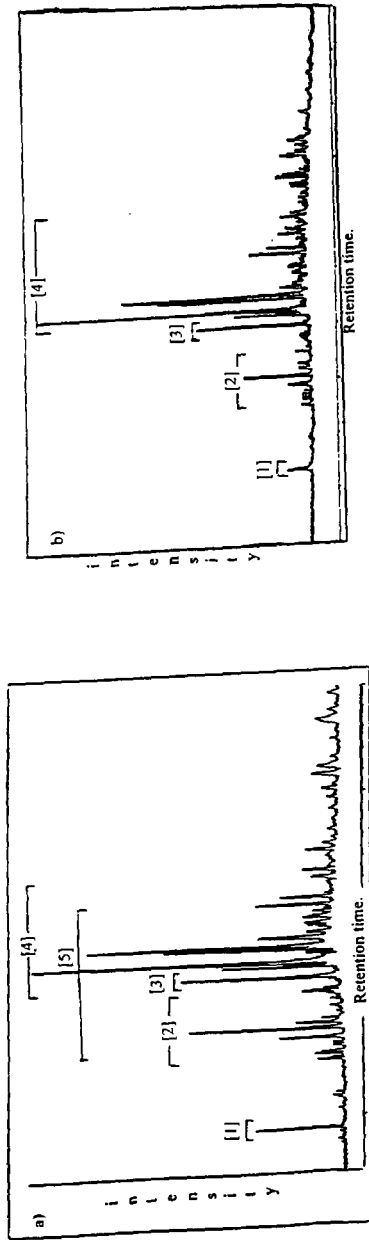


Figure 2. A coal tar pitch (S.P. 1050°C), heat treated at 350°C: a) AED 175nm channel and b) NPD nitrogen response. General assignments: [1] carbazole; [2] substituted carbazoles; [3] benzocridine and [4] benzocarbazoles. [5] See Figure 3b) for an enlargement of this region.

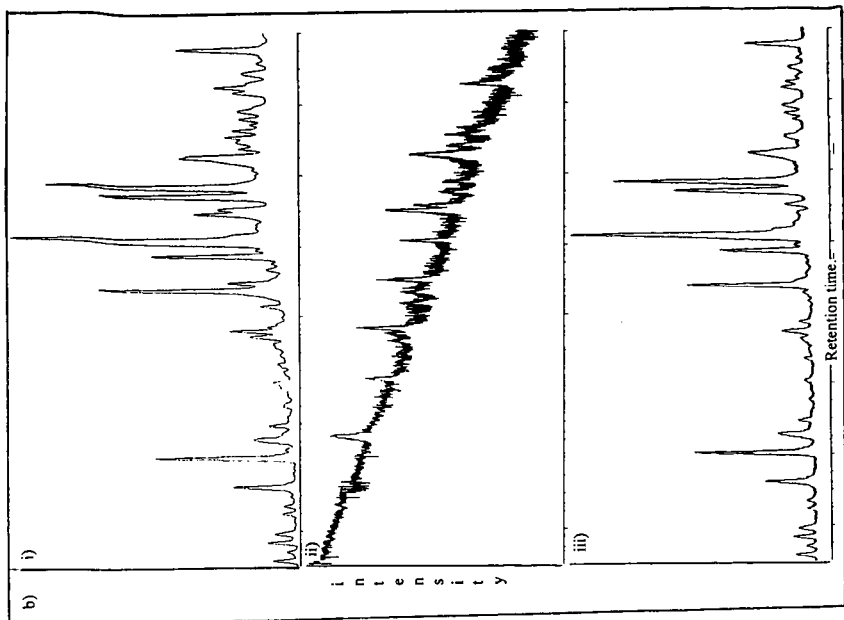
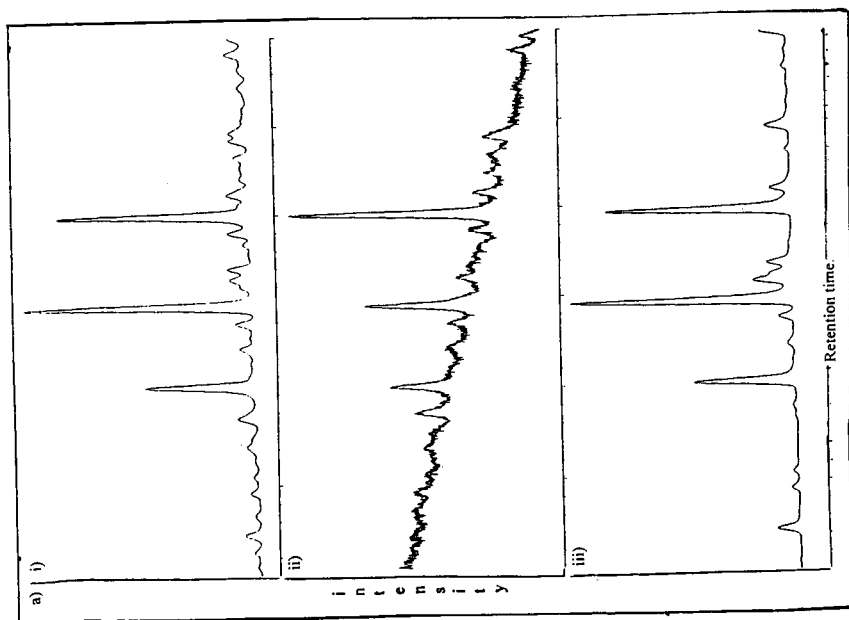


Figure 3. a) A supercritical gas extract of Mequinenza lignite: the GC-AED response on, i) the carbon 193nm channel; ii) the oxygen 777nm channel and iii) the sulphur 181 nm channel.
 b) A coal tar pitch (S.P. 105°C), heat treated at 350°C: the GC-AED response on, i) the carbon 193nm channel; ii) the oxygen 777nm channel and iii) the nitrogen 174nm channel.

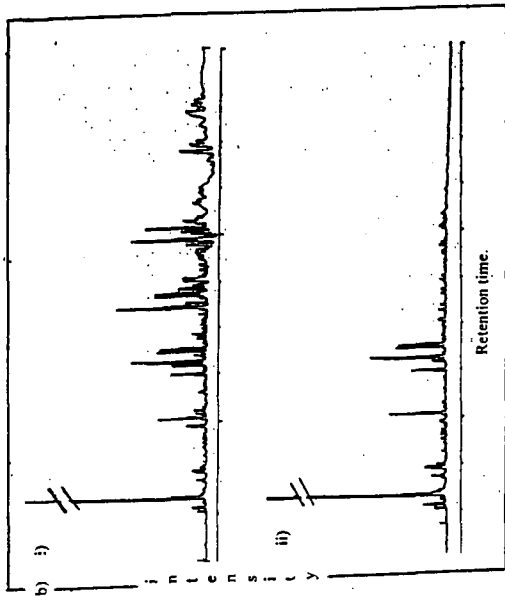
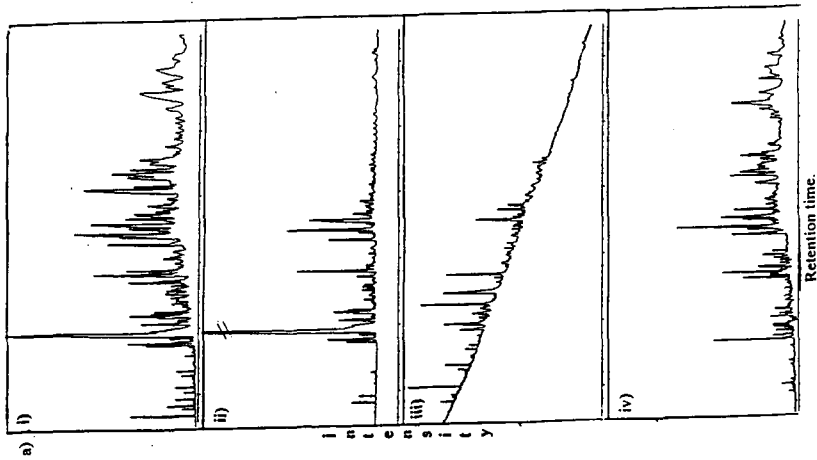


Figure 4. An untreated coal tar pitch (S.P. 35°C): a) the GC-AED response on: i) the carbon 193nm channel; ii) the nitrogen 175nm channel; iii) the oxygen 777nm channel and iv) the sulphur 181 nm channel. b) i) the FID carbon response and ii) the NPD nitrogen response.

COMPARISON OF SEVERAL CONTEMPORARY IONIZATION/MASS ANALYZER TECHNIQUES FOR LARGE COMPONENTS OF COMPLEX FOSSIL-DERIVED MATERIALS

Jerry E. Hunt and Randall E. Winans
Chemistry Division
Argonne National Laboratory
Argonne, IL 60439

Keywords: Argonne Premium Coals, mass spectrometry

INTRODUCTION

Coals and coal-derived samples provide a unique mixture for development and comparison of mass spectrometric techniques for high molecular weight analyses. The Argonne Premium Coal samples (APCS), a broad array of research grade standards collected, prepared, and stored under controlled conditions, are convenient for assessing classical and novel mass spectrometric techniques. Vacuum pyrolysis mass spectrometry of APCS 4 (Pittsburgh #8) has been reported.¹ Alkyl-substituted aromatic compounds and hydroxy- and dihydroxy-substituted aromatic compounds were observed. Newer techniques such as laser desorption (LD), as well as in-beam techniques, such as desorption chemical ionization (DCI) and desorption electron ionization (DEI) are better suited to the studies of mixture characterization as presented by fossil fuels.

We have previously reported laser desorption of coal extracts that show only low molecular weight ions (<1000 amu).^{2,3} The latter report compares LD with fast atom bombardment and DCI mass spectrometry. All three techniques produce similar data that differ only in minor details. Hanley reported LDMS of pyridine extracts produces a distribution of ions between 150 and 1500.⁴ Field ionization mass spectrometry shows similar patterns.⁵ Recently, others have interpreted their LD results in terms of high mass species (>12,000) being desorbed.^{6,7} The authors present data taken from single laser shots. We believe that the data presented can best be interpreted as electronic "noise" and that the observed signals are not related to the sample. In our hands, laser desorption mass spectrometry of coals and coal-derived materials does not show any reproducible ion intensity above 2000 u. Our results have been obtained on two different time-of-flight instruments, one constructed in-house and one a commercial instrument (Kratos Kompact MALDI III).

Laser desorption mass spectrometry has recently been used to identify high molecular weight proteins of mass in excess of 100,000 amu. Thus, if there are indeed large molecular species in coals or coal extracts, LDMS is an attractive technique. However, the conditions whereby large molecular ions can be desorbed intact are very specialized. The extension of LD to heavier molecules is made possible by embedding the sample in a chemical matrix (matrix-assisted laser desorption ionization, MALDI). Without this matrix, large mass species are not observed. Recently, Herod reported results using a time-of-flight mass spectrometer designed for MALDI analysis.⁸ He concluded that high mass species (up to 200,000 u) are observed in the mass spectrum. We have used our two TOF mass spectrometers for coal analysis by MALDI, have carefully analyzed our data and the instrumental conditions, and conclude that only low molecular weight ions (up to 1500 u) are observed. We interpret our results quite differently from Herod. First, results from both of our mass spectrometers are similar, i.e., ion intensities are in the mass range from about 200 to 1500. No ion peaks are observed at higher masses in either instrument. We did observe a problem with the detector in the Kratos instrument that may result in an over-interpretation of the data. The detector in the Kratos instrument is very sensitive to ion saturation, that is, high ion currents cause spurious peaks to be observed at times of flight which are uncorrelated in time and, thus, uncorrelated in mass. These may be incorrectly interpreted as "true" ion signals of high mass. If, indeed, large molecules do exist in coal, new matrices will need to be identified which are applicable to the types of compounds found in coal. We are currently investigating this area.

This study focuses on a number of complementary approaches that have been used to investigate fossil fuel-derived materials. LD, DCI, and DEHRMS are compared as methods of volatilizing high molecular weight species present in coal samples. Also, DEHRMS on a high resolution three-sector tandem mass spectrometer is compared to laser desorption with laser photoionization on a time-of-flight instrument for high mass mixture selectivity.

EXPERIMENTAL

The coals used in this study are the Argonne Premium Coal Samples 1 (Upper Freeport mvB) and 2 (Wyodak-Anderson subB). A complete discussion of the characteristics of the coals used in this study has been reported.⁹ Vacuum pyrolysis tars were prepared by heating coal in a vacuum at 400 °C and collected at room temperature. Pyridine extracts and KOH/glycol solubilization procedures have been reported.¹⁰ The EI and DCI mass spectra were recorded on a Kratos MS 50 triple analyzer. The reagent gas for the DCI studies was isobutane. The solids and extracts were heated in the source on a small platinum wire coil from 200 °C to 700 °C at 100 °C/min. with the source heated at 200 °C. The laser desorption and laser ionization mass spectra were recorded on a linear time-of-flight mass spectrometer constructed in-house and a Kratos Kompact MALDI III reflectron time-of-flight mass spectrometer. The fluence of the desorption laser is held constant at 10-100 mJ/cm² at a repetition rate of 20 Hz. For direct ion desorption the laser is operated close to the ionization threshold to minimize fragmentation of the desorbing material. The laser is operated at lower fluences for neutral ion desorption. The neutral molecules are then ionized by vacuum ultraviolet light. The 118 nm laser pulses are produced by third harmonic conversion of 355 nm light from a Nd:YAG laser in a high pressure Kr cell.

RESULTS

Figure 1 shows a comparison mass spectrum of the vacuum pyrolysis tars from APCS 1. The lower panel is the direct laser desorption mass spectrum and the upper panel the DCI mass spectrum of the same sample. In each spectrum there are only a small number of low intensity peaks below $m/z=200$, indicating the overall soft ionization of each technique. The two methods show similar peaks, with some variation in intensity. Overall the LD spectrum shows fewer peaks up to a mass of about 275 as compared to a more dense region for the DCI data. In LD the more volatile species sublime and are not observed. Above this mass the spectra are quite similar. The peaks in the DCI data are generally +1 species as compared to the LD data, indicating the formation of $(M+H)^+$ ions. Several homologous series are observed in the LD and DCI data. Possible structures can be assigned to each of these series based on PyHRMS results from the same coal sample. The prominent series (especially in the LD data) at $m/z = 230, 244, 258, 272$ is assigned to alkyl-pyrenes or fluoranthenes. Another series contains two different species, alkylphenyl-naphthalenes and alkylhydroxy-pyrenes or fluoranthenes. Thus, there is good agreement in mass, if not intensity, for these two techniques.

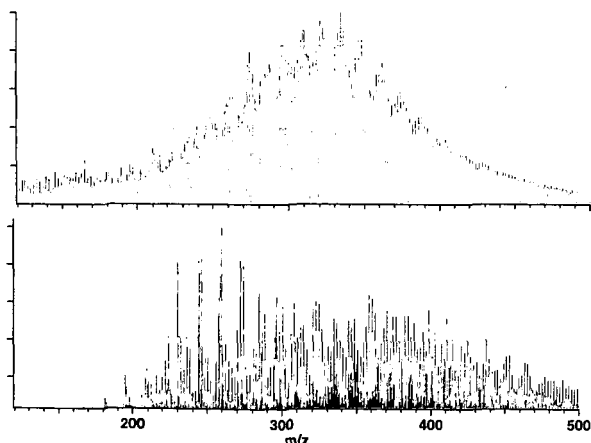


Figure 1. Comparison of LD (lower panel) and DCI (upper panel) methods for vacuum pyrolysis tars of APCS 1 (Upper Freeport mvB).

At higher masses there is also good agreement between the techniques. Several homologous series appear at these higher masses. A series at $m/z = 292, 306, 320, 334, 348, 362, 376$ is possibly alkylphenylpyrenes. Another series between 306 and 362, form an oxygen containing series with a suggested structure of methylbenzopyrenofuran.

The mass spectra of the demineralized pyridine extract of APCS 1 is shown in Figure 2. Spectrum A is the direct laser desorption mass spectrum of the pyridine extract and spectrum B the EI mass spectrum. Again the overall absence of ion intensity below 225 in the LD indicate soft ionization, i.e., the molecular fragmentation is minimum. Also, in laser desorption low molecular weight (volatile) molecules will be lost due to the high vacuum.

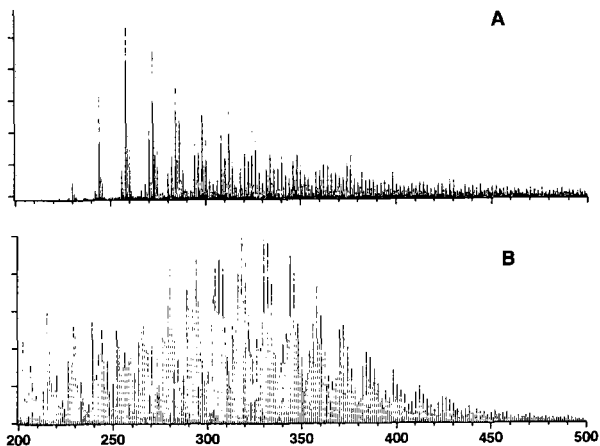


Figure 2. The pyridine extract of demineralized APCS 1. A, the LD and B, the EI mass spectrum.

Table 1. Major Ion Series in Laser Desorption of Pyridine Extract of APCS 1

Ion Series	Structural Type
230, 244, 258, 272, 286, 300, 314	alkyl pyrene or fluoranthene
242, 256, 270, 284, 298	alkyl chrysenes
252, 266, 280, 294, 308	alkyl benzopyrene or benzofluoroanthene
292, 306, 320, 334, 348, 362, 376	alkyl phenylpyrenes and pyrenobenzofuran
195, 209, 223, 237, 251	alkyl carbazoles
276, 290, 304, 318, 332	alkyl benzoperylene

In general the direct laser desorption mass spectra favor the aromatic compounds over the aliphatic, producing a simpler, cleaner mass spectrum, while the EI spectra show aliphatic as well as aromatic species.

Since direct laser desorption favors aromatic species at the expense of aliphatic species a method to enhance LD was employed. First, at low fluence, neutral molecules are desorbed, then a second laser pulse of 10.5-eV is used to ionize the neutrals. Since multiple photons can be absorbed increased ionization efficiency is expected for aliphatic species. A comparison of DEIHRMS and LD of neutral with photoionization is shown in Figure 3. The sample in this case is the hexane extract of the KOH/glycol reaction of APCS 2 (Wyodak-Anderson). The overall similarity of the spectra is compelling. The peak from $m/z = 368$ to 508 are assigned as acid with the base structure $H(CH_2)_nCO_2H$, $n = 23-33$. An important difference in the spectra is the appearance of high mass ions in the LD/LI spectra. Coupled with time of flight mass spectrometry, the spectra exhibit parent ion abundance which conventional 70 eV electron impact lack. The peaks near $m/z = 800$ do not appear in the DCI MS spectra. These peaks may be assigned as very long chain fatty acids on the order of C_{30} .

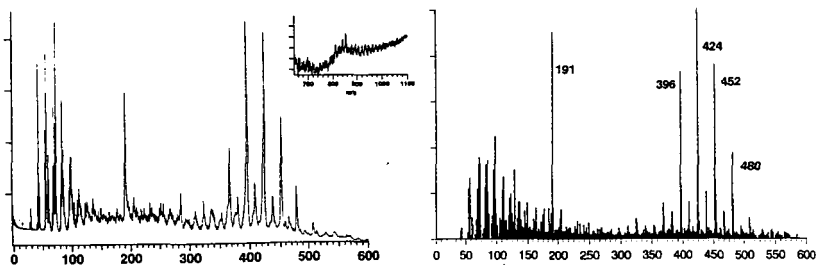


Figure 3. The laser desorption/laser ionization mass spectrum (left) and DEIHMS (right) of the hexane extract of KOH/glycol reaction of APCS 2.

CONCLUSION

The mass spectra show different molecular weight distributions, but similar ion series. In general LD, DCI, and EI give progressively lower distributions. Furthermore, the ions present in the LD and DCI spectra are directly comparable, while LD and EI produce different ion distributions. Information on neutrals is available from LD-photoionization. The appearance of an ion series in the $m/z = 700-1000$ range demonstrates an advantage of 10.5-eV ionization and TOF analysis. Mass spectral data from both LDMS, DCIMS, and EIHRMS are being analyzed for all eight Argonne Premium Coal samples.

ACKNOWLEDGMENT

This work was performed under the auspices of the Office of Basic Energy Sciences, Division of Chemical Sciences, U.S. Department of Energy, under contract number W-31-109-ENG-38.

REFERENCES

1. Yun, Yongseung; Meuzelaar, Henk L.C.; Simmleit, N.; Schulten, H.-R. *Energy Fuels* **1991**, *5*, 22-29.
2. Hunt, J.E.; Lykke, K.R.; Winans, R.E. *Preprints, Am. Chem. Soc., Div. Fuel Chem.* **1991**, *36*, 1325-1328.
3. Winans, R.E.; McBeth, R.L.; Hunt, J.E.; Melnikov, P.E. *Proc., 1991 International Conference on Coal Science*; University of Newcastle upon Tyne, UK, September 16-20, 1991, pp. 44-47.
4. Burroughs, J.A.; Cadre, B.M.; Hanley, L. *Proc., 41st American Society of Mass Spectrometry*; San Francisco, CA, May 30-June 4, 1993, p. 441.
5. Herod, A.A.; Stokes, B.J.; Schulten, H.-R. *Fuel* **1993**, *72*, 31-43.
6. John, P.; Johnson, C.A.F.; Parker, J.E.; Smith, G.P.; Herod, A.A.; Gaines, A.F.; Li, C.-Z.; Kandiyoti, R. *Rap. Commun. Mass Spectrom.* **1991**, *5*, 364-367.
7. Herod, A.A.; Kandiyoti, R.; Parker, J.E.; Johnson, C.A.F.; John, P.; Smith, G.P.; Li, C.-Z. *J. Chem. Soc., Chem. Commun.* **1993**, 767-769.
8. Herod, A.A.; Parker, J.E.; Johnson, C.A.F.; John, P.; Smith, G.P.; Li, C.-Z.; Kandiyoti, R. *Proc., 7th International Conference on Coal Science*; Banff, Alberta, Canada, September 12-17, 1993, pp. 1282-1285.
9. Vorres, K.S. *Energy Fuels* **1990**, *4*, 420-425.
10. Winans, R.E.; McBeth, R.L.; Hunt, J.E. *Preprints, Am. Chem. Soc., Div. Fuel Chem.* **1993**, *38*, 561-564.

HIGH PERFORMANCE LIQUID CHROMATOGRAPHY OF COAL LIQUEFACTION
PROCESS STREAMS USING NORMAL-PHASE SEPARATION WITH DIODE ARRAY
DETECTION.

Daniel E. McKinney¹, David J. Clifford¹, Lei Hou¹, Michael R. Bogdan², and Patrick G.
Hatcher¹

1. Fuel Science Program, Department of Materials Science and Engineering, The Pennsylvania
State University, University Park, PA 16802.

2. Sci-Tech, Inc., 200 Innovation Blvd., State College, PA 16803.

Keywords: HPLC, liquefaction, process streams

INTRODUCTION:

Since its introduction as an analytical method in the late 1960s and early 1970s, high performance liquid chromatography (HPLC) has become widely used in environmental studies, especially for the analysis of PAHs^{1,2}. PAHs are widespread environmental contaminants and much effort has been devoted to the development of liquid chromatographic columns which are sensitive to PAH separation. Reverse-phase HPLC on chemically bonded C₁₈ has become the method of choice for the separation of PAHs³⁻⁶, and a review by Wise *et al.*¹ has described general protocols for the separation of PAHs using reverse-phase HPLC. However, direct analysis of PAHs in complex fuel mixtures using reverse-phase HPLC is complicated as sample preparations have become elaborate, due in large part to the fact that most complex organic materials contain compounds that are not usually miscible in acetonitrile, the solvent of choice for reverse-phase HPLC separations of PAHs. These materials routinely are fractionated first into general compound class categories⁷ (i.e. aliphatics, polar compounds, aromatics, resins, and asphaltenes) before separation of PAHs can be performed, and usually normal-phase HPLC is relegated to general cleanup and isolation of the total PAH fraction. The development of "charge-transfer" stationary phases for separation of π -electron rich PAHs⁸⁻¹⁰ allows for the separation of PAHs and their isomers in the normal-phase using solvents which are generally miscible with complex organic systems.

Another problem associated with HPLC analysis of complex fuel mixtures and other extracts of natural samples is that, in the past, normal-phase and reverse-phase HPLC have depended upon either fluorescence detection or monochromatic UV absorbance detection. Fetzer and Biggs² have pointed out, these detection methods are too selective and many compounds go unobserved due to varying optimal wavelengths for different compounds. Developments in the last fifteen years of a full spectrum UV absorbance detector (i.e. diode array detector or DAD) enable full spectrum detection of HPLC eluates. A distinct advantage of the diode array HPLC technique, which provides UV spectra of separated fractions as a function of time, is its ability to identify, by spectral comparisons, the molecular components of the eluates, including the isomers of PAHs.

In this paper, we demonstrate a sensitive method for the detection and analysis of PAHs in coal liquefaction process stream samples. This is accomplished by the normal-phase separation of PAHs and their alkylated derivatives using a TCPP-modified silica column⁸ (Hypersil Green PAH-2) in combination with UV-diode array detection. This method allows for a more sensitive detection and efficient separation of multi-ring PAHs and their isomers without elaborate sample preparations or on-line coupling of a reverse-phase HPLC system.

EXPERIMENTAL:

Instrumentation: The dilute coal liquefaction process stream samples were analyzed and separated using a Waters 600E HPLC and Waters 991 photodiode array detector. The column used for HPLC separations was a Hypersil Green PAH-2 column purchased from Keystone Scientific, Inc.(Bellefonte, PA).

Mass spectral data were collected for each fraction using the solids injection probe of a Kratos MS-80 double-focusing high-resolution mass spectrometer. The ionization mode on the mass spectrometer was electron impact (EI, 70 eV). Instrument control and data collection were accomplished by using a computer-aided Data General DS90 software system.

Sample Description: A standard consisting of a mix of 16 PAH's was obtained from Supelco, Inc., Bellefonte, PA. The coal derived liquids used for two-dimensional, normal phase HPLC separation, were supplied by CONSOL, Inc. and consisted of five liquefaction process streams representing different liquefaction systems, different feed coals, and different degrees of catalytic activity (Table I).

Procedure: The standard PAH mix is subjected to HPLC analysis to derive response factors for internal standard quantitative calculations. The internal standards were benzo[b]fluoranthene and benzo[g,h,i]perylene, which were added to each diluted coal liquefaction stream sample at an appropriate concentration level. The former was used as the internal standard for samples 1, 2, and 3 because the compound elutes in a region containing few intense peaks in the sample eluates. For samples 4 and 5 we used the latter internal standard because some significant peaks were observed in the elution range of benzo[b]fluoranthene and these would co-elute with the standard.

The coal liquids are then filtered through 0.2 μ m filters (Supelco brand ISO-DISC N-32 3mm diameter, nylon membrane, 0.2 μ m pore size filters) in order to remove any insoluble

material. The column, equilibrated with 100% hexane, was operated in the gradient elution mode. Samples are injected onto the PAH-2 column, and following an initial 10 minute isocratic period, a linear gradient from 100% hexane to 100% dichloromethane is used up to 80 minutes followed by a final hold for 5 minutes.

RESULTS AND DISCUSSION:

Knowing that coal liquefaction process streams contain numerous amounts of polynuclear aromatic hydrocarbons and that the PAH-2 column successfully separated PAHs in a known standard, we had reason to be optimistic about its use for coal process stream liquids. The separation obtained for liquefaction process stream samples is demonstrated by 1-D maxplots in Figure 1. Peak identifications listed in Table II were made by comparison of retention times with the PAH standard and by fraction collection combined with heated probe/mass spectrometry. The use of the latter method was deemed necessary, because many peaks did not have retention times that coincided with those of compounds in the standard, notably the alkylated PAHs.

In general, the HPLC traces are characterized by both sharp peaks identified in Table II and broad regions representing unresolved components. The broad region of unresolved peaks between 0 and 20 minutes is constituted predominantly by two and three ring aromatics as determined by mass spectrometry. Most of the compounds are alkylated PAHs having very similar UV spectra, and some compounds are alkylated hydronaphthalenes. The second broad region of absorbance extends from 20 minutes retention time through to the end of the run, containing multiring PAHs and alkylated PAHs having from three to nine condensed rings. The most notable peaks (7, 8 and 9) are those of pyrene and its multialkylated homologs, the internal standard, benzo(b)fluoranthene (peak 11), benzo(g, h, i)perylene (peak 12), and coronene (peak 16).

We can ascribe several important features to each chromatogram, but basically three samples (sample 1 and sample 2), the pressure filtered liquids, show very similar characteristics and differ markedly as a group from the chromatograms of the composite heavy distillates, samples 4 and 5.

Although the three pressure filtered liquid (PFL) samples from the HRI facility generally show similar features, there are subtle differences in the relative distributions of compounds reflecting process conditions. The chromatogram of sample 1, a PFL from the liquefaction of the Wyodak/Anderson coal, differs from those of sample 2 and sample 3 which were obtained from liquefaction conditions using the Illinois #6 coal as feedstock. While pyrene and alkylated pyrenes are major components of all three samples, the two process streams from the Illinois #6 coal contain relatively larger amounts of PAHs with more than four rings, compared with the sample from the Wyodak/Anderson coal. This is perhaps due to the fact that the Illinois #6 coal is of higher rank. All three samples contain significant chromatographic intensity in the two broad unresolved regions described previously. Compared with sample 3, sample 2 appears to contain more intensity in the broad unresolved region in the early eluting portion of the chromatogram ascribed to two and three-ring PAHs. This could indicate that there is a relative build up of more refractory multi-ring material as Run CC-16 progressed.

The chromatograms (maxiplot) for the two high temperature distillates shown in Figure 1 differ from the chromatograms of pressure filtered process streams in that they contain a predominance of compounds with generally fewer than five rings and virtually no compounds with more than five rings other than coronene. This data is consistent with the gc/ms data presented elsewhere¹³. The dominant peaks are those of pyrene and its alkylated homologs (peaks 7 and 8) and dihydro-benzopyrene and its alkylated homolog (peaks 9 and 10). Wyodak coal (sample 5) appears to yield a higher proportion of dihydro-benzopyrene than Illinois #6 coal (sample 4) in its high temperature distillate. This is also consistent with the gc/ms data¹³. Unresolved components dominate the early part of the chromatogram but not the later retention time range. Unlike the pressure filtered process streams, the distillates contain no significant "hump" for unresolved components between retention times of 40 and 80 min. Obviously, the samples from the Wilsonville facility, comprised of distillates boiling below 850°F, contain lower boiling PAHs, in contrast to the samples obtained from the HRI facility which were not subjected to distillation. This is also demonstrated by the solubility data (Table I), in that samples 1, 2, and 3 have lower solubilities, consistent with higher molecular weight components, compared to the higher solubilities of samples 4 and 5, consisting of lower molecular weight components.

Table II contains the quantitative data for the five samples. As mentioned above, the dominant compounds exist as 1-3 ring aromatic/hydroaromatic compounds of undetermined structure. These account for more than half of the products detected. Other multiring PAHs individually account for between 0.05% and 1.3 % of the sample weights of the samples 1-3. Summing of the concentrations of peaks 1-19 in each chromatogram for samples 1-3 reveals that 18% to 32% of the sample weights can be accounted for as detected PAHs. Samples 1 and 2, filtered process streams from two different coals at the HRI facility, appear to have similar overall concentrations of PAHs, even though the distributions are slightly different as mentioned above. The difference between samples 2 and 3, from the same coal, appear to be related to changes in process time, since they represent samples taken from different days. Samples 4 and 5, from the Wilsonville reactor, appear to have significantly lower concentrations of all detected compounds, ranging from 0.007% to a maximum of 2.3%. The significant decrease in concentrations compared to the samples from the HRI facility is indicative of the differences in liquefaction methodology. Not only are the yields of PAHs lower, but the distributions are different, as discussed previously. The low yields initially seemed puzzling, but examination of the gc/ms data presented in a previous report¹³ indicates that significant amounts of unresolved complex materials having intense *m/z* fragment ions characteristic to structures of C_nH_{2n-3} are present. It is likely that the parent compounds of these fragment ions do not yield significant

absorptions in the UV range, thus, explaining why they remain undetected by the HPLC method. If the compounds are undetectable by UV-absorption, then they fall out of our analytical window, a pitfall for this method.

CONCLUSIONS:

The results outlined in this report from experiments performed in our laboratory have proved very encouraging. We were successful in the separation, characterization, and quantification of PAHs of a limited series of select samples which depict a broad range of liquefaction process conditions, using a newly developed normal-phase HPLC column, the Hypersil PAH-2, coupled with a UV-diode array detector. We feel this method has great potential for the characterization of liquefaction process streams along with other extracts of natural products containing high concentrations of PAHs. The success of this method was based on the fact that it enabled us to identify both qualitative and quantitative differences among the limited sample set. Perhaps the most readily observed differences are noted between samples obtained from the HRI facility and the Wilsonville facility. Thus the technique can readily distinguish between sample types from these two liquefaction facilities, regardless of the feed coal used. Those compounds detectable by HPLC from the Wilsonville samples, 850°F distillates, appear to be of lower ring number than samples from the HRI facility, whose samples are composed of the whole process stream.

The HPLC method also allows differentiation among samples from the same facility but differing in their process conditions. For example, a different distribution of PAH's was obtained from the process stream samples in which different coal feedstocks were used. The sample liquefied from the Illinois #6 coal appears to have a higher amount of the multi-ring PAH's than the sample from the Wyodak, consistent with the fact that higher rank of coal is more likely to yield more of the higher condensed ring compounds. Another difference between samples indicative of differences in process conditions is that between samples 2 and 3. The former contains a significantly greater concentration of PAH's and, as a result, more of the sample can be quantified. The PAH distributions are similar, in a relative sense, which is indicative of the fact that the entire spectrum of PAH's is being reduced by the processing and could indicate a build-up of more refractory material as the run progressed. Subsequently, time resolved differences induce an overall decrease in PAH levels, which could be related to increased hydrogenation of the rings due to increased exposure to liquefaction conditions or to deactivation of the catalyst.

ACKNOWLEDGMENTS:

We thank Susan D. Brandes, Richard A. Winschel and Frank P. Burke (CONSOL, Inc.) for providing samples of liquefaction process streams and funding through a subcontract on U. S. Department of Energy Project DE-AC22-89PC89883.

REFERENCES:

1. Wise, S. A., Sander, L. C., May, W. E., *J. Chromatogr.*, **1993**, *642*, 329.
2. Fetzer, J. C., Biggs, W. R., *J. Chromatogr.*, **1993**, *642*, 319.
3. Wise, S. A., *Handbook of Polycyclic Aromatic Hydrocarbons*, vol. I, Marcel Dekker, New York, 1983, Ch. 5, p. 183.
4. Wise, S. A., *Handbook of Polycyclic Aromatic Hydrocarbons - Emission Sources and Recent Progress in Analytical Chemistry*, Vol. II, Marcel Dekker, New York, 1985, Ch. 5, p. 113.
5. Fetzer, J. C., *Chemical Analysis of Polycyclic Aromatic Compounds*, Wiley, New York, 1989, Ch. 5, p. 59.
6. Bartle, K. D., Lee, M.L., Wise, S. A., *Chem. Soc. Rev.*, **1981**, *10*, 113.
7. Akhlaq, M. S., *J. Chromatogr.*, **1993**, *644*, 253.
8. Holstein, W., *Chromatographia*, **1981**, *14*, 468-477.
9. Grizzle, P.L. and Thomson, J.S., *Anal. Letters*, **1987**, *20*(8), 1171-1192.
10. Nondek, L. and Malek, J., *J. Chromatography*, **1978**, *155*, 187-190.
11. Lochmuller, C. H., in D. E. Leyden and W. Collins (Editors), *Silylated Surfaces*, Gordon and Breach, New York, **1980**, 231.
12. Herren, D., Thilgen, C., Calzaferri, G., Diederich, F., *J. Chromatogr.*, **1993**, *644*, 188.
13. Clifford, D. J., McKinney, D. E., Hou, L., Hatcher, P. G., "High Performance Liquid Chromatography (HPLC) of Coal Liquefaction Process Streams Using Normal-phase Separation with UV Diode Array Detection"; Final Report, October 1993, DE-AC22-89PC89883, The Pennsylvania State University.

Table I: General information including percent solubilities for samples 1-5.

Sample #	Sample Designation ¹	Source ²	Run Number and Period	Feed Coal	Comments	Percent Solubility (%)
1	PFL	HRI	CC-15 11	Wyodak and Anderson	filtered process stream	91.7
2	PFL	HRI	CC-16 4	Illinois No. 6	filtered process stream	92.9
3	PFL	HRI	CC-16 13	Illinois No. 6	filtered process stream	92.6
4	V-1067 Dist.	W	257 Composite	Illinois No. 6	heavy distillate	96.8
5	V-1067 Dist.	W	262 Composite	Wyodak and Anderson	heavy distillate	97.6

1) PFL = pressure filter liquid; V-1067 Dist. = 850°F- distillate of second-stage flashed bottoms

2) HRI = Hydrocarbon Research Inc.; W = Wilsonville

Table 2: Assignments and weight percents for peaks labeled in Figure 1

Peak Number	Peak Assignment	Weight % in sample #1	Weight % in sample #2	Weight % in sample #3	Weight % in sample #4	Weight % in sample #5
1	one & two ring hydro-aromatics	8.97	12.6	6.43	1.74	2.36
2	two & three ring hydro-aromatics	16.2	14.4	6.72	2.21	1.42
3	C ₁ -anthracene	0.463	0.397	0.656	0.0470	0.0390
4	phenylmethyl-naphthalene* C ₄ -phenanthrene C ₅ -phenanthrene	0.746	0.504	0.698	0.0590	0.0460
5	dihydro-pyrene	ND	0.115	0.0640	0.0220	0.0380
6	hexahydro-benzopyrene	ND	0.0530	0.0220	0.00700	0.0190
7	pyrene	1.29	1.10	0.887	0.111	0.0980
8	C ₁ -Pyrene* C ₂ -Pyrene C ₃ -Pyrene	0.650	0.598	0.498	0.0660	0.0600
9	dihydro-benzopyrene	0.407	0.563	0.379	0.0530	0.123
10	C ₁ -dihydro-benzopyrene* C ₂ -dihydro-benzopyrene hexahydro-benzo[g,h,i]perylene	0.449	0.387	0.200	0.0180	0.0390
11	benzo[b]fluoranthene	internal standard	internal standard	internal standard	ND	ND
12	benzo[g,h,i]perylene	0.326	0.384	0.349	internal standard	internal standard
13	C ₁ -benzo[g,h,i]perylene	0.148	0.169	0.140	ND	ND
14	C ₂ -benzo[g,h,i]perylene* C ₃ -benzo[g,h,i]perylene	0.0660	0.0960	0.0730	ND	ND
15	dihydro-dibenzopyrene* C ₁ -dihydro-dibenzopyrene C ₂ -dihydro-dibenzopyrene	0.0600	0.109	0.0770	ND	ND
16	coronene	0.246	0.276	0.265	ND	ND
17	dihydro-benzocoronene	0.105	0.151	0.133	ND	ND
18	bisanthene* C ₁ -bisanthene	0.0360	0.0370	ND	ND	0.00200
19	benzobisanthene* C ₁ -benzobisanthene	ND	0.0180	0.0160	ND	ND

ND=not detected

* = predominant contributor

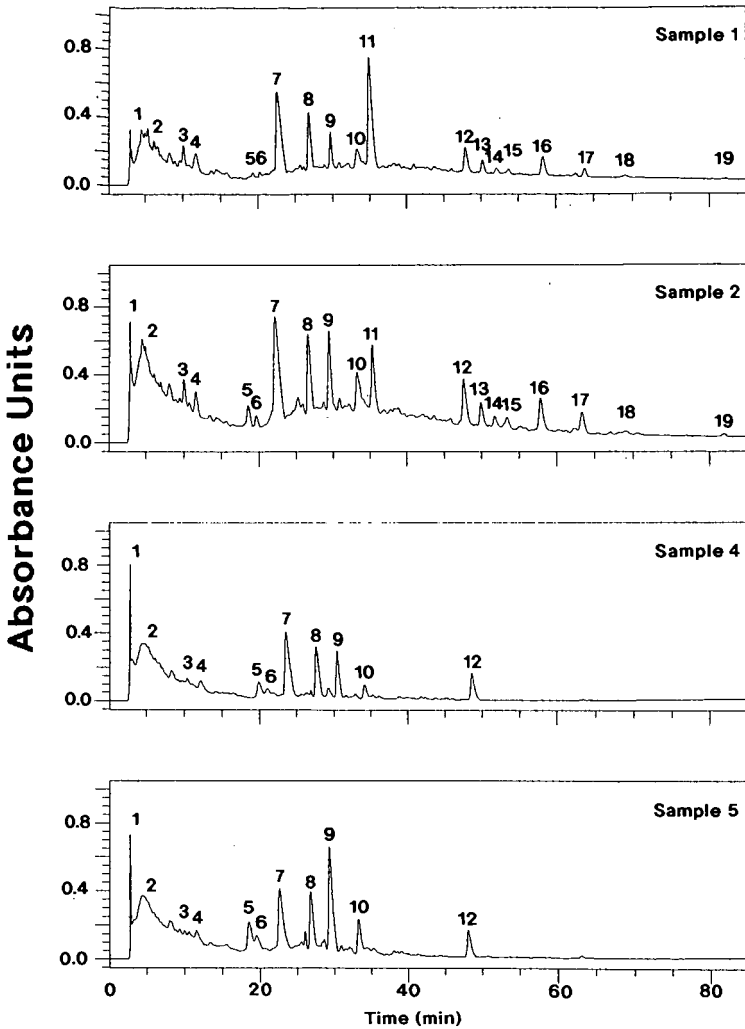


Figure 1. Maxiplots of the HPLC chromatograms for four of the five samples examined. Sample #3 is not included because its chromatogram is similar to that of Sample #2.

MOLECULAR BEAM MASS SPECTROMETRIC CHARACTERIZATION OF BIOMASS PYROLYSIS PRODUCTS FOR FUELS AND CHEMICALS¹

F.A. Agblevor, M.F. Davis, and R.J. Evans.
National Renewable Energy Laboratory,
1617 Cole Boulevard, Golden, CO 80401

Key words: Biomass pyrolysis, multivariate analysis, molecular beam mass spectrometry.

ABSTRACTS

Converting biomass feedstocks to fuels and chemicals requires rapid characterization of the wide variety of possible feedstocks. The combination of pyrolysis molecular beam mass spectrometry (Py-MBMS) and multivariate statistical analysis offers a unique capability for characterizing these feedstocks. Herbaceous and woody biomass feedstocks that were harvested at different periods were used in this study. The pyrolysis mass spectral data were acquired in real time on the MBMS, and multivariate statistical analysis (factor analysis) was used to analyze and classify Py-MBMS data into compound classes. The effect of harvest times on the thermal conversion of these feedstocks was assessed from these data. Apart from sericea lespedeza, the influence of harvest time on the pyrolysis products of the various feedstocks was insignificant. For sericea lespedeza, samples harvested before plant defoliation were significantly different from those harvested after defoliation. The defoliated plant samples had higher carbohydrate-derived pyrolysis products than the samples obtained from the foliated plant. Additionally, char yields from the defoliated plant samples were lower than those from the foliated plant samples.

INTRODUCTION

The U.S. Department of Energy has embarked on a major program to explore alternate energy sources including biomass. Biomass is an attractive alternative energy source because if energy crops are managed sustainably, a fuel cycle results that will contribute little or no net greenhouse gases to the earth's atmosphere. Biomass feedstocks vary considerably in source and composition and some examples of biomass feedstocks are waste woods from the pulp, paper and lumber industries; demolition wood from urban areas; and agricultural residues and cultivated herbaceous and woody energy crops. It is projected that biomass energy could contribute 11 quads of the United States' energy requirement if all the biomass resources are fully developed [1].

To embark on a large scale production of biomass energy, the quality of the feedstock, that may be influenced by the time of harvest, must be assessed. Seasonal variations give rise to changes in nitrogen, minerals and carbohydrate content of the plants [2]. These changes in turn influence the pyrolysis pathways of the biomass feedstocks. Low alkali metal content of biomass species promotes cellulose decomposition pathways that favor levoglucosan formation whereas the high ash content of biomass favors hydroxyacetaldehyde and char formation reactions [3]. Similarly, a high nitrogen content of biomass favors char formation because of interaction between the amino acids and carbohydrate decomposition products [4]. Thus by judiciously selecting the harvest time of the biomass, it may be possible to influence the pyrolysis products of the feedstock.

In addition to feedstock quality, the conversion technology is equally important for a successful biomass energy program. Several technologies including pyrolysis, gasification, liquefaction and biochemical conversion are currently under development. Fast pyrolysis technologies are receiving considerable attention because they can produce a more dense and easily transportable fuel compared to the original feedstock. The pyrolysis oils can conceivably be used as a chemical feedstock for other processes.

Efficient pyrolytic conversion of biomass to fuels and chemicals requires a thorough understanding of the pyrolysis process and an efficient tool for analyzing the pyrolysis products. The molecular beam mass spectrometer (MBMS) is a unique tool that is capable of analyzing biomass pyrolysis products in real time. However, the MBMS alone offers only qualitative and semiquantitative capability, but when combined with multivariate statistical analysis, it offers a powerful tool to analyze biomass and other pyrolysis products.

¹ This paper will be published as a preprint of the ACS Fuels Division Meeting, August 21-26, 1994, Washington D.C.

In this paper, we discuss the application of MBMS and multivariate statistical technique in the classification and analysis of biomass feedstocks harvested at different periods. The influence of harvest time on the pyrolysis products of the feedstocks is discussed. The goal of the study is to develop a rapid method for characterizing biomass and other feedstocks pyrolysis products.

MATERIALS AND METHODS

Pyrolysis of Biomass Feedstocks

The biomass feedstocks used in this study were supplied by subcontractors of the National Renewable Energy Laboratory (NREL), Biofuels Program. The following feedstocks (harvested in various parts of the contiguous USA) were used in this study: hybrid poplar (*Populus deltoides x nigra* var. *Caudina*), sericea lespedeza (*Lespedeza cuneata* var. *Seralata*), black locust (*Robinia pseudoacacia* L.), and switchgrass (*Panicum virgatum* L.). Hybrid poplar samples were harvested from section #11 of Rocksbury Township, Pennington County, MN in November 1991 and March 1992; sericea lespedeza samples were harvested in October and December 1992 and black locust samples were harvested from 9-year-old plants at the Hind's Research Farm near Ames, IA in the fall of 1991 and spring 1992. Switchgrass samples were harvested from a 6-year-old stand located on the Koemel ranch 7 km south of Stephenville, TX in October 1991 and August 1992. About 1kg of each feedstock was shipped to NREL where they were prepared for pyrolysis. The feedstocks were air-dried at room temperature for 4-7 days to facilitate milling because wet samples tend to heat up during milling. The samples were milled in a Wiley mill (Model 4) until all the material passed through a 2 mm screen. The ground materials were then sieved to -20/+80 mesh size and riffled to homogenize them. We stored the sieved samples in freezers until such time the analysis were performed. The moisture content of the feedstocks prior to pyrolysis was 5-7%.

Biomass samples (20-30 mg) were weighed in quartz boats in triplicates and pyrolyzed in a quench pyrolysis reactor. The reactor consisted of a quartz tube (2.5 cm inside diameter) with helium flowing through at 5 L/min (at STP). The reactor tube was interfaced with the orifice of the molecular beam mass spectrometer (MBMS), Extrel™ Model TQMS C50, for pyrolysis vapor analysis (see detailed description of the MBMS in [5]). The reactor was electrically heated and its temperature maintained at 550 ± 5 °C. The temperature profile of the biomass samples once introduced into the reactor, is unknown, although the pyrolysis reaction was completed in 50 s. Total pyrolysis time was 90 s (including the time the quartz boat heats up to 550°C), but the residence time of the pyrolysis vapors in the reactor pyrolysis zone was ~75 ms and this prevented secondary cracking reactions. The pyrolysis vapors were sampled through the MBMS orifice in real time. During the sampling process, the pyrolysis vapors underwent free-jet expansion during their passage through the orifice and this sufficiently cooled the pyrolysis vapors to prevent secondary reactions or condensations. The cooled pyrolysis vapors passed through a skimmer to form a molecular beam that was fed to a 22.5 eV electron impact ionization triple quadrupole mass spectrometer for real time analysis. Mass spectral data for 15-300 Da were acquired on a Teknivet Vector 2™ data acquisition system.

Multivariate Analysis of Data

Mass spectral data acquired from the pyrolysis process were analyzed by multivariate statistical techniques. The data were first normalized to the total ion current to account for the sample size variation. Data reduction and resolution were carried out on the normalized data using the Interactive Self-modeling Multivariate Analysis (ISMA) program. The correlation around the mean matrix was used to select the significant number of factors for resolution of the mass spectral data into compound classes (see details of this methodology in [6]). In this method, the data set was mean-centered by subtracting the mean from each mass variable. Each variable was weighted by its standard deviation so that all masses (both large and small) were equally important. This method was used to show the differences between the pyrolysis products of the biomass species and the influence of harvest time on the samples. On the other hand, the correlation around the origin matrix was used to extract the relative fractional concentration of compound classes in the biomass pyrolysis products. In performing factor analysis around the origin, the absolute magnitude of the relative abundance for each mass variable was also factor analyzed. However, each variable is weighted by the standard deviation so that each mass is equally important in this method as well. This is in contrast to factor analysis around the mean where only the differences between samples are used for factor analysis. The latter technique is used when only differences between samples are needed, while the former is used when fractional concentrations of components are to be determined. This can be confusing to the reader who is accustomed to factor analysis around the mean and viewing plots of factor score 1 versus factor score 2. When factor analysis around the origin is used, this same information is contained in factor scores 2 and 3, and factor score 1 contains the information about the mean of each variable. The number of factors selected for the analysis was limited to significant factors (eigenvalues >1). Factor scores from the analysis were presented in two-dimensional plots to show compositional differences between various biomass materials. Materials with similar mass spectral intensities form clusters in the factor space. The factor analyzed data were resolved into three components corresponding to lignin, hexosans and pentosans. These resolved pyrolysis products of the biomass

feedstocks were used to determine the influence of storage time on the composition of the biomass.

RESULTS AND DISCUSSION

Pyrolysis-molecular beam mass spectra (Py-MBMS) for the different biomass materials (hybrid poplar, black locust, sericea lespedeza, and switchgrass) that were harvested at two different times of the year show visual similarity for all the species except sericea lespedeza. The Py-MBMS spectra can be divided into three main classes representing pentosans with typical m/z 43, 85, 96, and 114; hexosans with typical m/z 31, 60, 73, 97, 126, 144, and 162; and lignins with typical m/z 124, 137, 150, 154, 167, 180, 194, 210, and 272. A small region, which is typical of phenolic esters and phenylpropane lignins (m/z 94, 120, and 150), is prominent in the switchgrass pyrolysis mass spectra.

The influence of harvest time cannot be readily discerned from visually inspecting most of the spectra of the feedstocks (see Figure 1a and 1b) except by multivariate statistical analysis. In the case of sericea lespedeza, the Py-MBMS from the two harvests are visually discernible (see Figure 2a and 2b). In Figure 2b, the pyrolysis products that derive from the carbohydrates are higher for the December harvest compared to the October harvest.

The Py-MBMS spectral data were further analyzed using the ISMA program to highlight the differences between the harvests. The analysis of the mass spectral data using the correlation around the mean matrix indicated that 87% of the variance in the data set could be explained using four factors. The four factors were used to perform factor analysis using a correlation around the origin matrix. The factor-score plot (Figure 3a) showed four main groups corresponding to hardwoods, switchgrass, the October sericea lespedeza harvest, and the December sericea lespedeza harvest. The repeatability of the pyrolysis runs is indicated by the triangles in the factor score plot. The variance diagram in Figure 3b also confirms the clusters in the factor score plot.

The different clusters shown in the factor space for the two sericea lespedeza harvests suggests that the pyrolysis products of these two feedstocks are different. The major difference between the pyrolysis products of the two harvests is the carbohydrate component of the feedstocks. The resolution of the pyrolysis spectra showed a relatively high concentration of carbohydrate component in the December harvest of the sericea lespedeza compared to the October sericea lespedeza harvest. This observation is similar to the seasonal carbohydrate cycles noted in deciduous trees in the temperate climate. Carbohydrate contents of stems and branches of deciduous trees are maximized near the time of leaf fall and start to decrease in late winter [2]. Although sericea lespedeza is technically not a tree, it is a woody shrub that defoliates in the fall like the deciduous trees. It is probable that the total reserve carbohydrate accumulation in this shrubby species follows a similar cycle to those observed for the trees.

In addition to the high carbohydrate content of the December sericea lespedeza harvest, the char produced during the pyrolysis was lower ($16.2 \pm 1.0\%$) than that for the October sericea lespedeza harvest ($21.4 \pm 1.0\%$). The difference in char yields was attributed to the significant differences between the nitrogen and ash contents of the two harvests. The October sericea lespedeza harvest had a high leaf to stem ratio (0.26) and consequently a high nitrogen content ($1.14 \pm 0.10\%$) compared to the December sericea lespedeza harvest that was defoliated and had a nitrogen content of $0.75 \pm 0.10\%$. The ash contents of the October and December sericea lespedeza harvests were 2.1 ± 0.3 and $1.3 \pm 0.4\%$ respectively. Both the nitrogen and ash components of the biomass are known to promote char formation. Nitrogen compounds are known to react with carbohydrate decomposition products during the pyrolysis process resulting in char [4].

For switchgrass samples, although the repeatability triangles do not overlap, the differences between the pyrolysis products of the two harvests appear to be very small and statistically insignificant. The factor analysis of the data indicates that the switchgrass samples have a higher concentration of components that are rich in m/z 120 and 150 compared to the sericea lespedeza and the woody species. These masses derive from phenolic ester units known to occur in grass lignins. Nitrogen (0.59 ± 0.08 and $0.56 \pm 0.066\%$) and ash (5.2 ± 0.4 and 4.8 ± 0.2) contents of the two harvest were similar, and hence char yields from both harvests were very similar (18.6 ± 0.3 and $18.4 \pm 1.4\%$).

Py-MBMS and factor analysis of the woody biomass species (black locust and hybrid poplar) indicated that there are no significant differences in the yield of pyrolysis products because of harvest time. The repeatability triangles overlap as shown in Figure 3a. The variance diagram also indicates that the hardwoods are richer in lignin components compared to the non-woody species (switchgrass and sericea lespedeza). The woody species have very strong peak intensities at m/z 138, 154, 167, 180, 194, and 210 which are typical lignin decomposition products. Nitrogen and ash contents of the woody species from the two harvests were very similar and hence the char yields were also very similar. Although seasonal variations in minerals, nitrogen, and reserved carbohydrates contents have been reported for hardwoods,

the influence of these changes on the pyrolysis products of the woody biomass feedstocks analyzed by our method appear to be minimal.

CONCLUSIONS

The multivariate analysis of the biomass feedstocks studied shows that the influence of harvest time on the composition of the biomass pyrolysis products is only significant for the herbaceous biomass feedstock (*sericea lespedeza*). The pyrolysis products of woody biomass feedstocks appear to be less affected by the time of harvest. Thus, for fuel production from *sericea lespedeza* this factor must be taken into account. Small changes in the biomass feedstocks can be detected by MBMS and their subsequent influence on converting the feedstocks to fuels and chemicals can be assessed. The Py-MBMS technique for analyzing biomass feedstocks has some advantages over conventional chemical analysis in that sample preparation is minimal, very small samples are required for analysis, pyrolysis time is very short, and the pyrolysis data is acquired in real time. This technique may also find application in coal and other fossil fuel analysis.

ACKNOWLEDGEMENT

The authors acknowledge H.L. Chum and R. Overend for their involvement in initiating this study; A.E. Wiseloglel, the NREL Terrestrial Biomass Feedstocks Interface Program coordinator, and N. Hinman, the NREL Biofuels Program manager, for their continued support. P. Ashley prepared the biomass feedstocks for the pyrolysis studies. The work was sponsored by the U.S. Department of Energy Biofuels Systems Division through the Biofuels Program (R. Moorer, R. Costello, and J.Ferrell).

REFERENCES

1. Sunderman, D. "Using Biomass and Wastes Productively: Research Advances at the National Renewable Energy Laboratory." In *Energy from Biomass and Wastes XVI*, (D.L. Klass, ed.) Institute of Gas Technology (IGT): Chicago, 1993; pp. 1-13.
2. Kramer, P.J. and Kozlowski, T.T. *Physiology of Woody Plants*; Academic: New York, 1979; Chapters 7, 9, and 10. .
3. Evans, R.J.; Agblevor, F.A.; Chum, H.L.; Wooten, J.B.; Chadwick, D.B.; and Baldwin, S.D., "New Approaches to the Study of Cellulose Pyrolysis," *ACS Fuel Div., Preprints* (1991), 36 (2), 714-724.
4. Theander, O., and Nelson, D.A., "Aqueous High Temperature Transformation of Carbohydrates Relative to Utilization of Biomass," *Adv. Carbohydrate Chem. Biochem.*(1989), 46, 273-326 .
5. Evans, R.J., and Milne, T.A., "Molecular Characterization of the Pyrolysis of Biomass I, Fundamentals," *Energy and Fuels* (1987), 1 (2), 123-137.
6. Windig, W.; Haverkamp, J.; and Kistemaker, P.G., "Interpretation of Sets of Pyrolysis Mass Spectra by Discriminant Analysis and Graphical Rotation," *Anal. Chem.* (1983), 55, 81-88 .

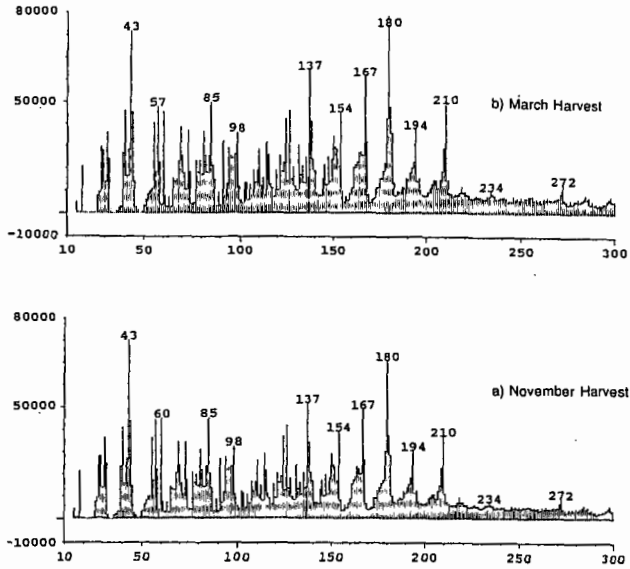


Figure 1. Pyrolysis mass spectra of hybrid poplar. Note the strong similarity in the spectra of a) the November harvest, and b) the March harvest.

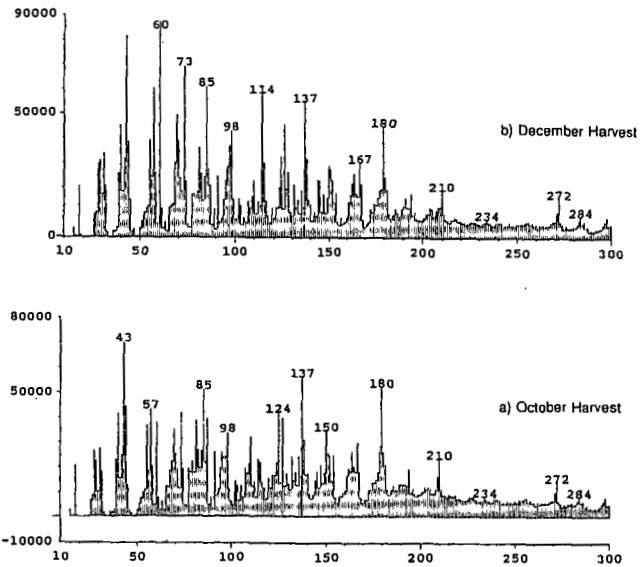


Figure 2. Pyrolysis mass spectra of sericea lespedeza. Notice the difference in the intensity of the low mass peaks (e.g., m/z 60, 73 and 114) in a) the October harvest, and b) the December harvest.

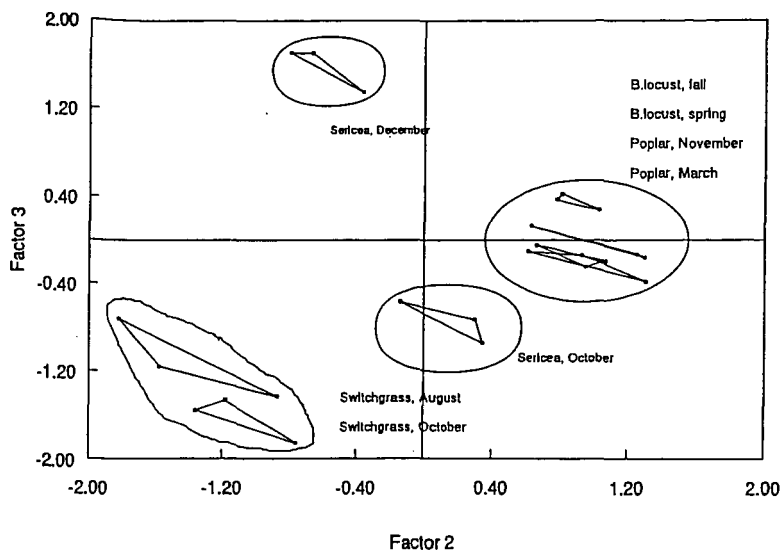


Figure 3a. Factor-score plot of Factor 2 versus Factor 3 of the different harvests of sericea, black locust, hybrid poplar, and switchgrass showing the clusters of the similar biomass samples in the factor space. The triangles show the repeatability of the pyrolysis runs.

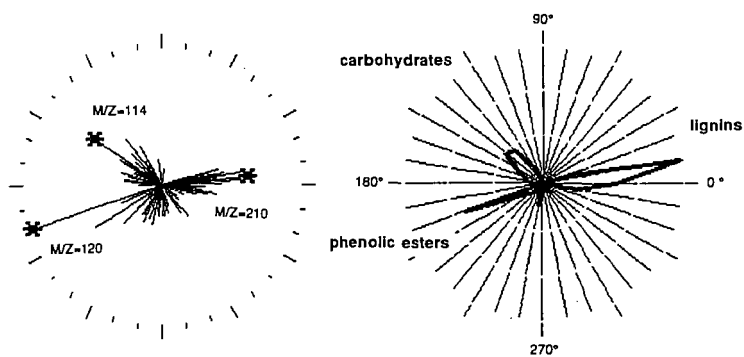


Figure 3b. Variance diagram of factor 2 versus factor 3 of the Py-MBMS of the biomass feedstocks showing compound classes in the spectra.